Today – the last lecture:

Feb. 23$^{th}$ – lecture 13 – and Feb. 28$^{th}$

Mar. 2$^{nd}$ – exam at CAMK at room 18/19
Be in person
Mar. 9$^{th}$ – overview of exam, signing cards
Be in person

Overview of this HW#6 – end of this lecture

# Summary after 12th :

## Extragalactic X-ray astronomy:

## ISM:

- **Soft X-ray emission of gas**
- **HIM – hot interstellar medium**
- **Local Hot Bubble model**
- **ISM extinction.**

## Nearby galaxies:

- **Point-like emission components**
- **Contribution of LMXB and HMXB**
- **Log(N) – Log(S) distribution**
- **Luminosity function of point like sources in our Galaxy and nearby galaxies**
- **ULX – ultra luminous X-ray sources**
- **Hot plasma component.**

## Cluster of galaxies – cooling flows:

- **ICM – hot intercluster plasma**
- **Mass profile for gas in hydrostatic equilibrium**
- **Temperature and brightness profiles from observations**
- **Commonly used density profile**
- **Spectra taken from concentric rings**
- **Problem of cooling flows.**

# Lecture 13th – AGN and their contribution to cosmic XRB:

A class of objects where X-ray emission from an accretions disk is prominent.

$$L_{bol} = \eta * \dot{M} * c^2$$

$$T_{disk} \propto 4 \times 10^6 \left( \frac{M_{BH,NS}}{10\, M_{Sun}} \right)^{-1/4}$$

For M = $10^8$ $M_{Sun}$:

$$T_{disk} \approx 10^5\, K$$

Magdziarz+ 1998 NGC 5548

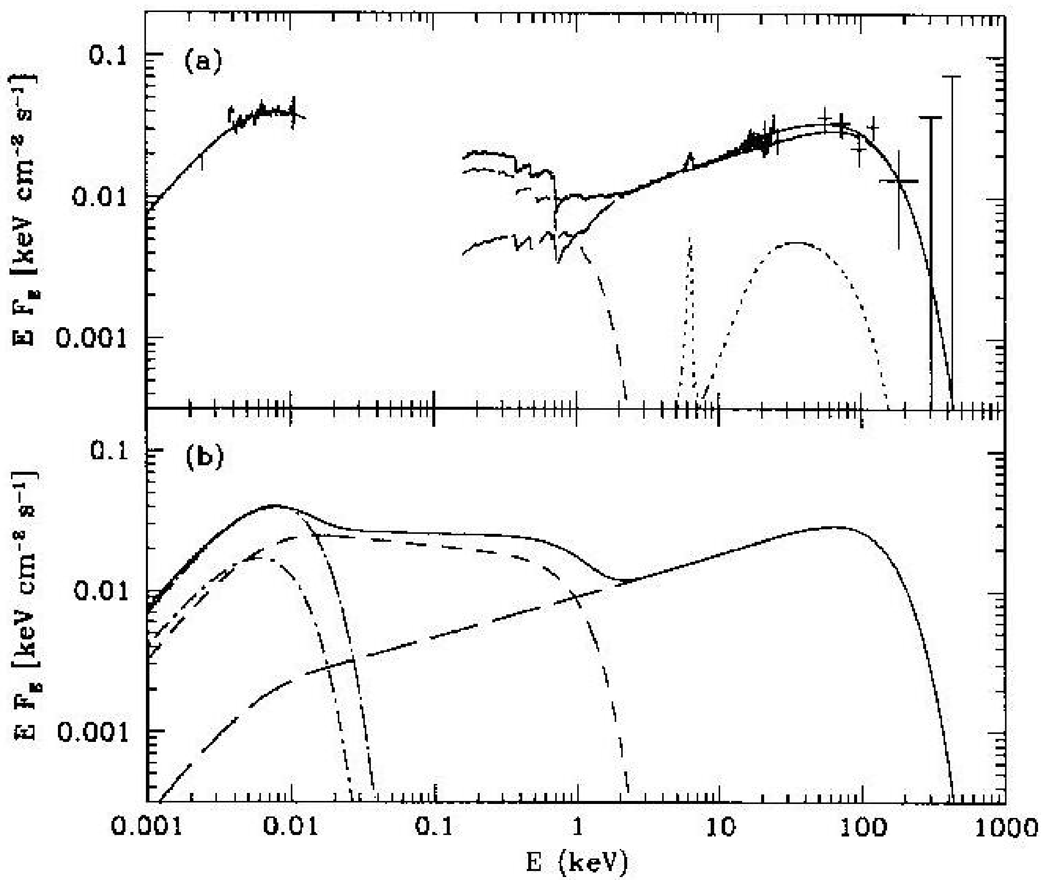

# X-ray binaries:

A class of objects where X-ray emission from an accretions disk is prominent.

$$L_{bol} = \eta * \dot{M} * c^2$$

$$T_{disk} \propto 4 \times 10^6 \left( \frac{M_{BH,NS}}{10\, M_{Sun}} \right)^{-1/4}$$

For $M = 1.4\, M_{Sun}$:

$$T_{disk} \approx 10^7\, K$$

Cyg X-1 Zdziarski + 2002

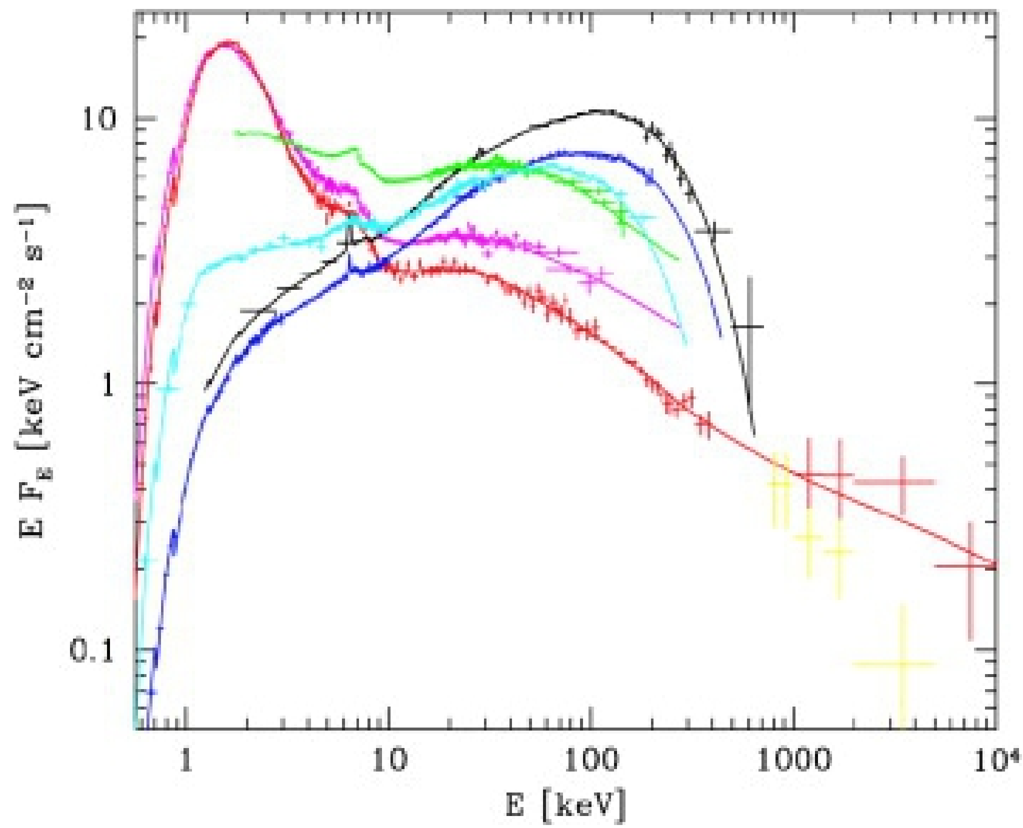

# Black hole systems:

## Active Galactic Nuclei (AGN)

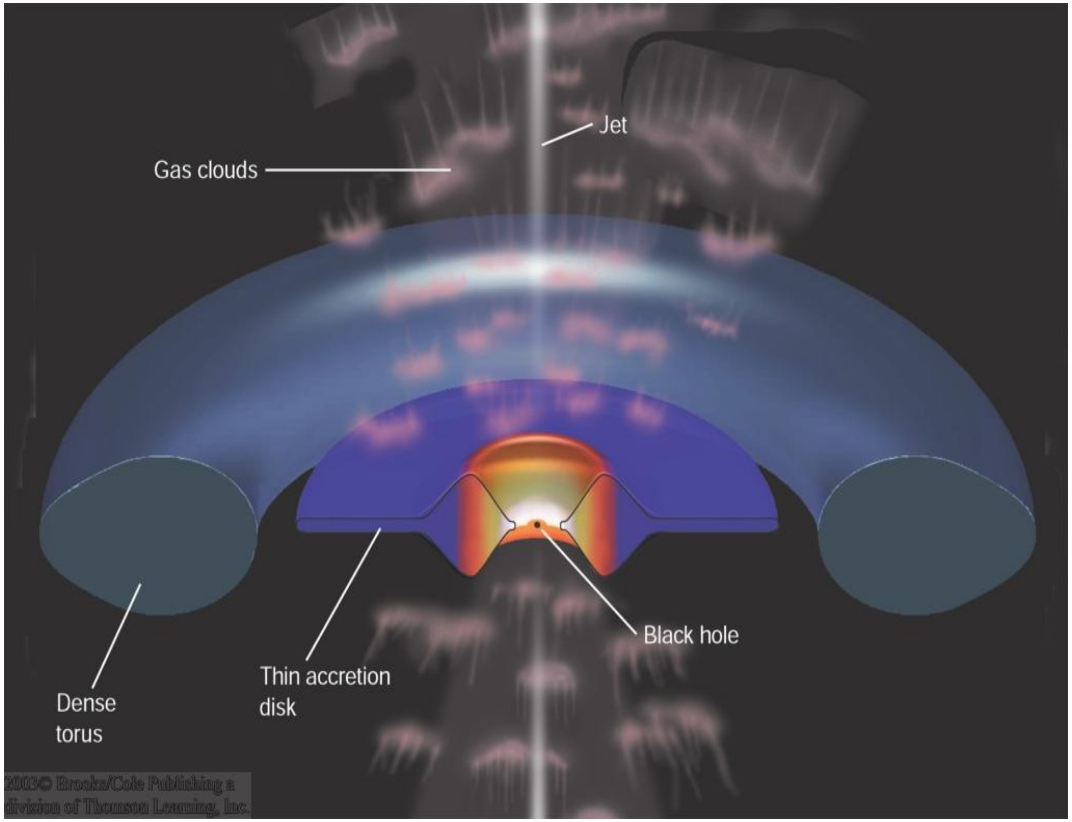


$M_{BH}=10^{7\text{-}9}\ M_{\odot}$

$T_{eff} < \text{few} \times 10^5$ K

## Black Hole Binaries (XRB)

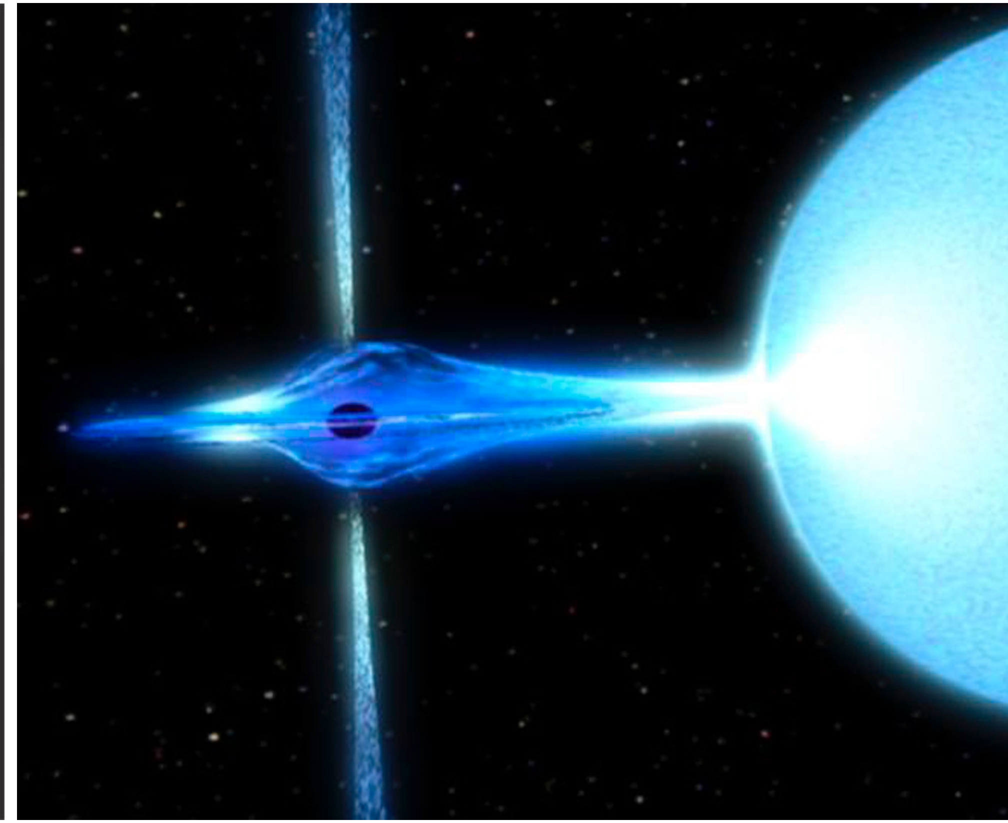

$M_{BH}=10\ M_{\odot}$

$10^6 < T_{eff} < \text{few} \times 10^7$ K

# AGN – classical picture:

Urry & Padovani cartoon
of unified AGN model:

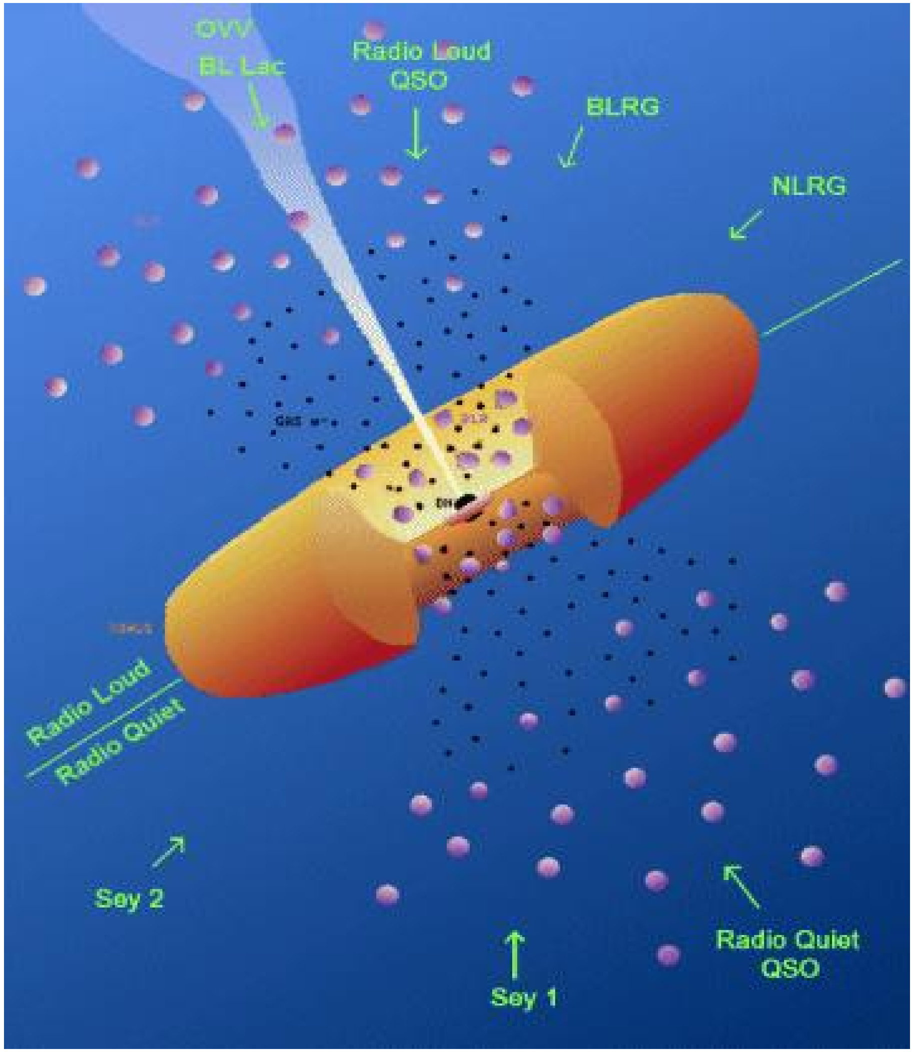


## Types of AGN:

**1) radio-load:**
**dominated by jet emission, no lines**

$$f_R(4.76\,GHz)/f_B > 1$$

**BL Lac, Blandford & Rees 1978,**

**2) OVV – optically violent variables, strong polarized radio emission, rare examples of lines,**

**3) radio-quiet:**
**dominated by accretion disk emission,**

**Seyfert's galaxies (1943) are radio quiet objects with strong emission lines about 8500 km/s.**

# Seyfert's galaxies:

Sy1 – two types of emission lines:

I) narrow forbidden emission lines originated in rare medium:

$$\rho \sim 10^3 - 10^6\, cm^{-3}$$

$$FWHM < 1000\, km/s$$

II) broad emission lines from larger density regions:

$$\rho \sim 10^9\, cm^{-3}$$

$$FWHM \sim 10000\, km/s$$

Khachikian & Weedman 1974

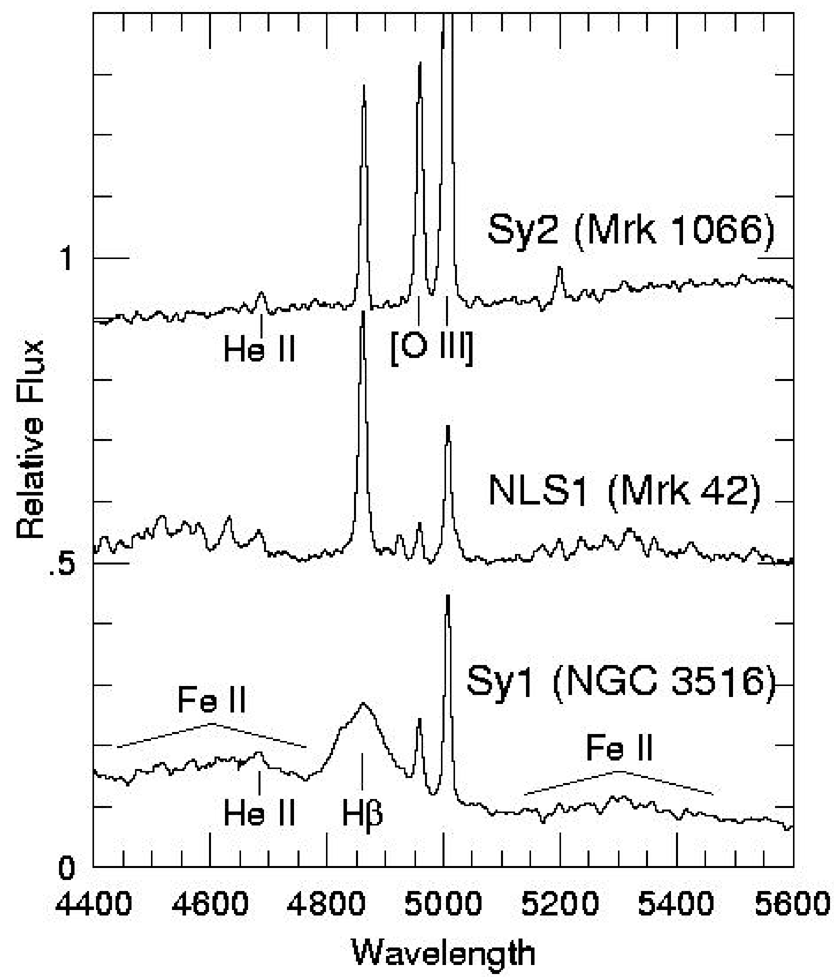


Fig. 1. Spectra in the region of Hβ of the NLS1 Mrk 42 (center), the Sy1 NGC 3516 (below), and the Sy2 Mrk 1066 (above).

Sy2 – only narrow lines,
one mag weaker than Sy1,

NLS1 – strong as Sy1, but emission line $H_{!}$ $< 2000$ km/s

# Unified model of radio quiet AGN:

Antonucci & Miller 1985

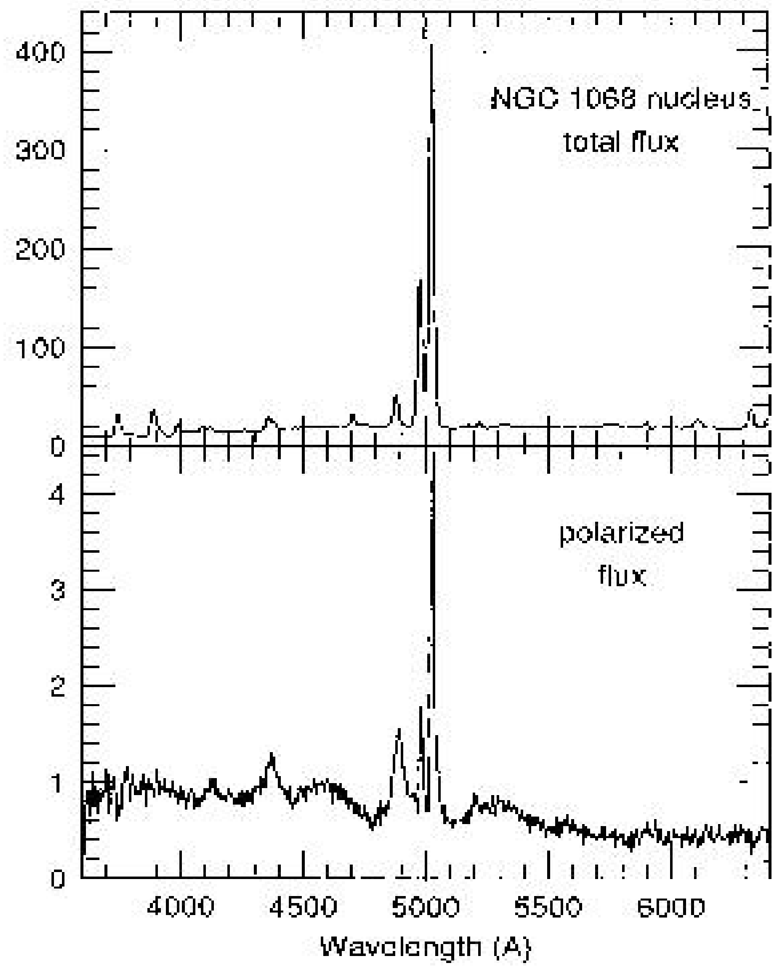


Emission lines are formed in clouds illuminated by continuum emission from the center of AGN
i.e. from an accretion disk.

NGC 1068 – Sy 2 galaxy with broad emission lines in polarized light.

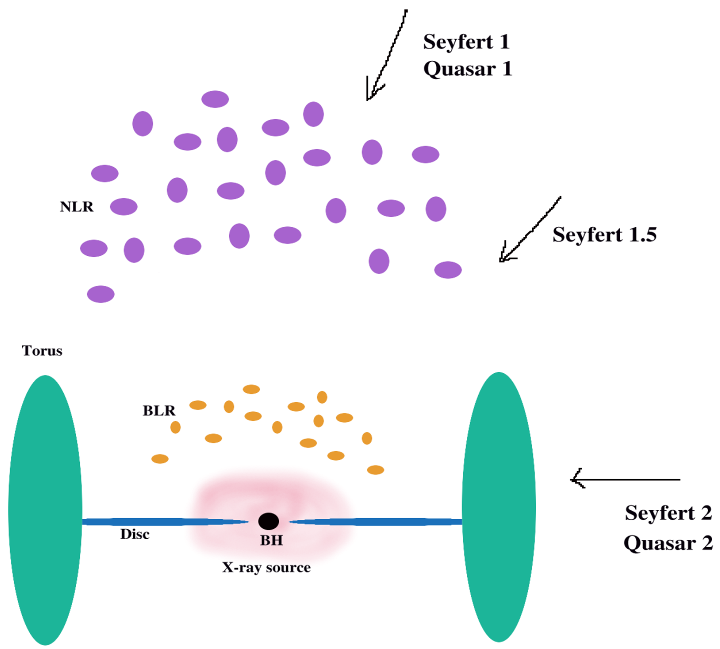

# Continuum energy distribution of radio-loud AGN:

BL Lac and OVV – blazars posses strong X-ray emission.
Jets are resolved by VLBI up to 1 pc.

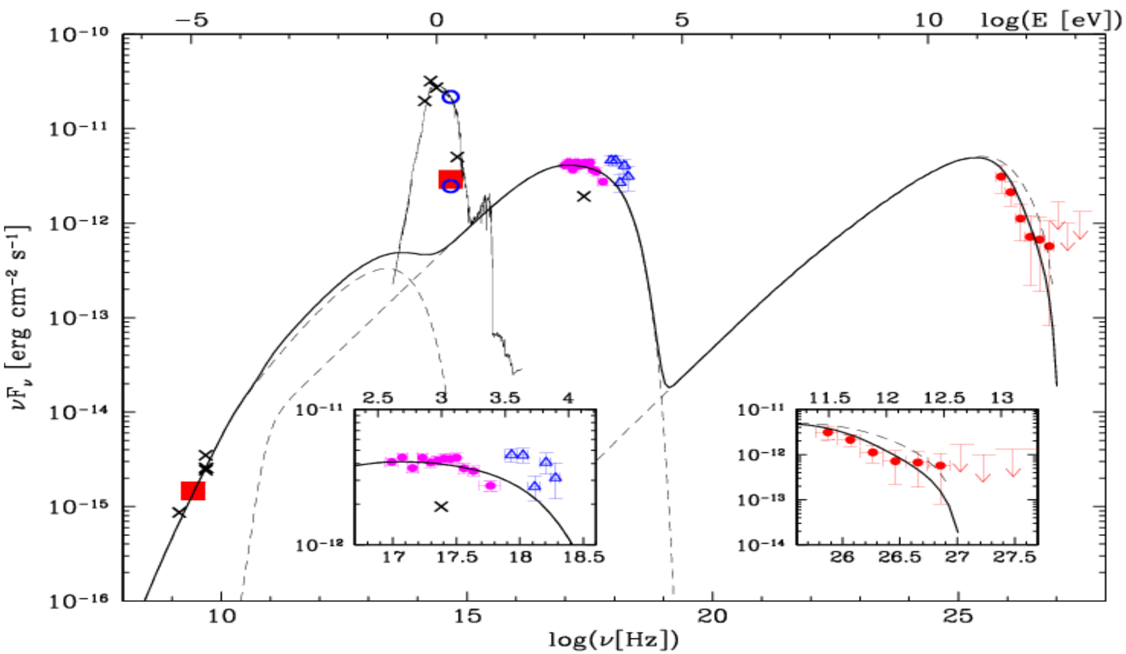


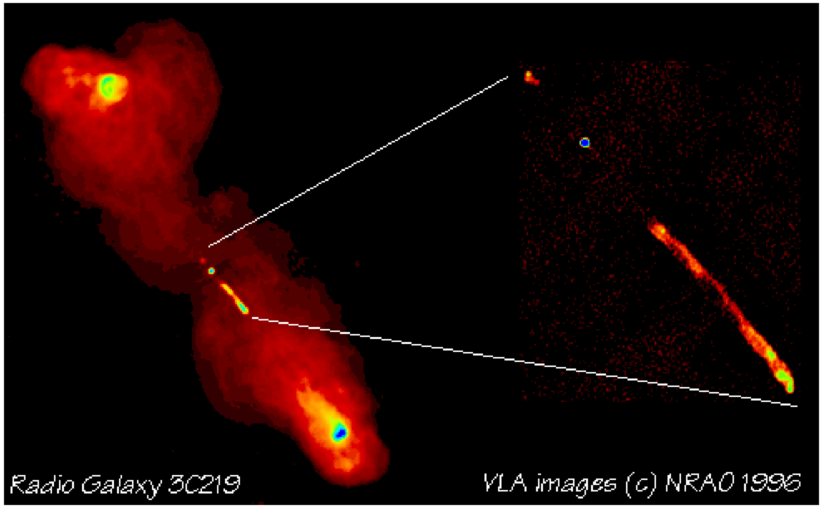


Acceleration in jests:
- X-rays as synchrotron emission,
- correlation of X-rays with TeV.

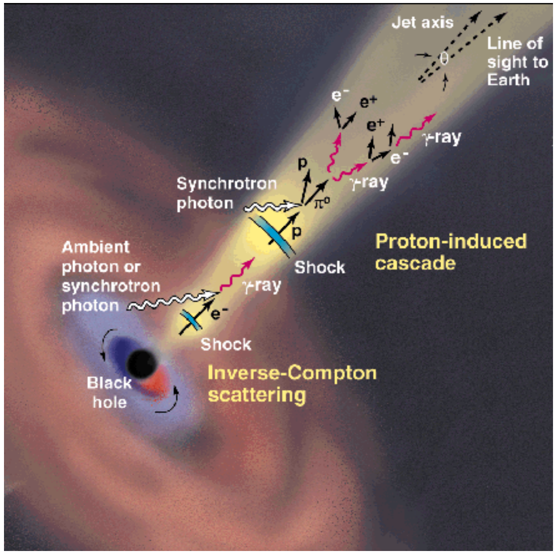

<u>Continuum energy distribution of radio-loud AGN:</u>

Mean spectra of blazars for different luminosities, about 132 objects observed by ROSAT.

Two maxima are observed they are shifted toward lower energies for more luminous objects.

The ratio of peak frequencies is almost constant, but the ratio of peak luminosities increases with total luminosity.

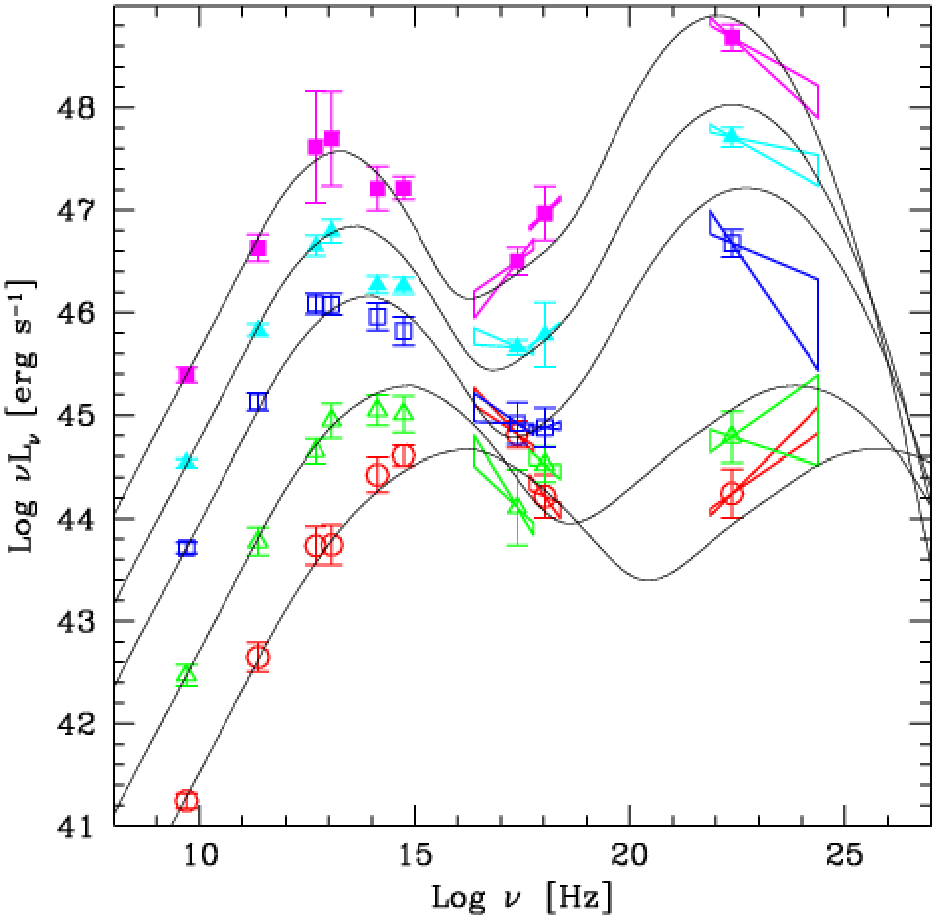

# Continuum energy distribution of radio-loud AGN:

**3C279, Ballo+ 2002**

Synchrotron radiation from jet

Emission from accretion disk

SSC -synchrotron self Compton

External Compton

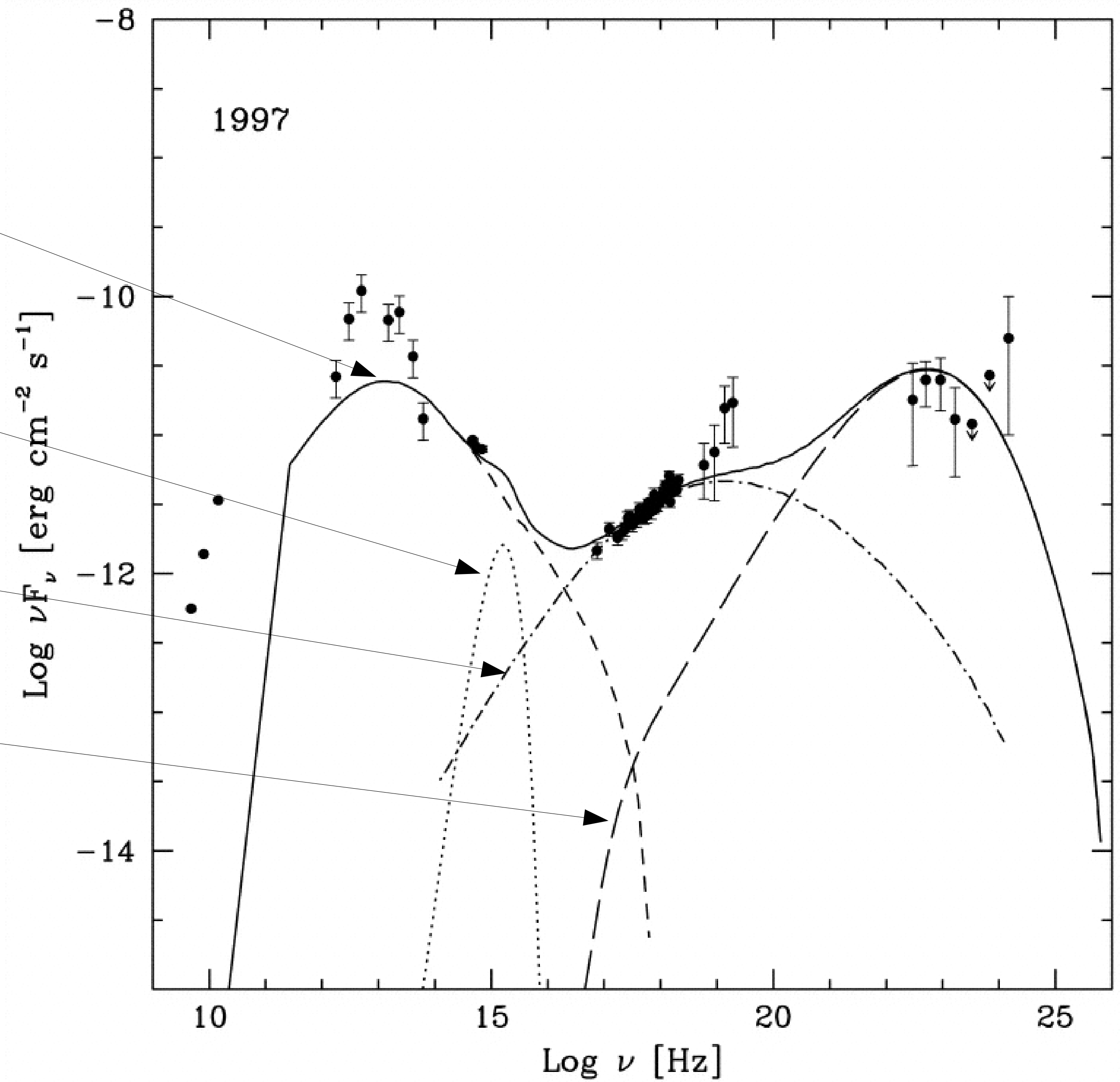

# Continuum energy distribution of radio-loud AGN:

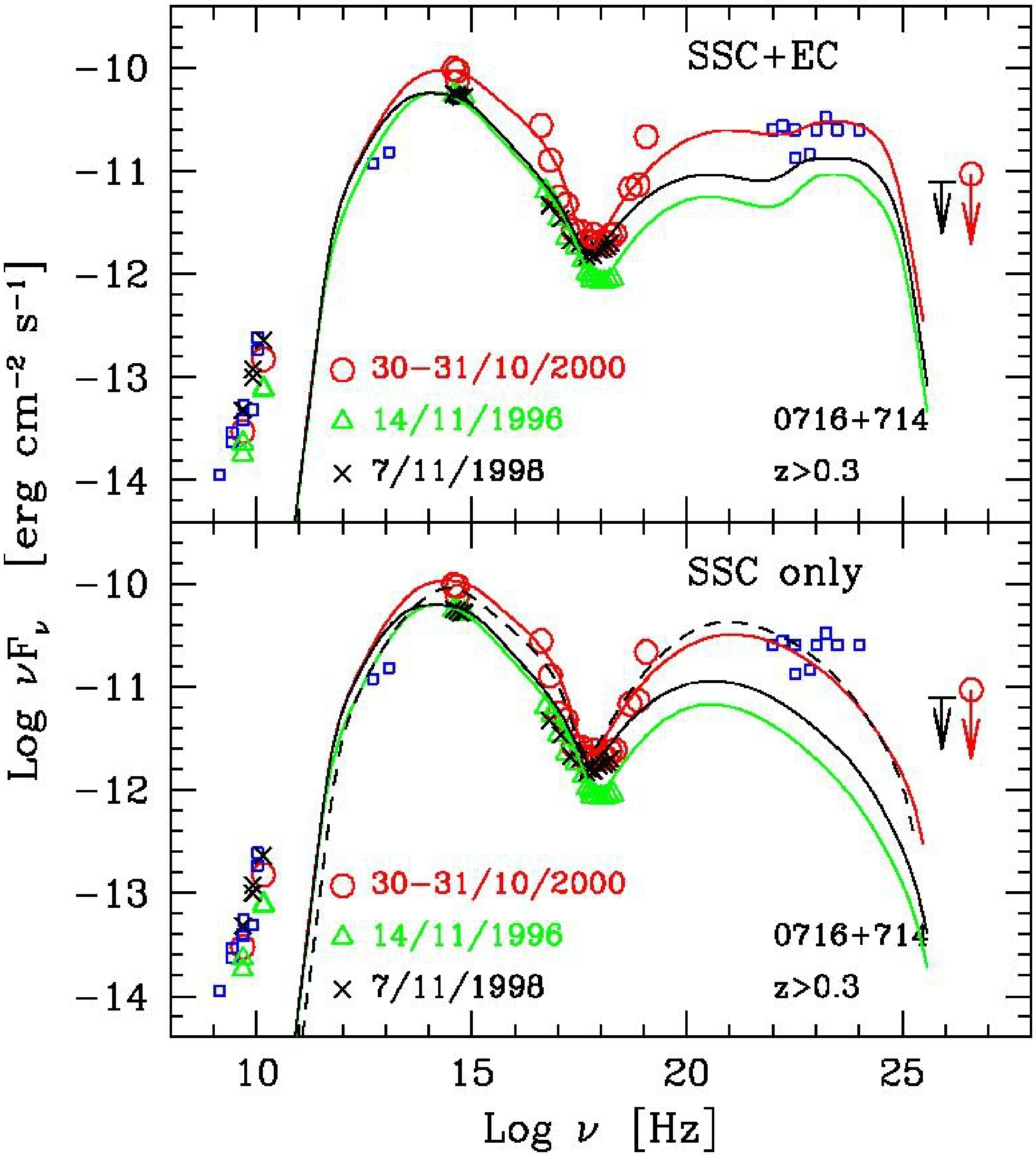


Synchrotron Self Compton SSC
- Comptonization of synchrotron radiation from the jet,

External Comptonization EC
- Comptonization of external photons most probably from the Broad Line Regions.

# Continuum energy distribution of radio-loud AGN:

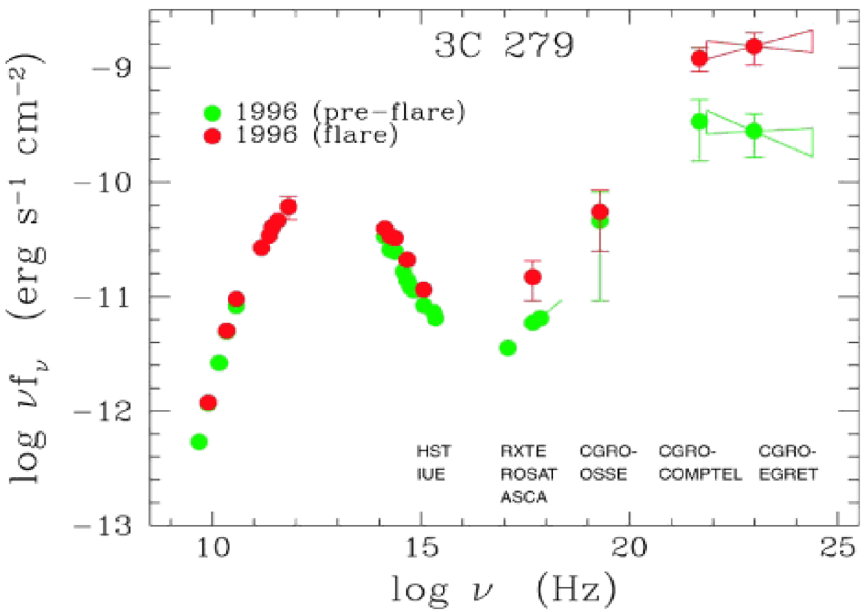


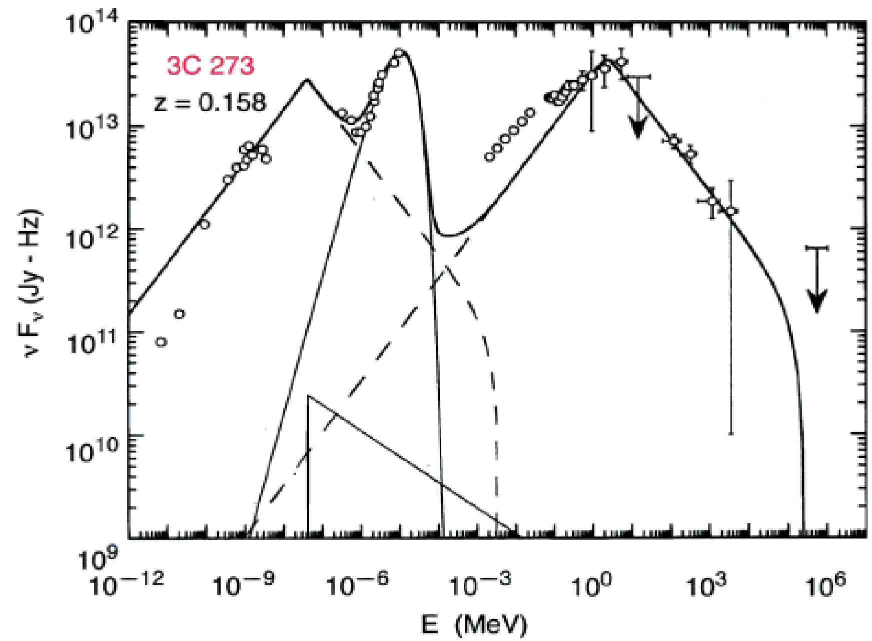


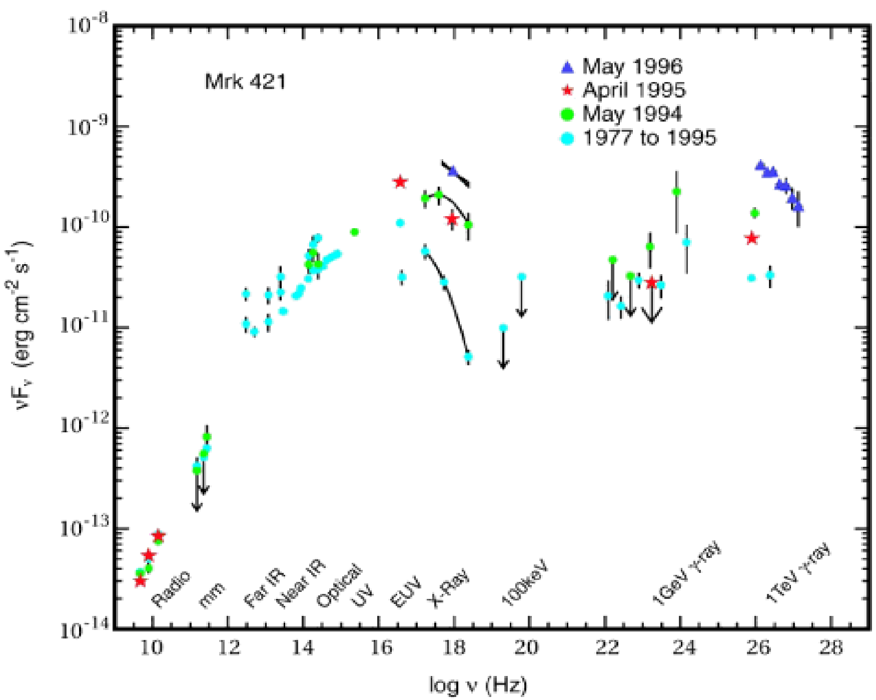


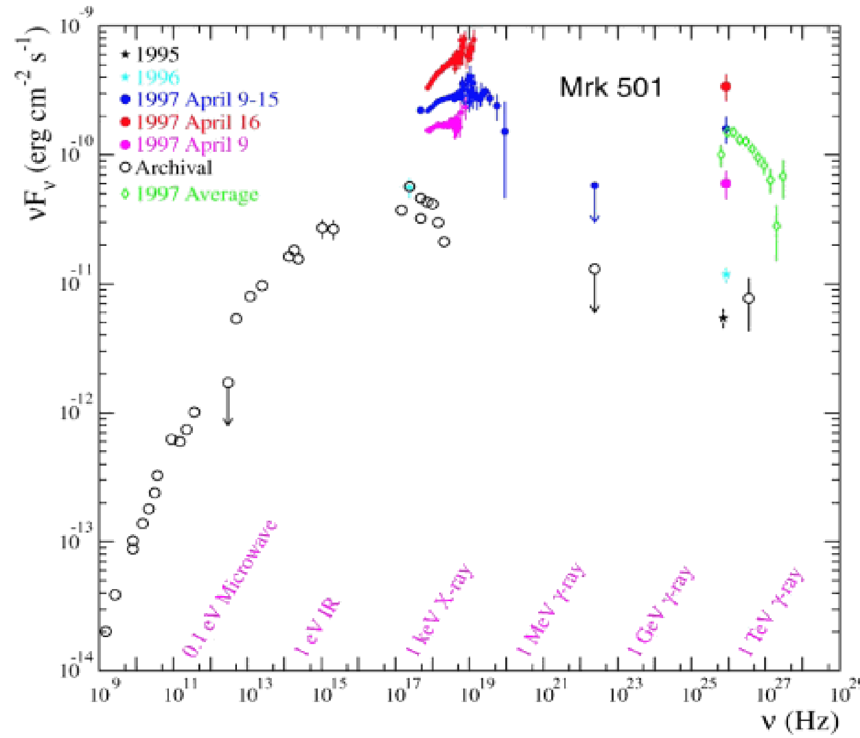

# Continuum energy distribution of radio-quiet AGN:

Magdziarz et al. 1998
NGC 5548 Sy1
HST, IUE, Rosat, Ginga, OSSE

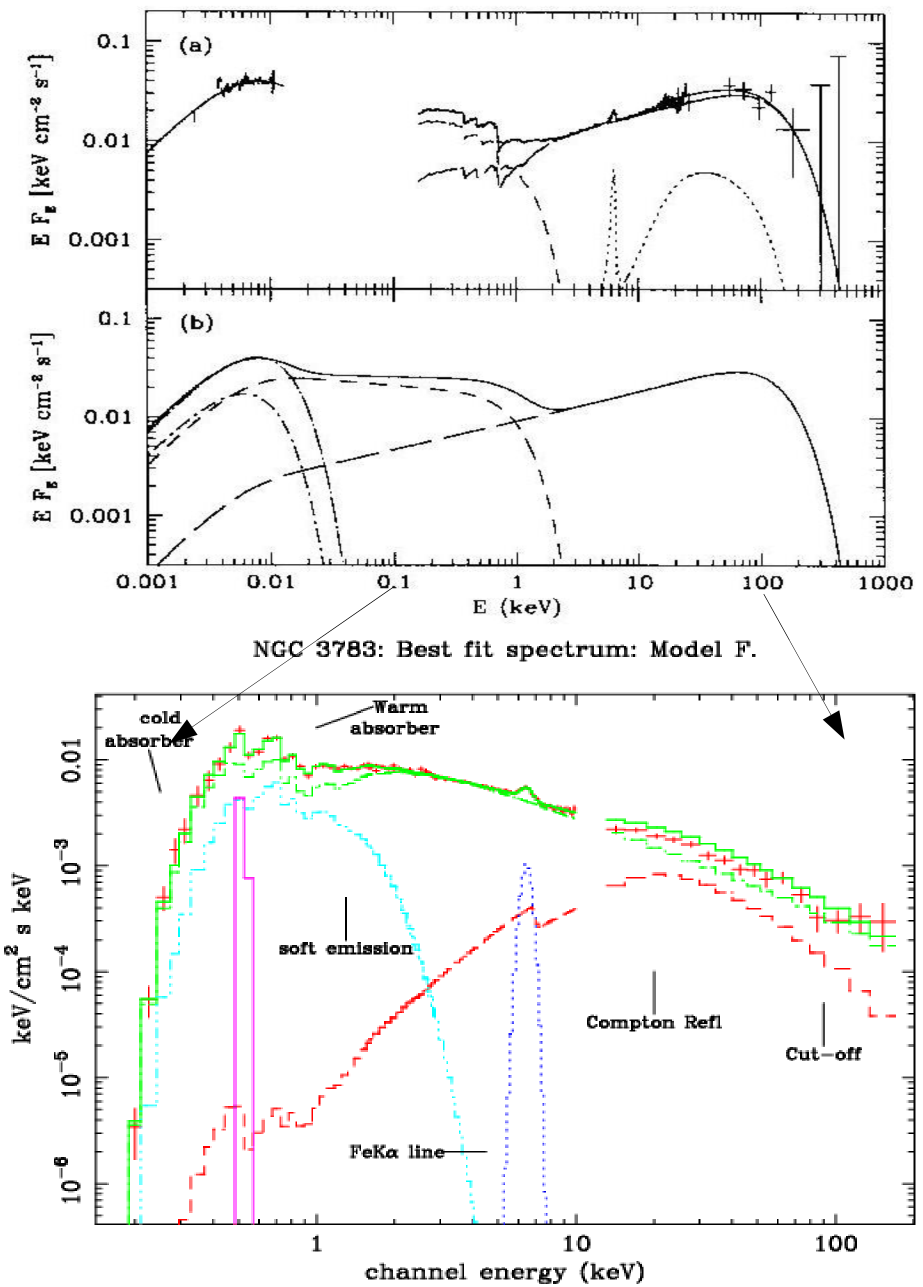


De Rosa et al. 2002
NGC 3783 Sy1

Broad-band spectrum
Beppo-SAX

# Continuum energy distribution of radio-quiet AGN:

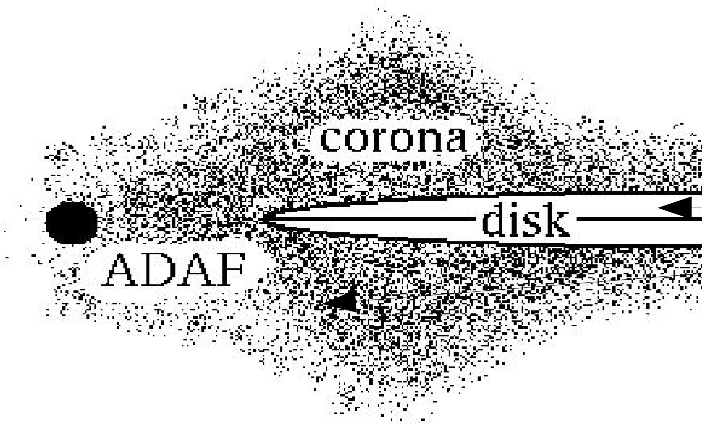


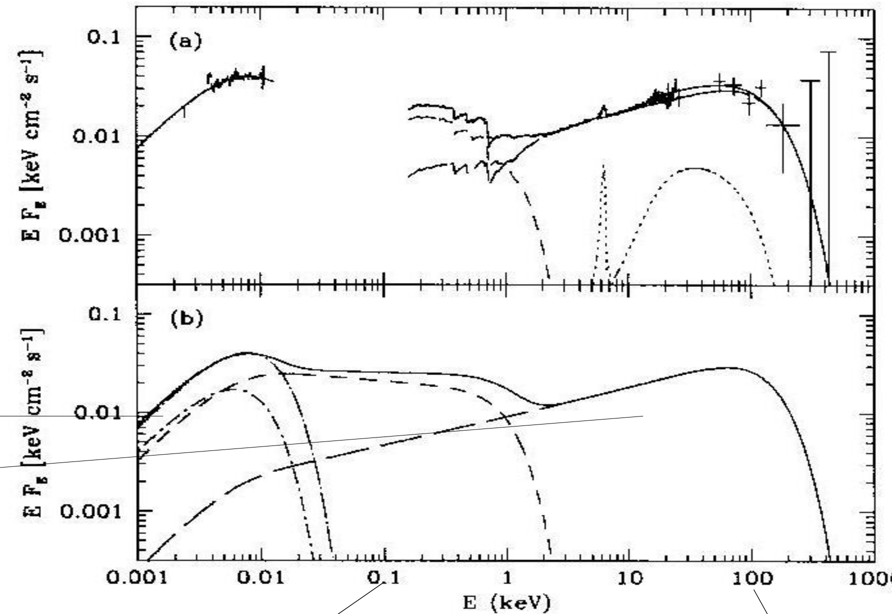


NGC 3783: Best fit spectrum: Model F.

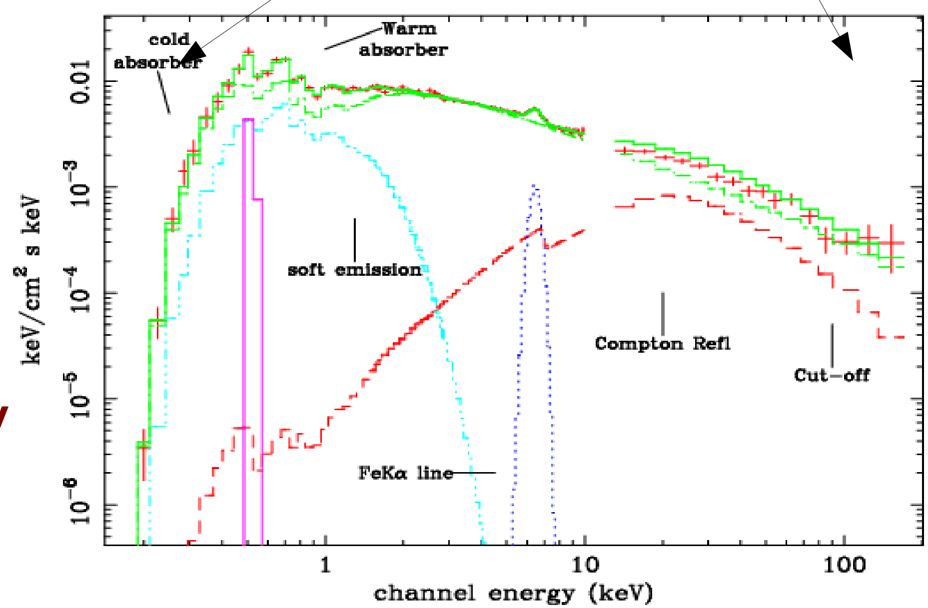


$$T_{disk} \approx 10^{4-5} K \quad ; \quad 0.01 \quad keV$$

Disk is too cold to produce spectra up to a few hundred keV

Hot corona above an accretion disk.

# Continuum energy distribution of radio-quiet  AGN:

## Radiative interaction of hard X-rays with colder disk matter:

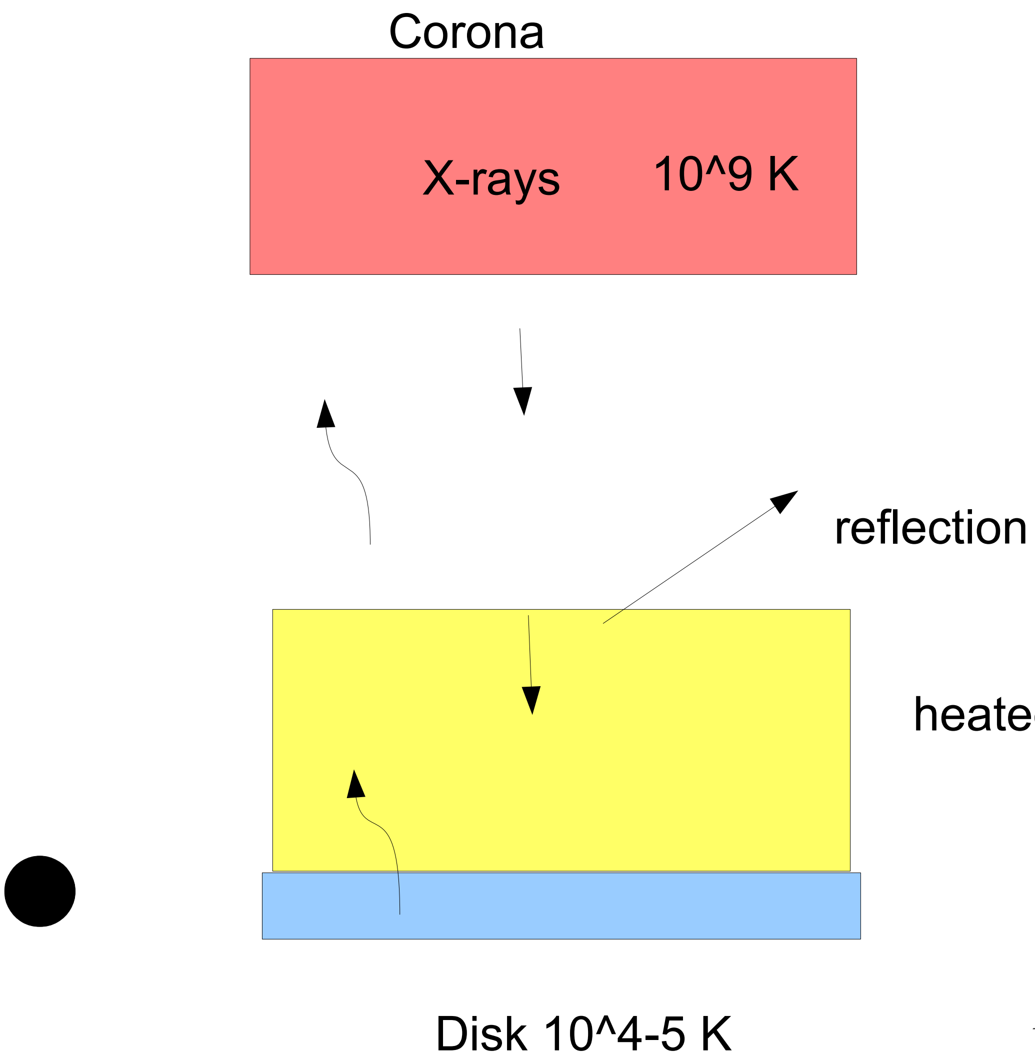


$$F_X = f_{cor} * \frac{3 G M \dot{M}}{8 \pi r^3} * b(r)$$

heated atmosphere up to few * 10^7 K.

$$F_{disk} = (1 - f_{cor}) * \frac{3 G M \dot{M}}{8 \pi r^3} * b(r)$$

# Corona – the source of hard X-rays:

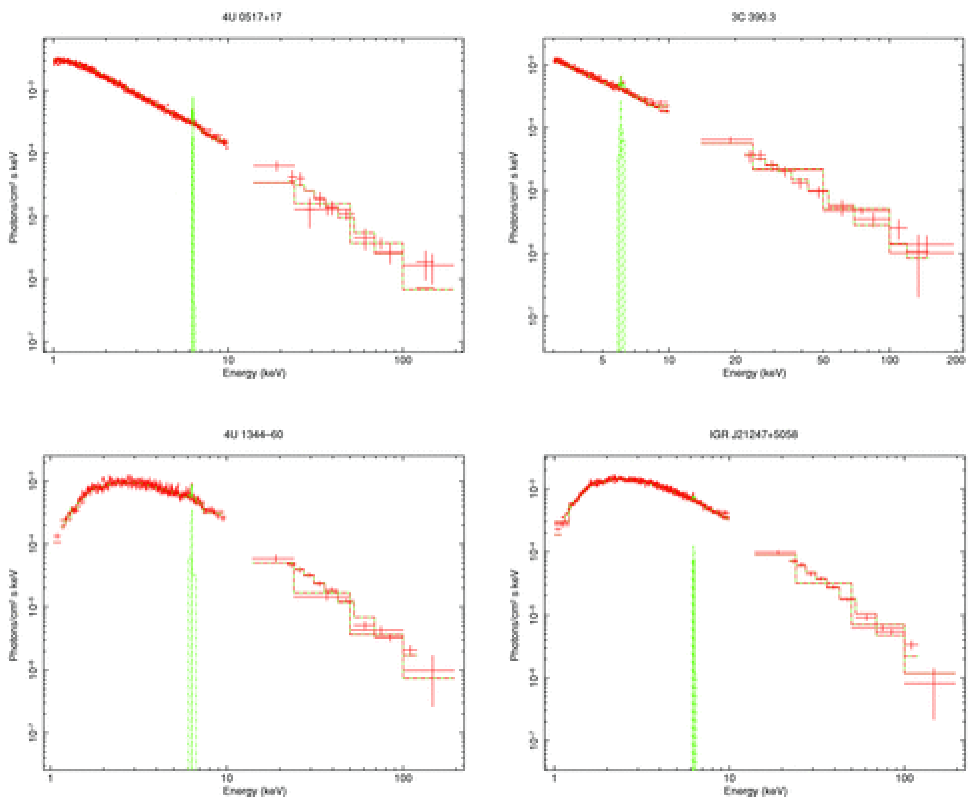


**Molina + 2009, Sy1**

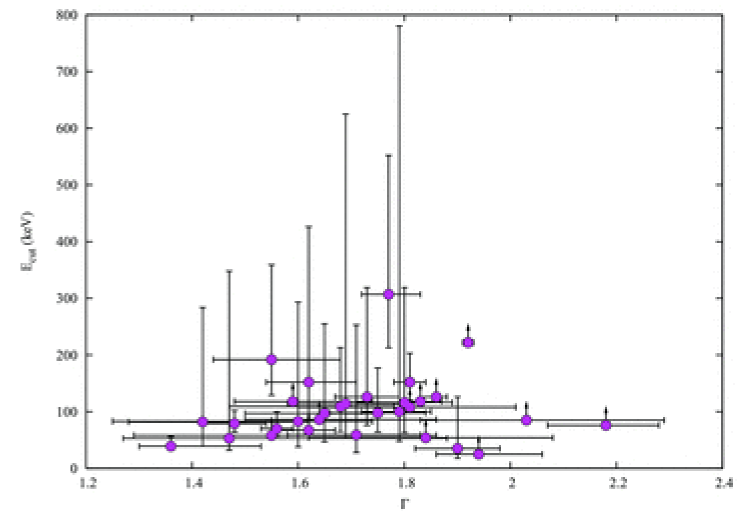

Integral data together with XMM-Newton obs. Hard component is fitted by power-law with photon index Γ, and hard energy cut-off:

$$N = A\,E^{(-\Gamma)}; \qquad F = B\,E^{(-\alpha)}; \qquad \Gamma = 1 + \alpha$$

# Compton up-scattering – cooling of X-ray corona:

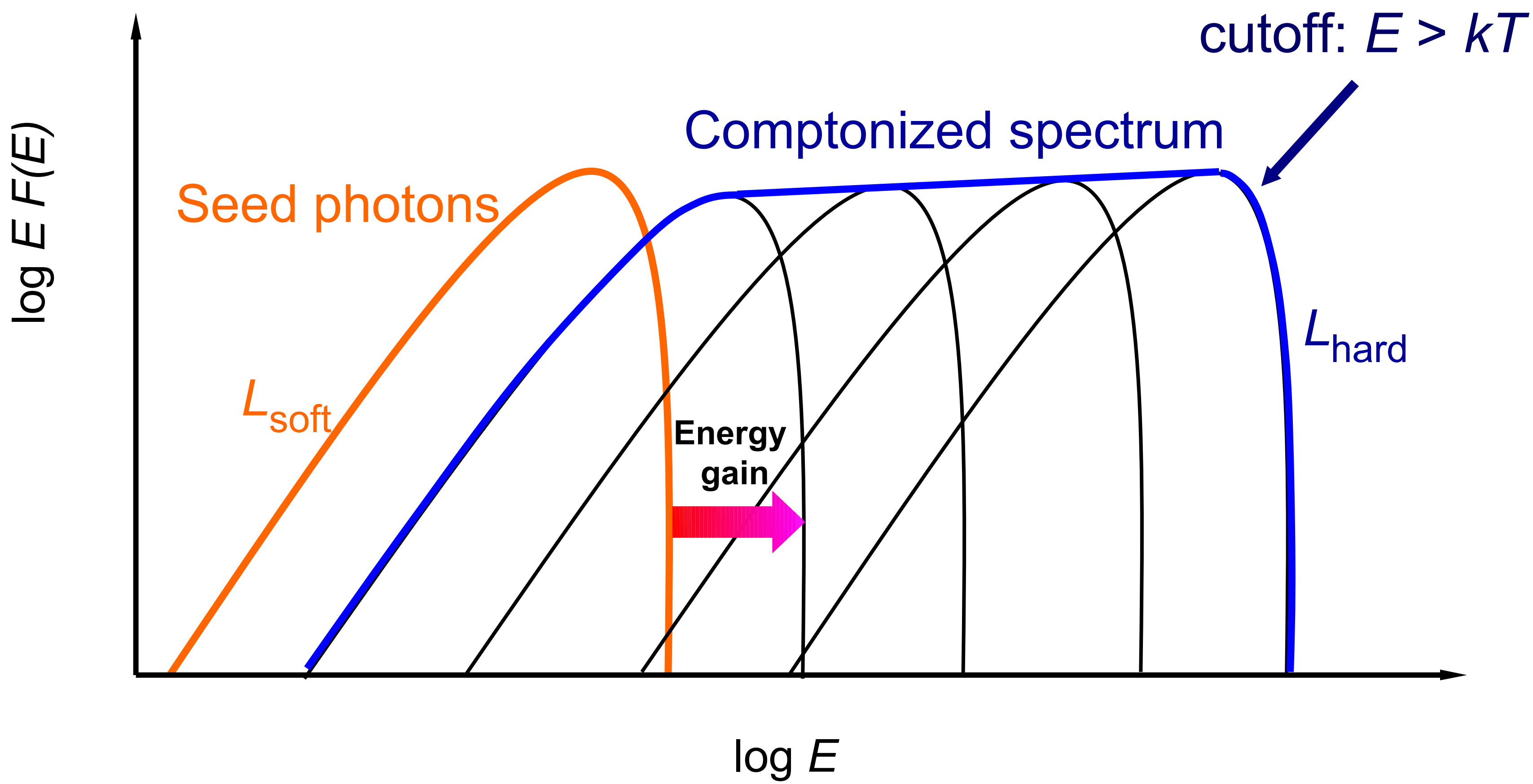


Soft disk photons are taking energy from hot electrons passing the corona – radiative cooling of the corona, power law forms.

# Corona – the source of hard X-rays:

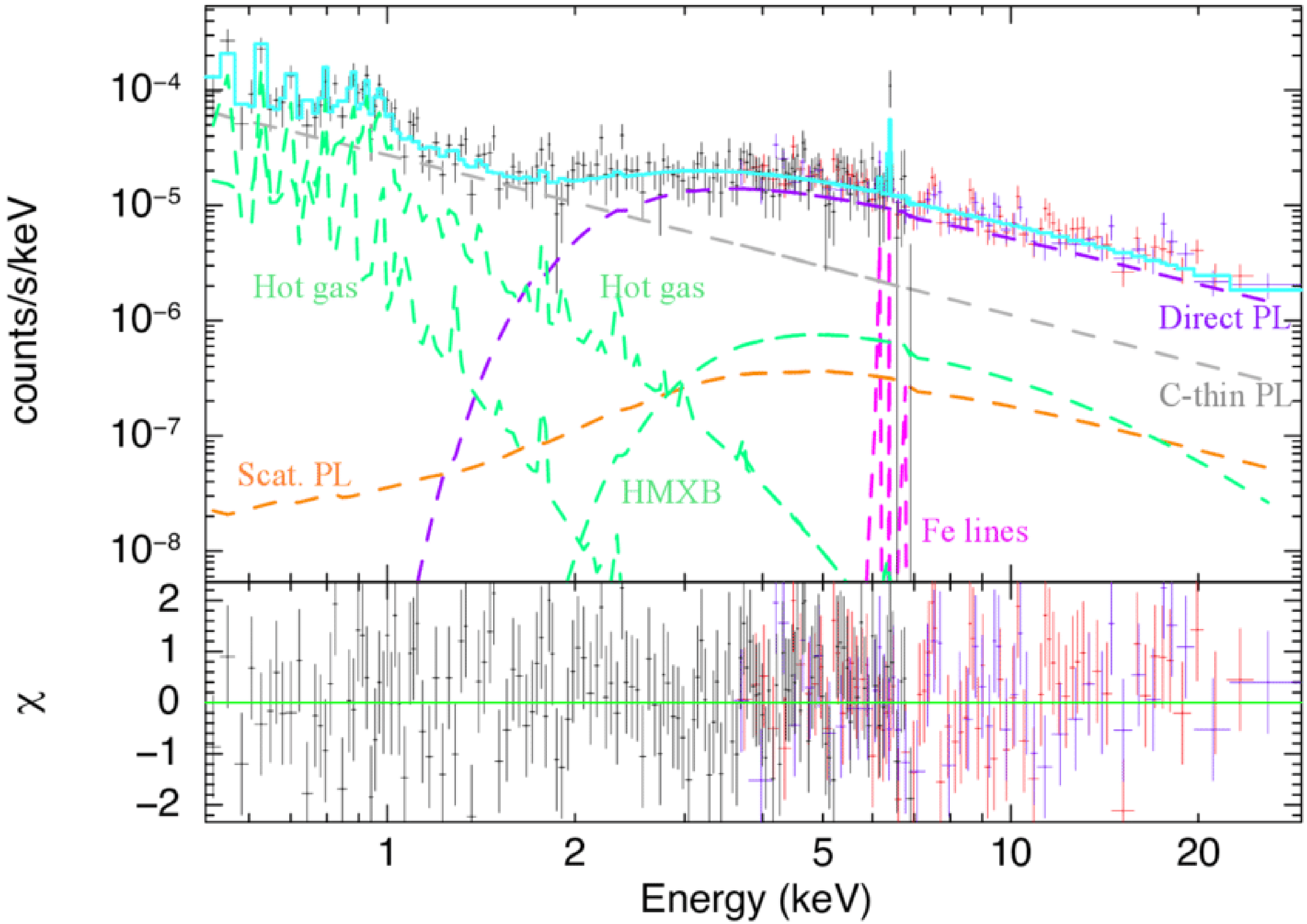


-Unfolded Chandra and NuSTAR spectra shown with the best-fit model components (dashed lines) with the total model in cyan. The starburst MEKAL and HMXB components are in green. The AGN component includes Compton-thin AGN emission unaffected by the absorber (grey), the "zeroth" order direct emission from the AGN transmitted through the absorber (purple), the scattered AGN emission through the absorber (orange), and the Fe K emission lines modeled self-consistently within MYTorus as well as the 6.7 keV Fe line (magenta).

# X-ray source of hard radiation in AGN:

Hot corona above accretion disk, two-phase accretion.
Haartd & Maraschi 1991:
- vertically averaged zone,
- Maxwell distribution of electrons - Te
- energy balance between disk and corona
- Comptonization of soft seed photons from the disk on hot electrons – cooling of the corona.

Free parameters of the model:
- amount of energy generated in the corona:

$$f_{cor} = \frac{F_{cor}}{F_{gen}}; \qquad F_{gen} = \frac{3}{8\pi} \frac{GM\dot{M}}{r^3} \left[ 1 - \left( \frac{r_0}{r} \right)^{1/2} \right]$$

- albedo: ~ 0.1 – 0.2,
- filing factor – how much corona covers the disk: ~ 1.

# X-ray source of hard radiation in AGN:

1. Solving energy balance assuming that disk is affected by half of the coronal emission :
   in the disk: $F_{disk} = (1 - f_{cor}) F_{gen} + (1 - a) \eta F_{cor}; \quad \eta = 0.5$

   in the corona: $F_{cor} = f_{cor} F_{gen} = (A - 1) F_{disk}$

$A = \exp(y) \qquad y = \tau_{es} \frac{4kT_e}{m_e c^2} \left(1 + \frac{4kT_e}{m_e c^2}\right) \qquad for\, \tau < 1 \Rightarrow \quad \alpha = \frac{-\ln \tau}{\ln A}$

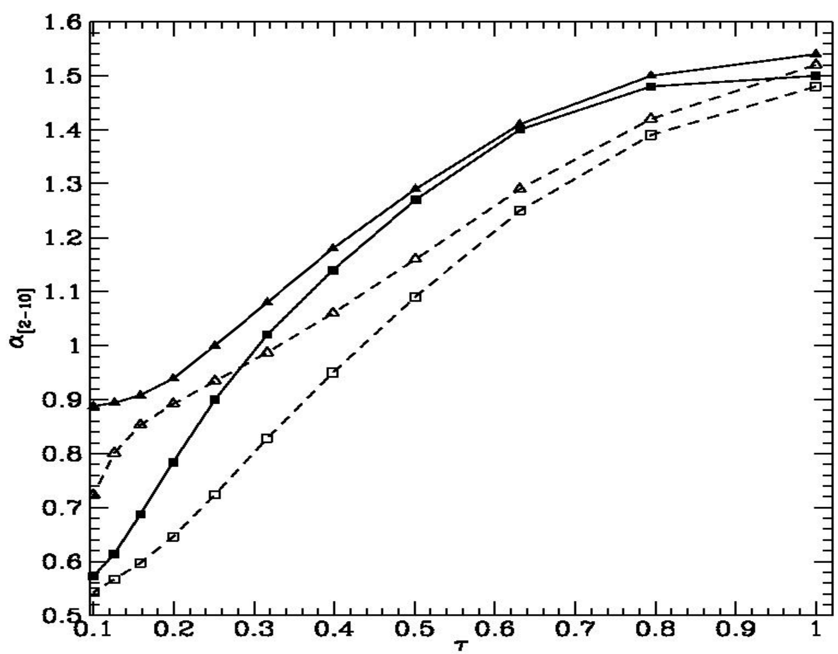


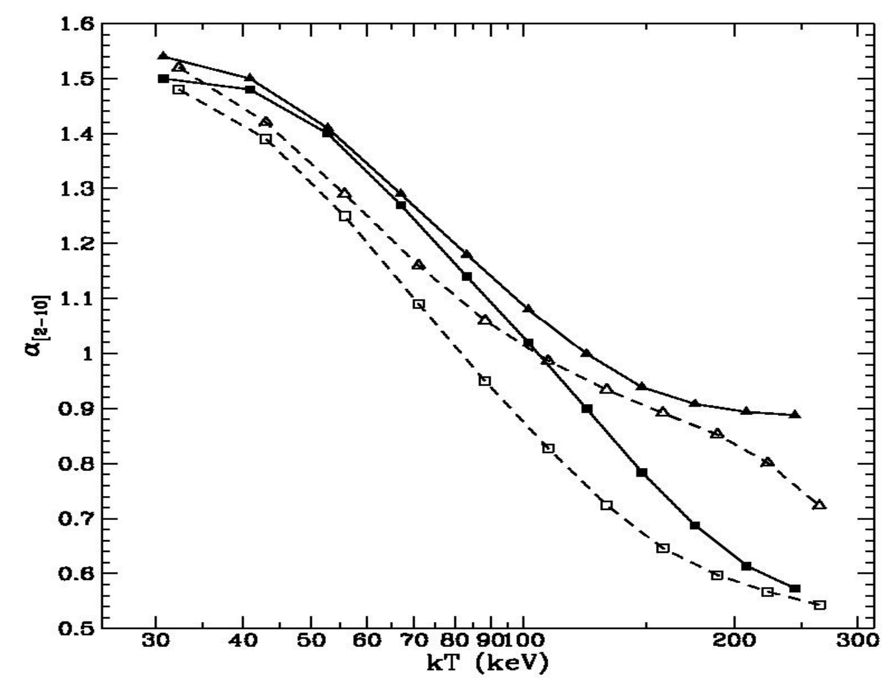

# X-ray source of hard radiation in AGN:

2. Compton cooling of corona by seed photons from the disk $F_{disk}$ of the black body distribution. Monte Carlo simulations compute probability of such scattering keeping constant amount of photons.

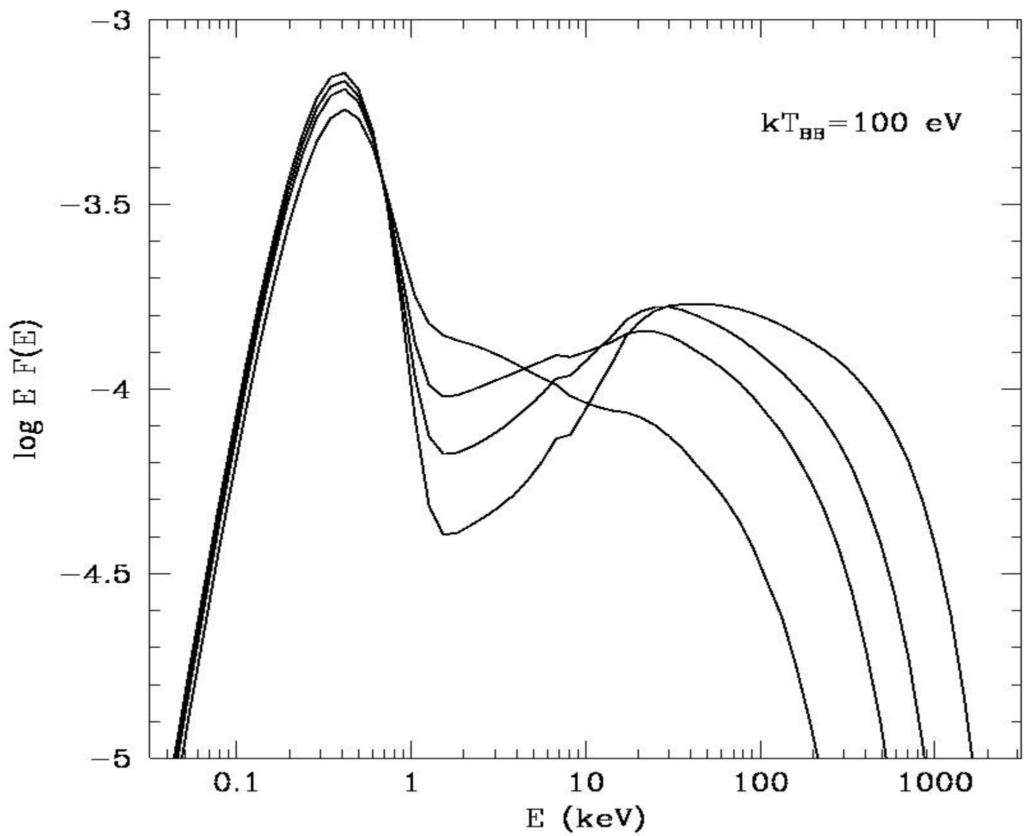


$$k\,T_{BB} = 100\,eV\,; \qquad \tau = 0.65\ldots0.1\,; \qquad kT/m\,c^2 = 0.11\ldots0.5$$

# X-ray source of hard radiation in AGN:

There is an additional mechanism to heat up the corona – for instance magnetic field reconnection.

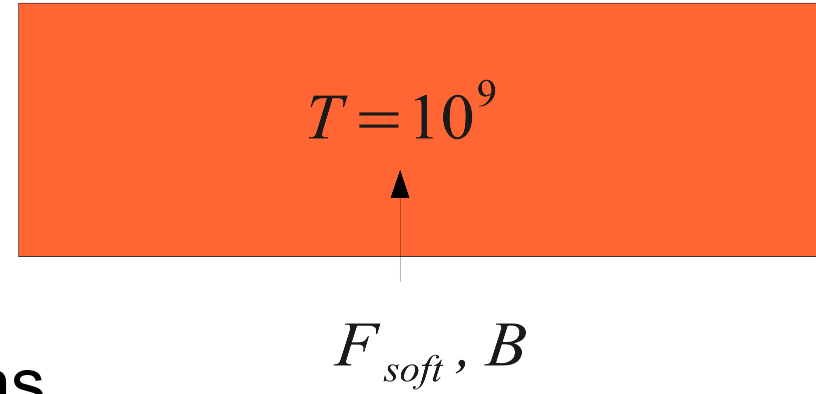


There has to be intrinsic seed photons radiation field.

$$f_{cor} \Rightarrow \tau, \alpha$$

Corona covers only part of the disk or bulk motion.

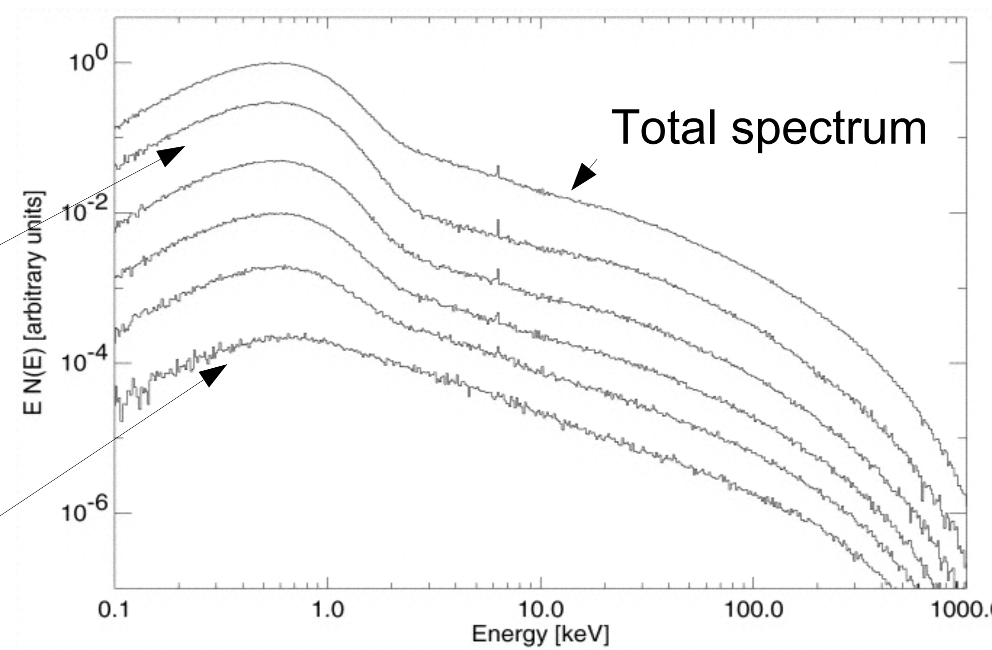


$$\mu = \cos(\theta)$$

$$\mu = 0.9, 0.7, 0.5, 0.3, oraz\, 0.1 ; \qquad k\langle T_c \rangle = 118\, keV ; \qquad kT_{BB} = 200\, eV$$

# X-ray source of hard radiation in AGN:

## GRMHD with RT

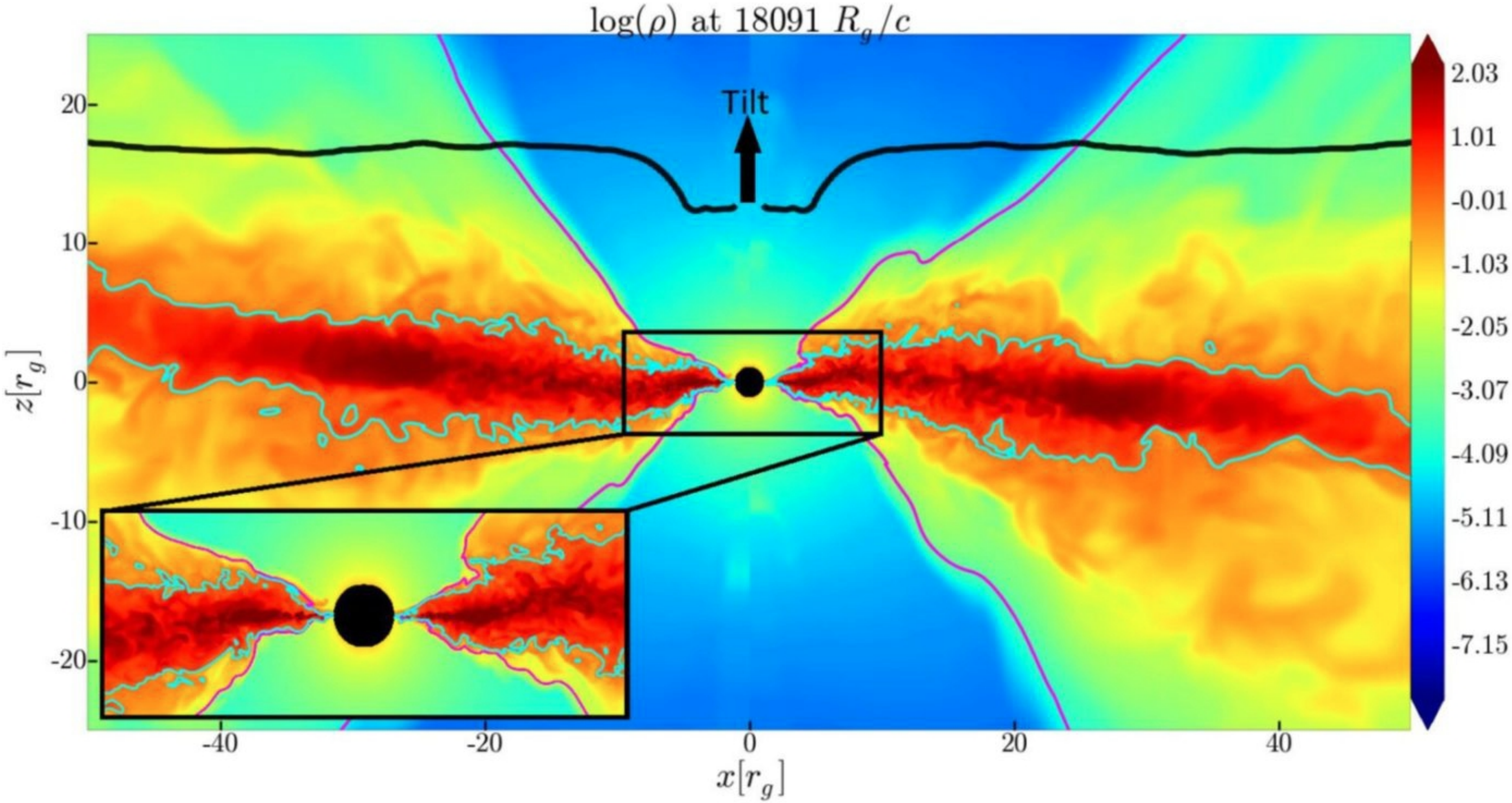


This image shows how the inner region of the accretion disk (red) aligns with the equatorial plane of the black hole. The outer disk is tilted away. The inner disk (where the black curve dips) is horizontal, signaling the long-sought Bardeen-Petterson alignment. Credit: Sasha Tchekhovskoy/Northwestern University; Matthew Liska/University of Amsterdam

# First observation of X-ray reflection:

Pounds+ 1990 Nature

Compton scattering
hard energetic photons
from colder matter.
An atmosphere is heated
by highly energetic photons
up to inverse Compton
temperature.

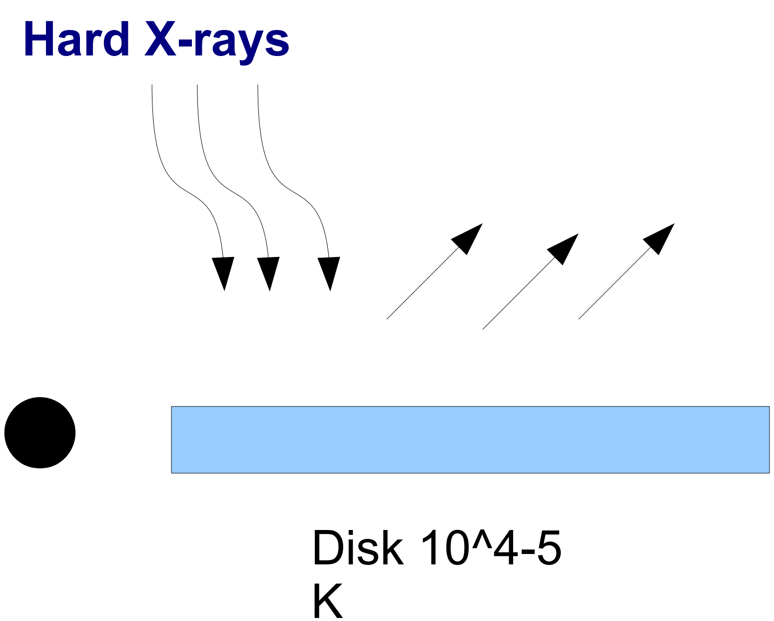


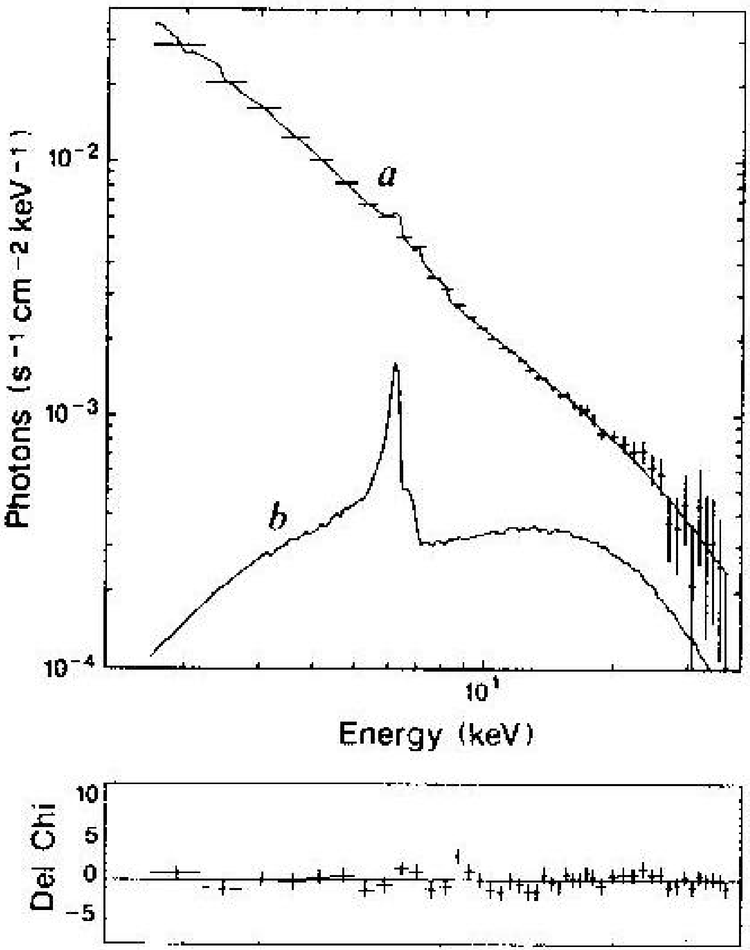


FIG. 2 a, Power law plus reflection and warm absorber model (as detailed in the text), together with residuals. b, Reflection component only.

NATURE · VOL 344 · 8 MARCH 1990

# Modeling of Compton reflection:

- Peak about 20 keV
- Fluorescent Fe line at 6.4 or 6.7 keV
- Bound – free absorption on the low energy cut-off
- Klein-Nishina and Compton down-scattering at hight energy cut-off.

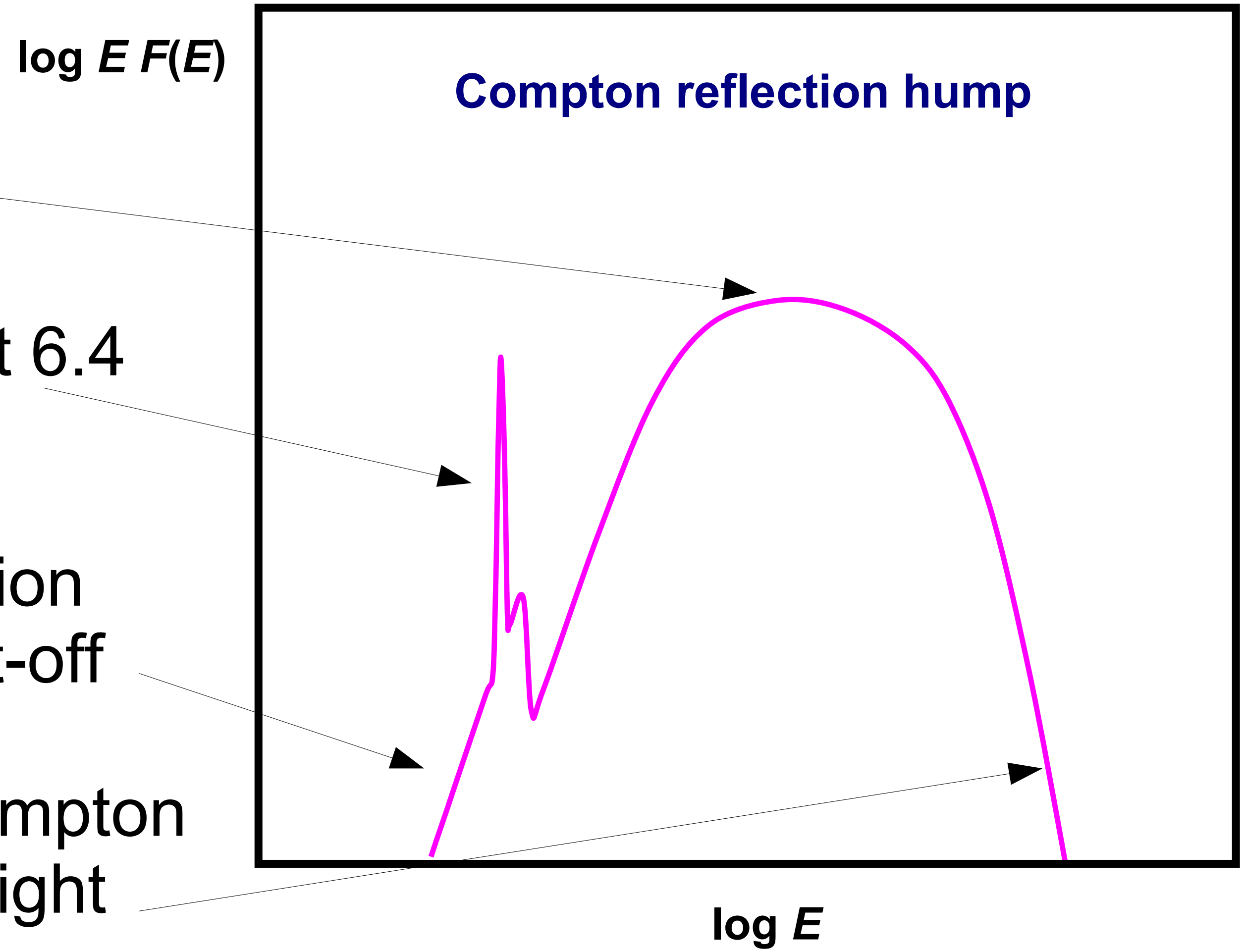


For AGN we observe Compton reflection hump as a separate component.

# The transition layer between an accretion disk and corona:

Corona - power-law, or
broken power-law emission.

Heating via photoionization,
Compton reflection.

Black Body from optically
thick accretion disk.

Compton scatering together with
absorption, the later diminishes photons.

Base of an atmosphere.

We know how to compute
transfer of radiation taking
into account illumination,
which predicts strength of lines
from an accretion disk.

The transition layer between an accretion disk and corona:

Compton heated atmosphere of an accretion disk:

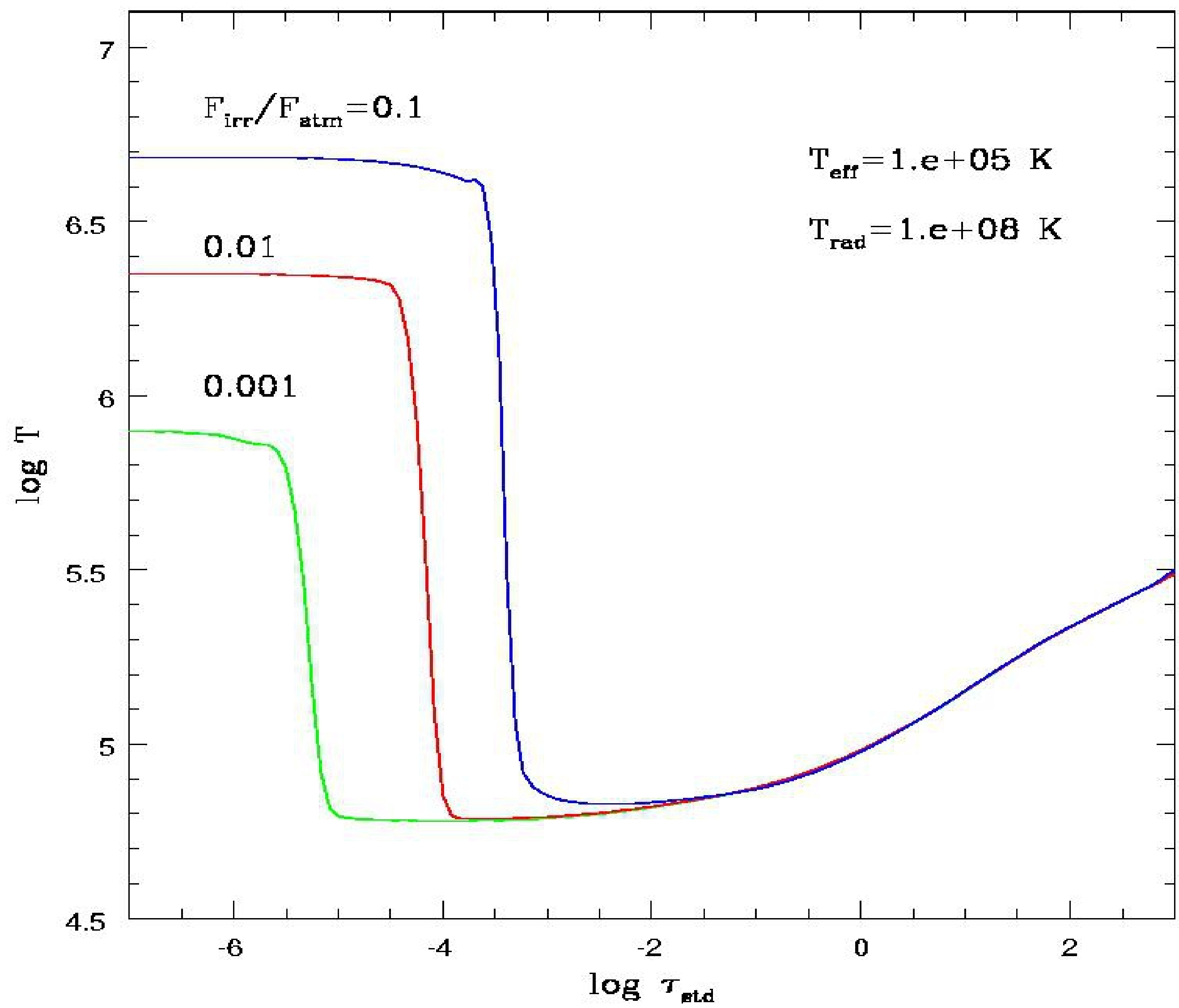

# The transition layer between an accretion disk and corona:

Redistribution of hard X-rays in soft X-ray energy band.

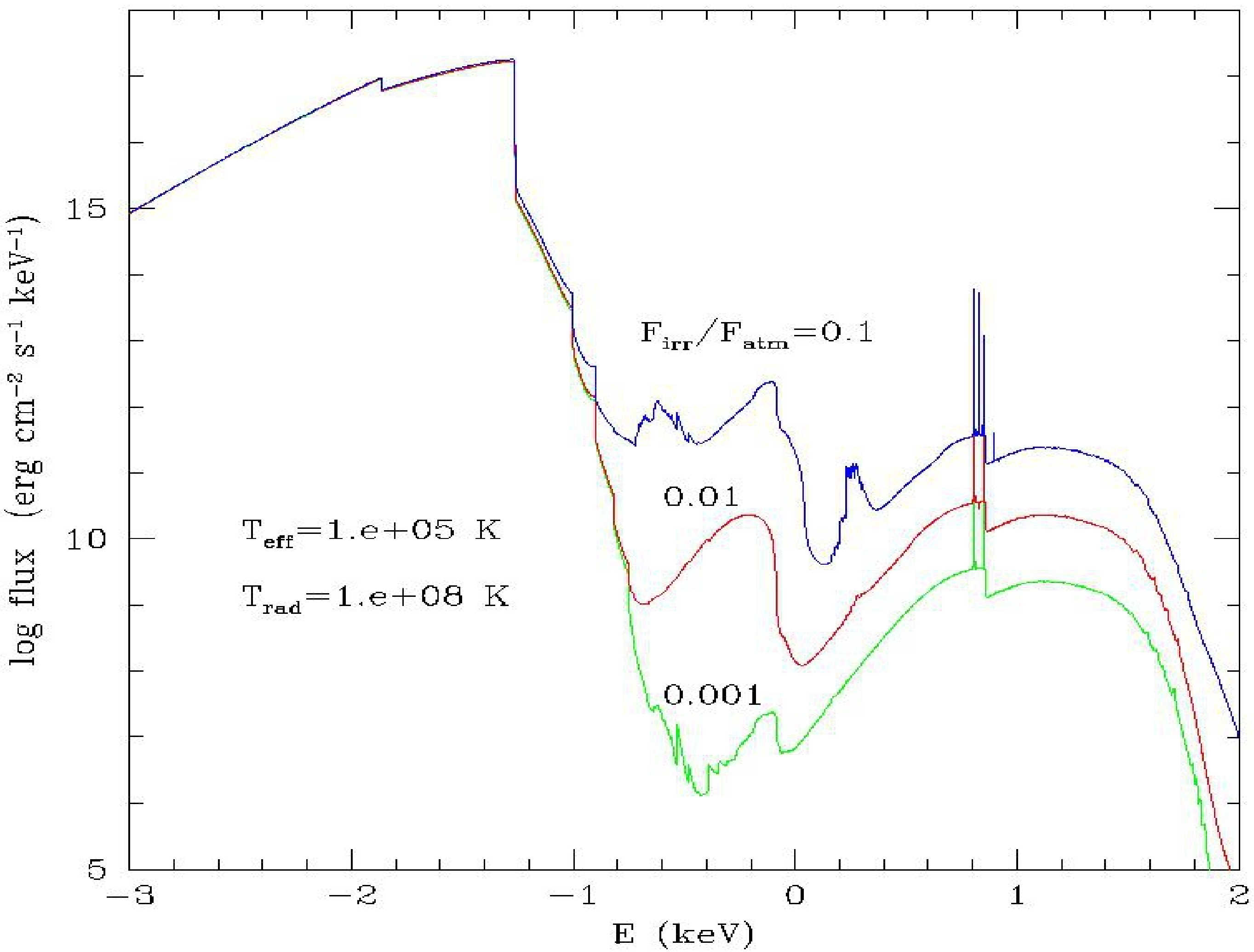

# The transition layer between an accretion disk and corona:

Nayakshin et al. 2000

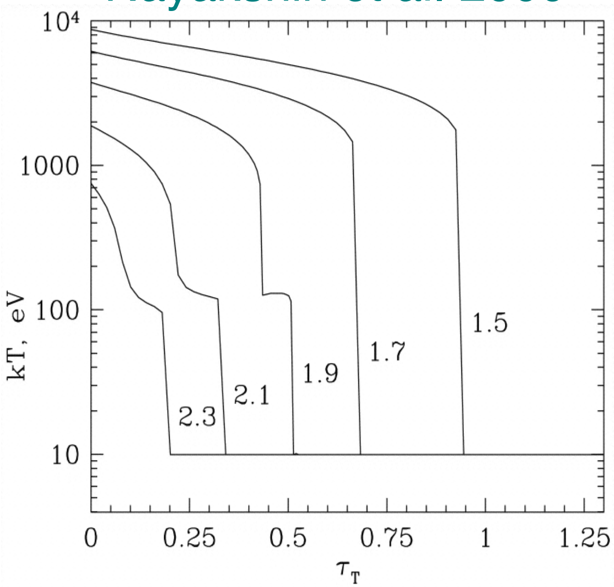


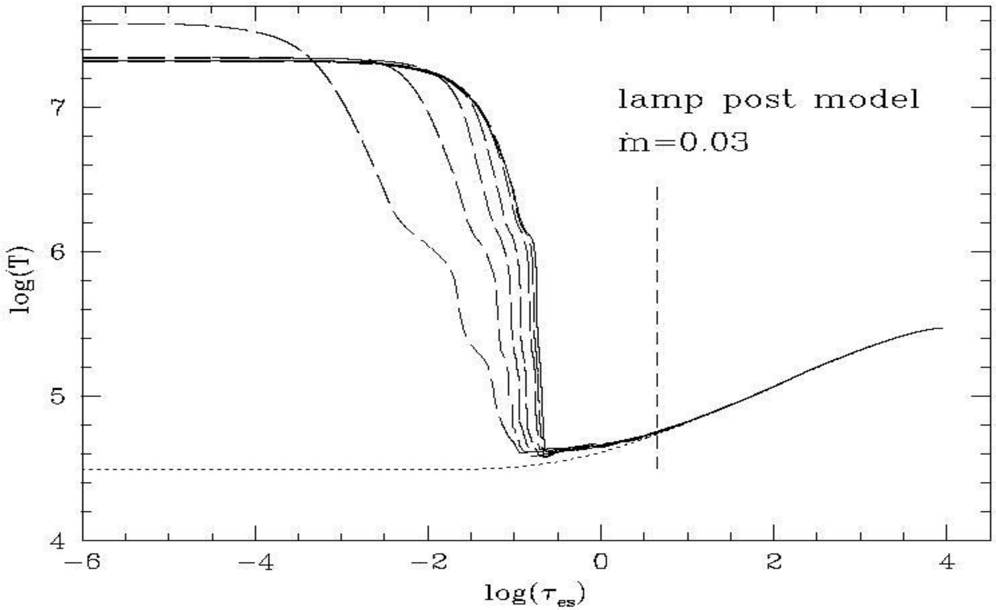


Ballantyne et al. 2001

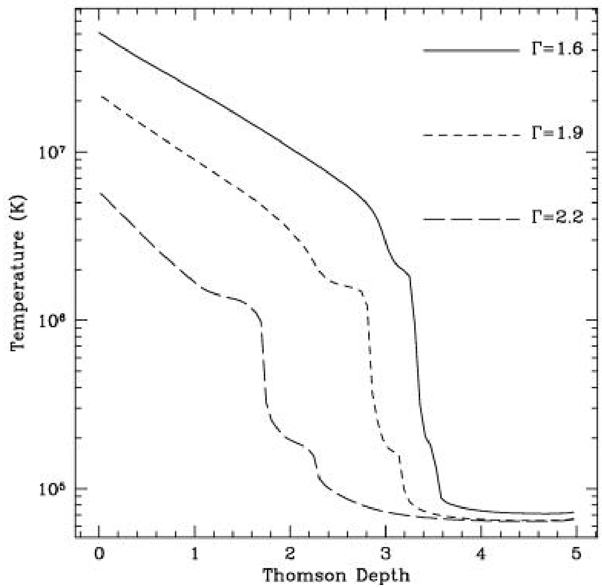


**TITAN** , Różańska et al 2002

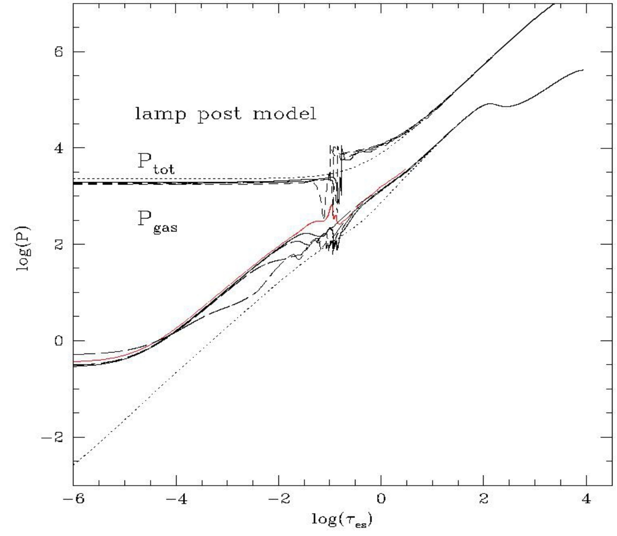

# The transition layer between an accretion disk and corona:

Comparing of work by: Nayakshin, Ballantyne and **TITAN** :

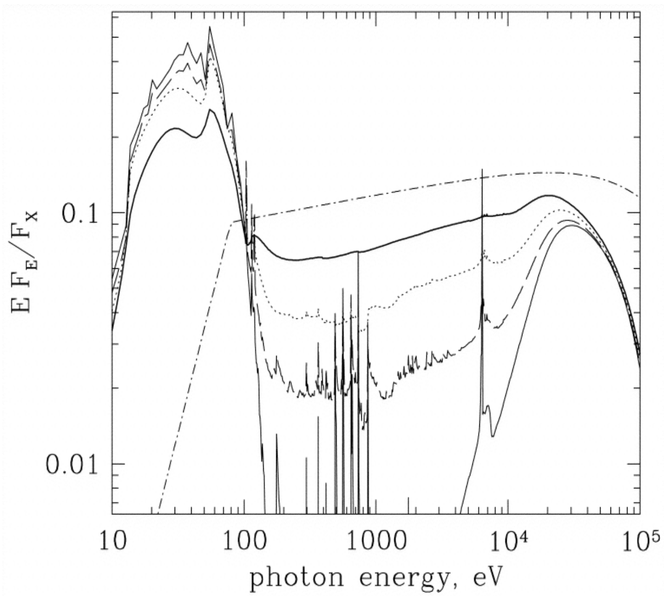


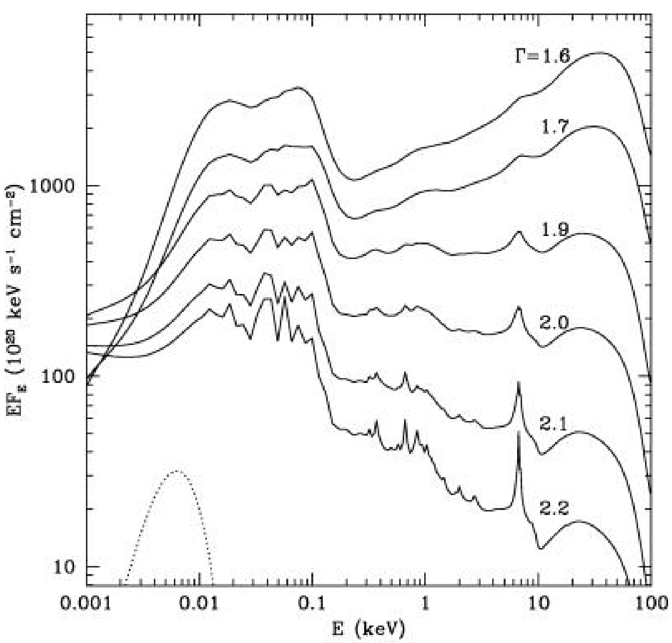


non-LTE,
external illumination
900 atomic
bound-bound
transitions.

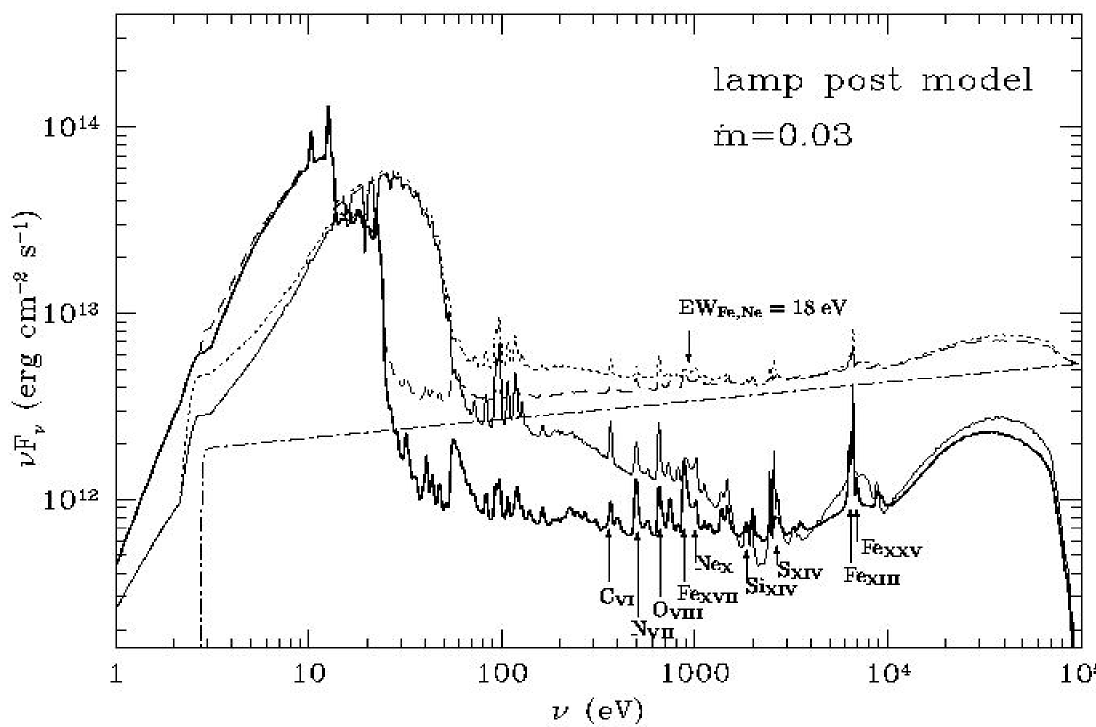

# Fluorescent iron Kα line from AGN:

Tanaka + 1995, NATURE , ASCA

MCG-6-30-15

Fabian + 2002, MNRAS Letter XMM-Newton

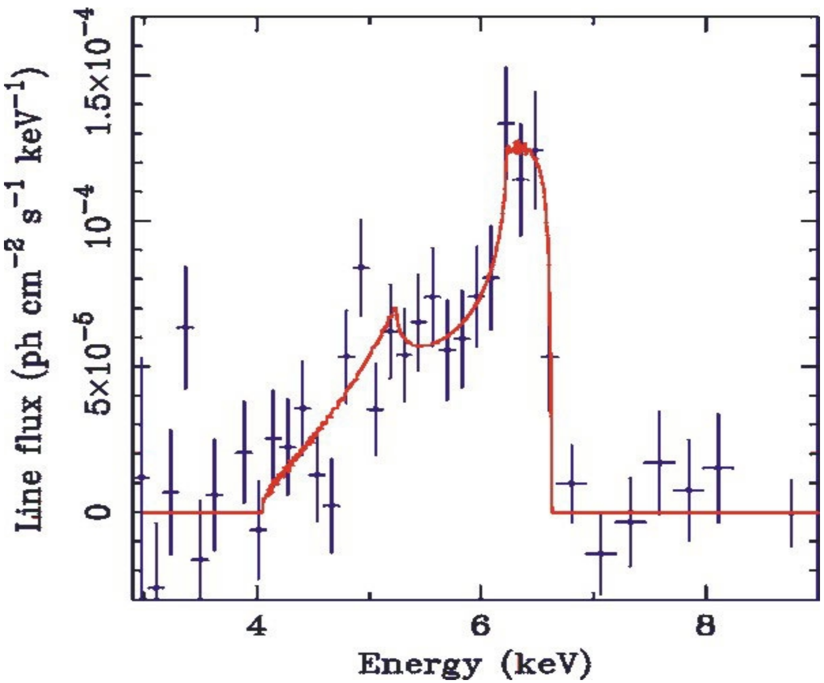


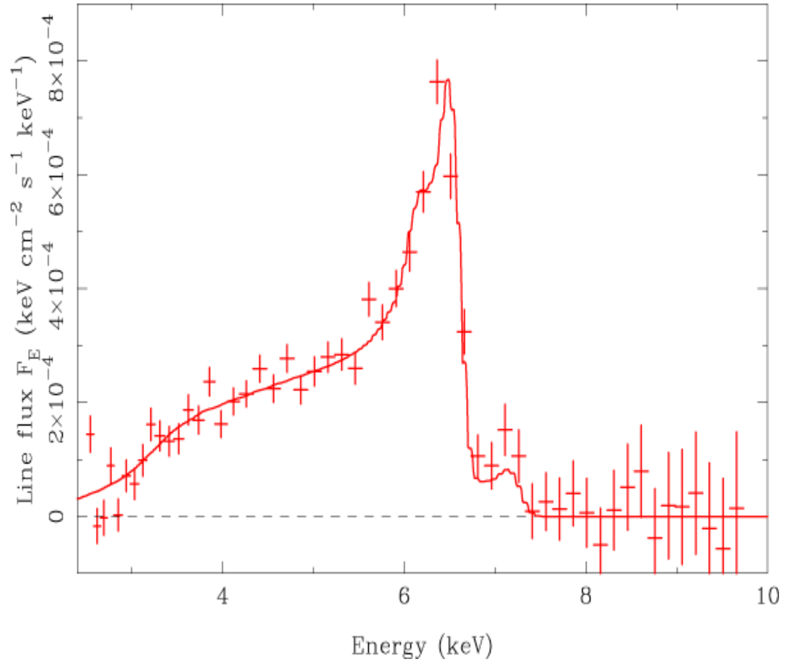


Since energy of line centroid is 6.4 keV, matter is weakly ionized almost neutral – agrees with accretion disk temperature in AGN.

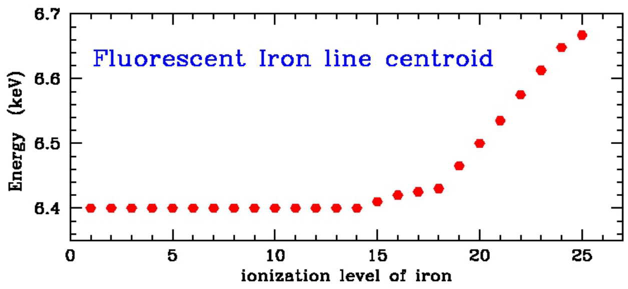

<u>Fluorescent iron Kα line from AGN:</u>

Assuming that the line is created as a reflection from an accretion disk we have to take into account spacial and general relativistic corrections: Fabian + 1989

1) Doppler shift due to the didk rotation,

2) gravitational redshift ,

3) beaming of the radiation emitting toward an observer,

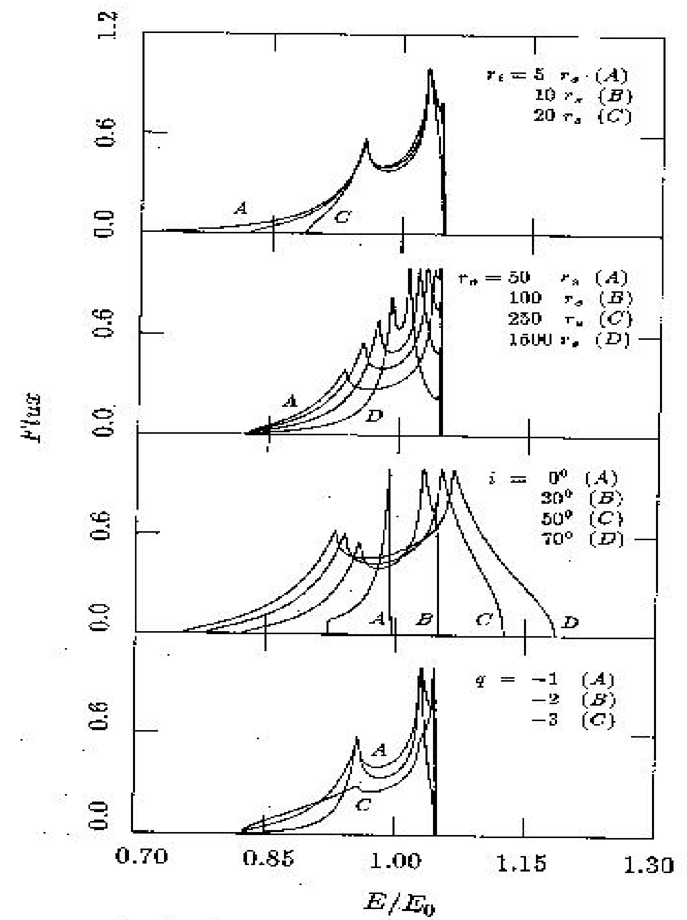


This is usually taken into account in “ray tracing” codes.

# Fluorescent iron Kα line from AGN:

This is usually taken into account in "ray tracing" codes

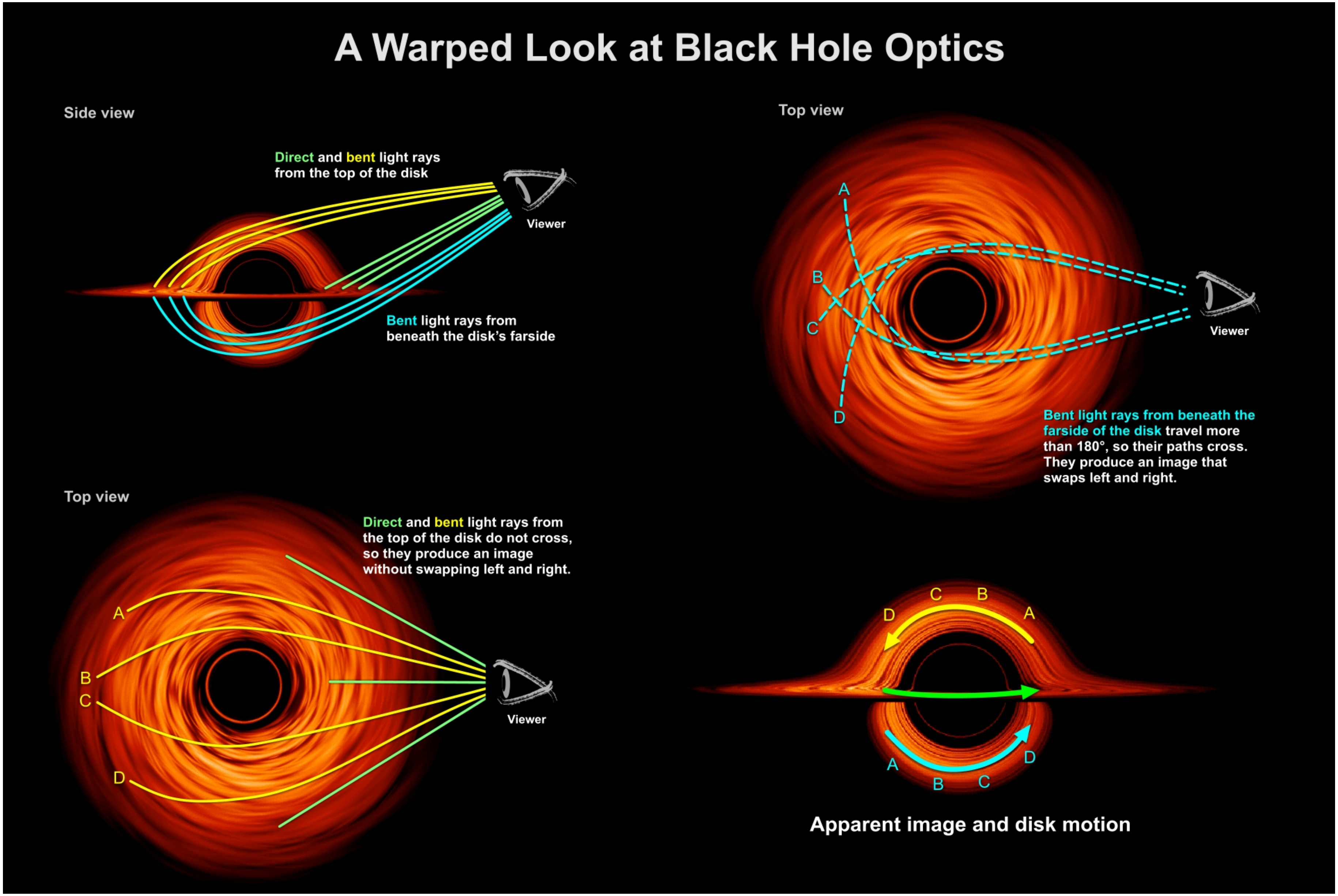

# Fluorescent iron Kα line from AGN:

Black hole spin determination

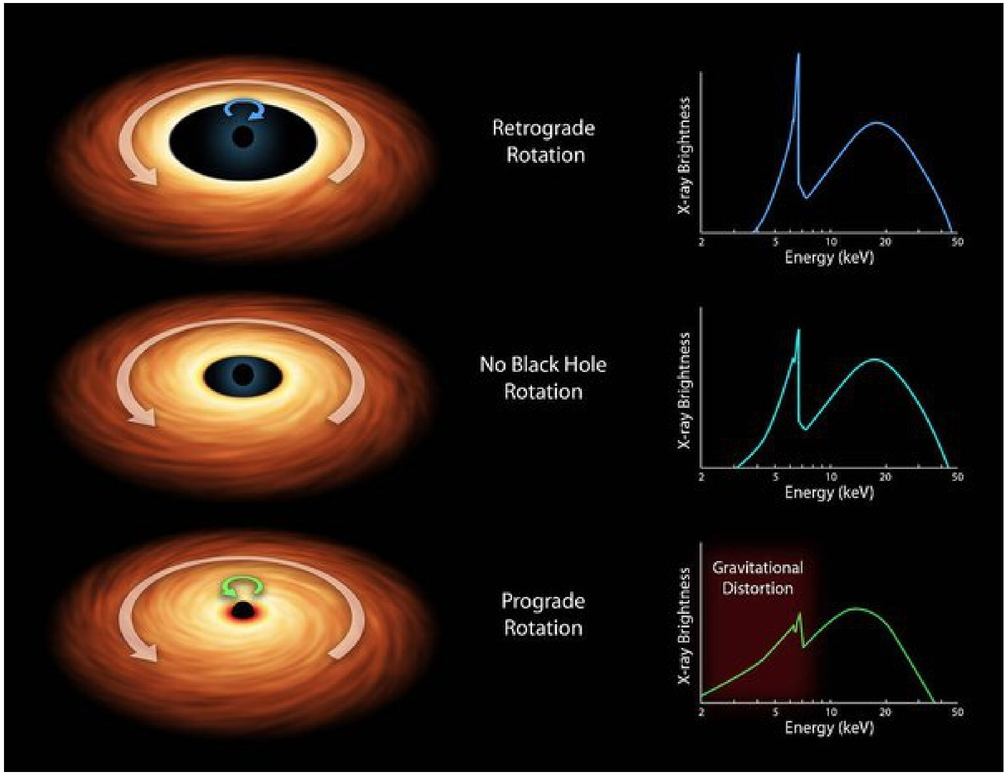


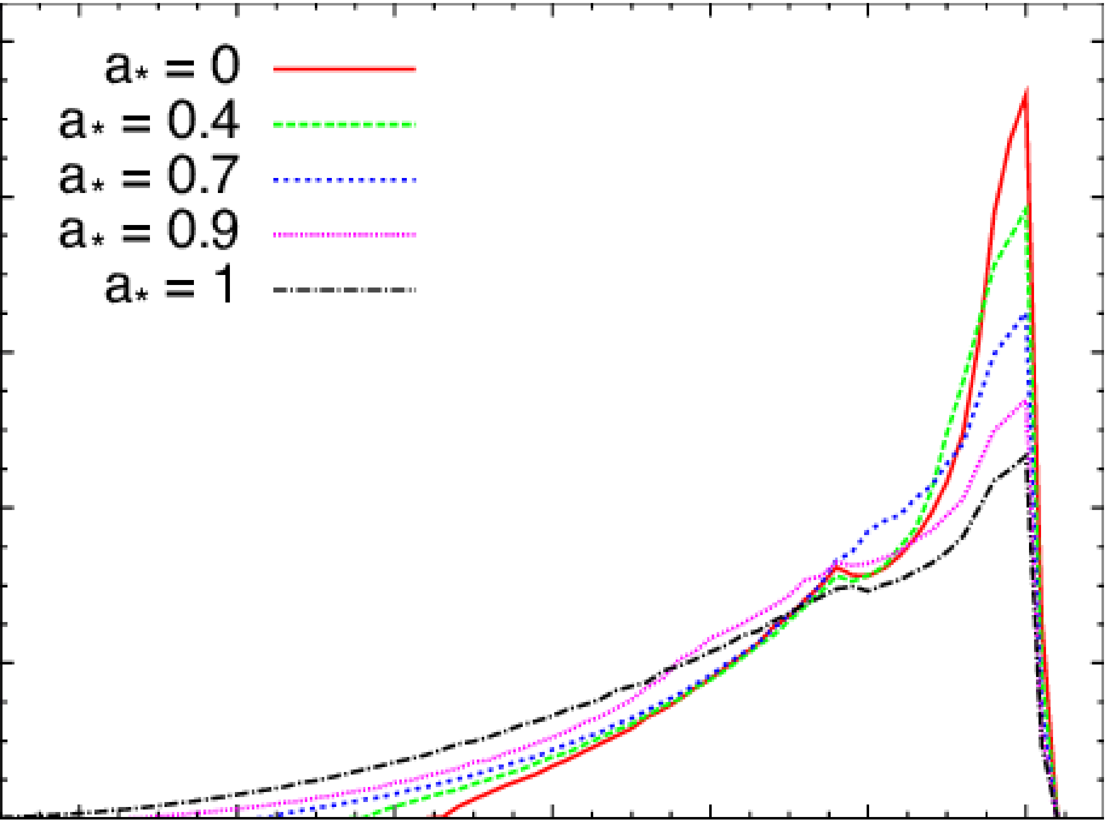

# Fluorescent iron Kα line from AGN:

Chandra Yaqoob + 2004

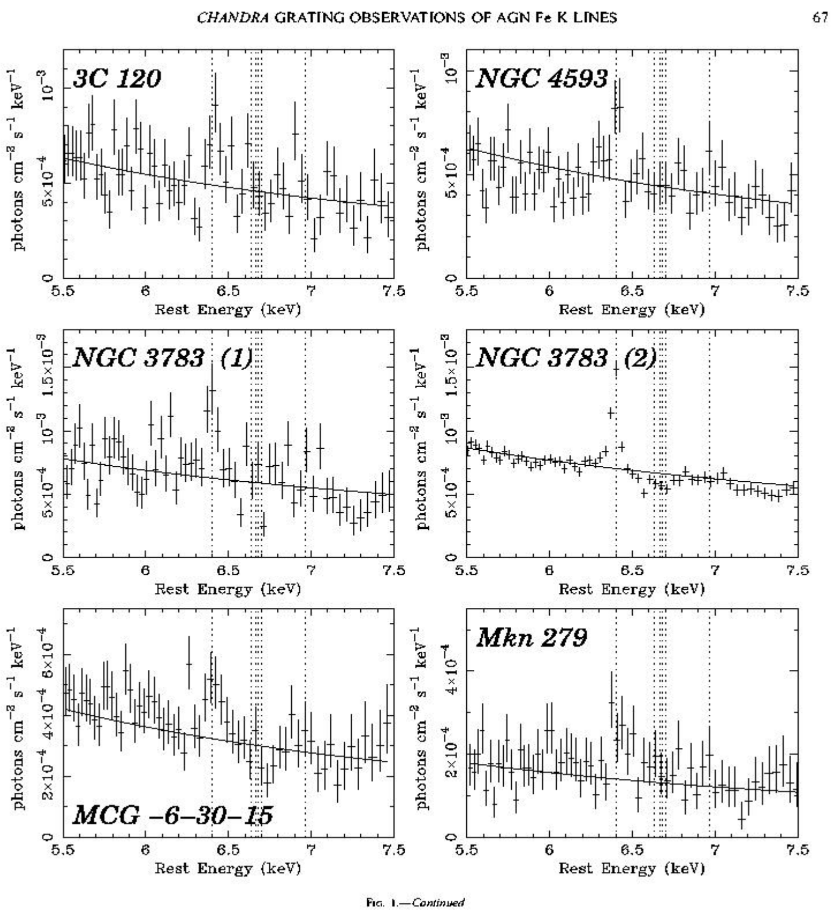


Mrk 205
XMM, Reeves + 2001

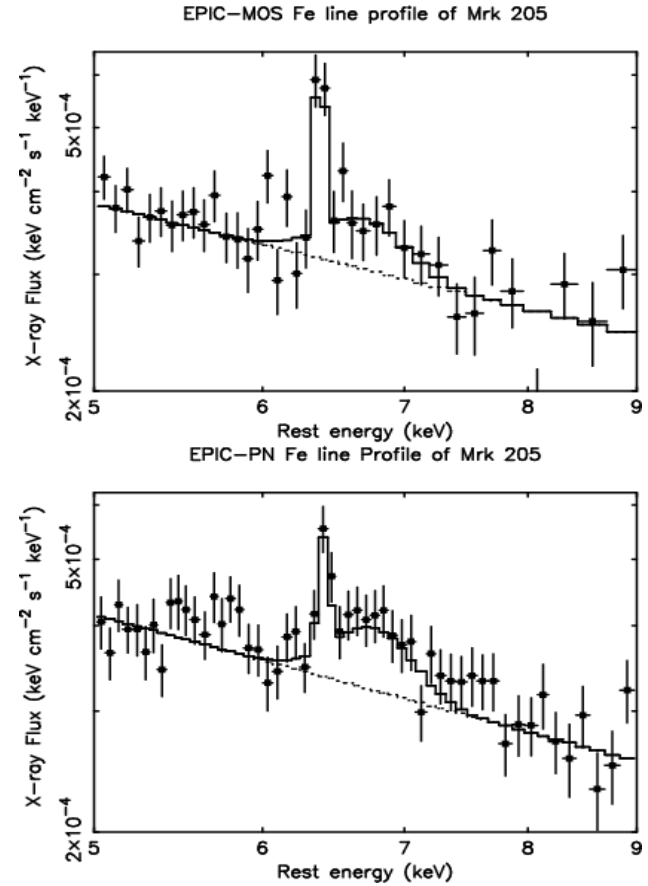


In some objects line is very weak and better satellites are needed to solve the problem.

# Fluorescent iron Kα line from AGN:

Turner + 2011 (conference presentation)
old concept of Collin+ 2000. Compton scattering from many clouds creatures Compton Shoulder:

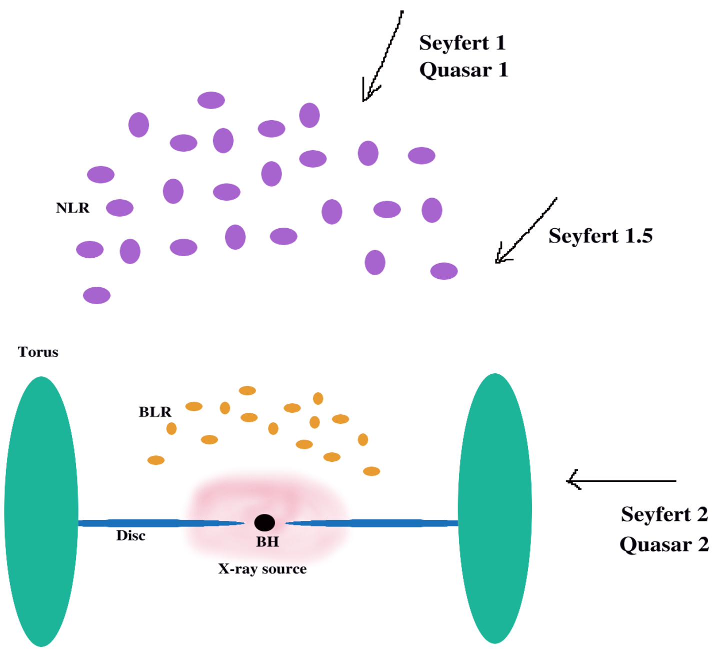


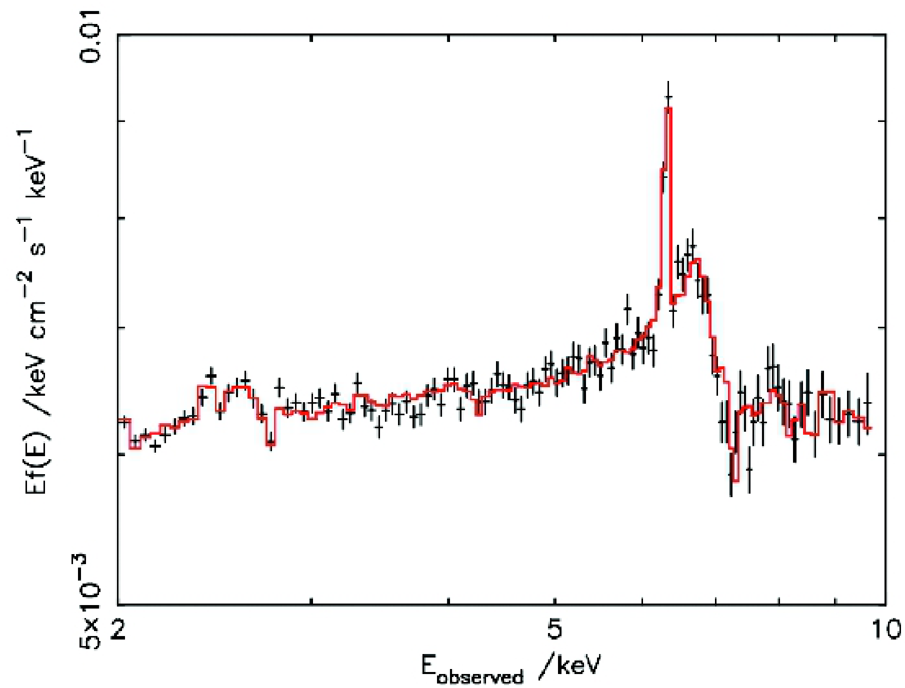


**Figure 13.** The best-fitting wind model fit to the mean 2–10 keV spectrum of Mrk 766, plotted in units of Ef(E), showing model and 'unfolded' data.

# Warm absorber in AGN:

**MR 2251-178** (z=0.06398) **Halpern 1984, EINSTEIN HRI**

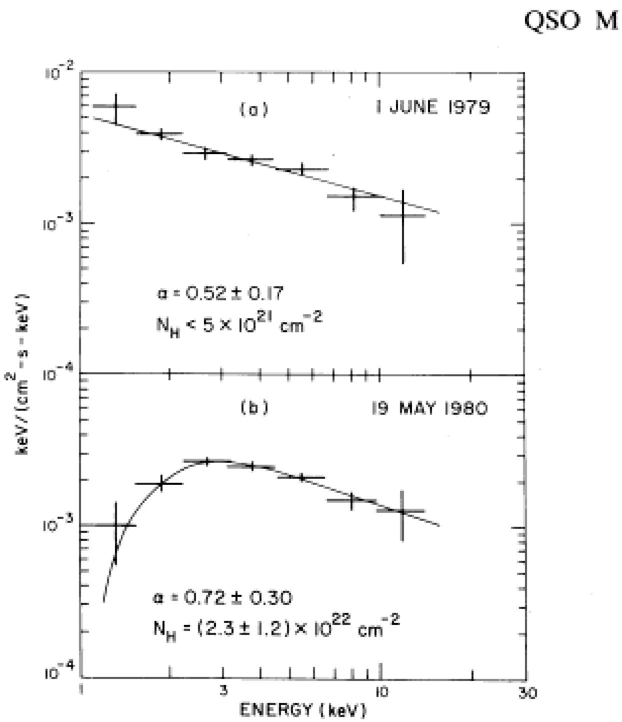


FIG. 1.—*Einstein* MPC spectra for MR 2251−178: (*a*) 1979 June 1; (*b*) 980 May 19.

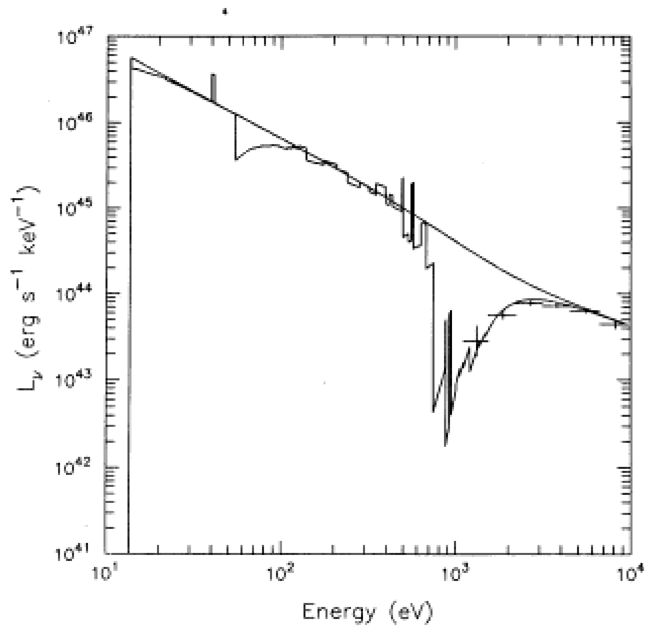


FIG. 3.—Incident and emergent spectra for a shell of column density $6.2 \times 10^{22}$ and log $U = 0$, normalized to the MPC spectrum of 1980 May. Prominent absorption edges are due to He II, O VII, and O VIII at 54.4, 739., and 870. eV respectively.

Warm absorber – partially ionized gas on the way toward obsrever,

**O VII 0.739 keV, O VIII 0.870 keV**

# Warm absorber in AGN:

Nandra + 1992, NATURE , ROSAT
MCG-6-30-15 Sy1.2 (z=0.00775), edge O VIII 0.825±0.017 keV

1993 – 2000 ASCA, BeppoSAX

1999 – up to now, Gratings on the board of CHANDRA, XMM

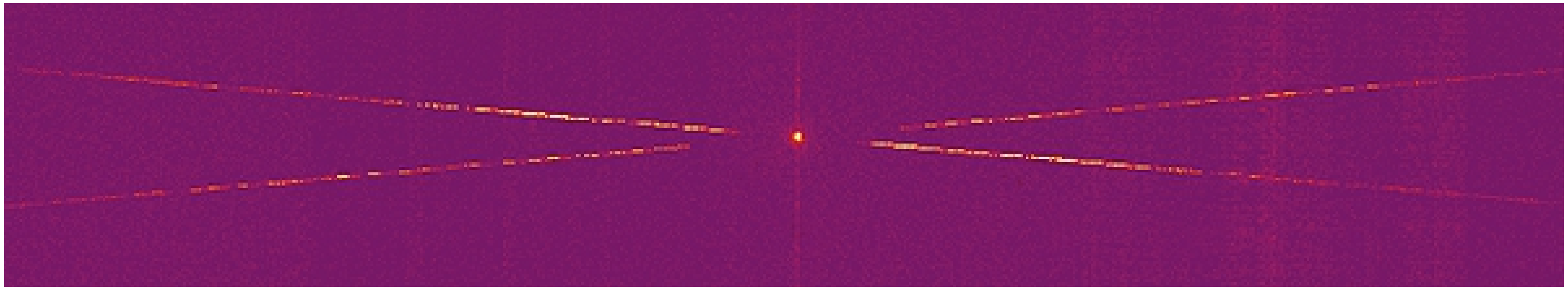

**NGC 3783, High Energy Transmission Grating**

# Warm absorber in AGN:

**NGC 3783 Sy1**

CHANDRA Kaspi + 2002 — 900 ksec

XMM Blustin + 2003 — 280 ksec

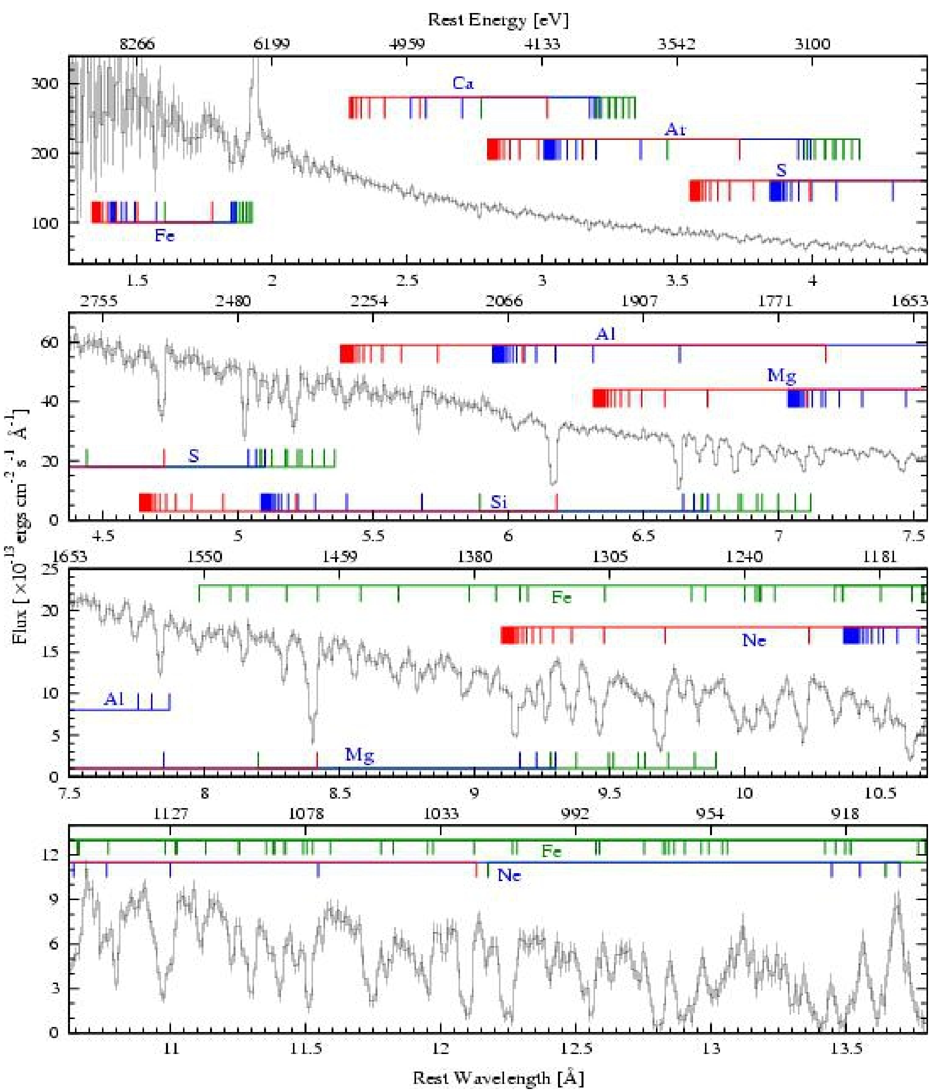


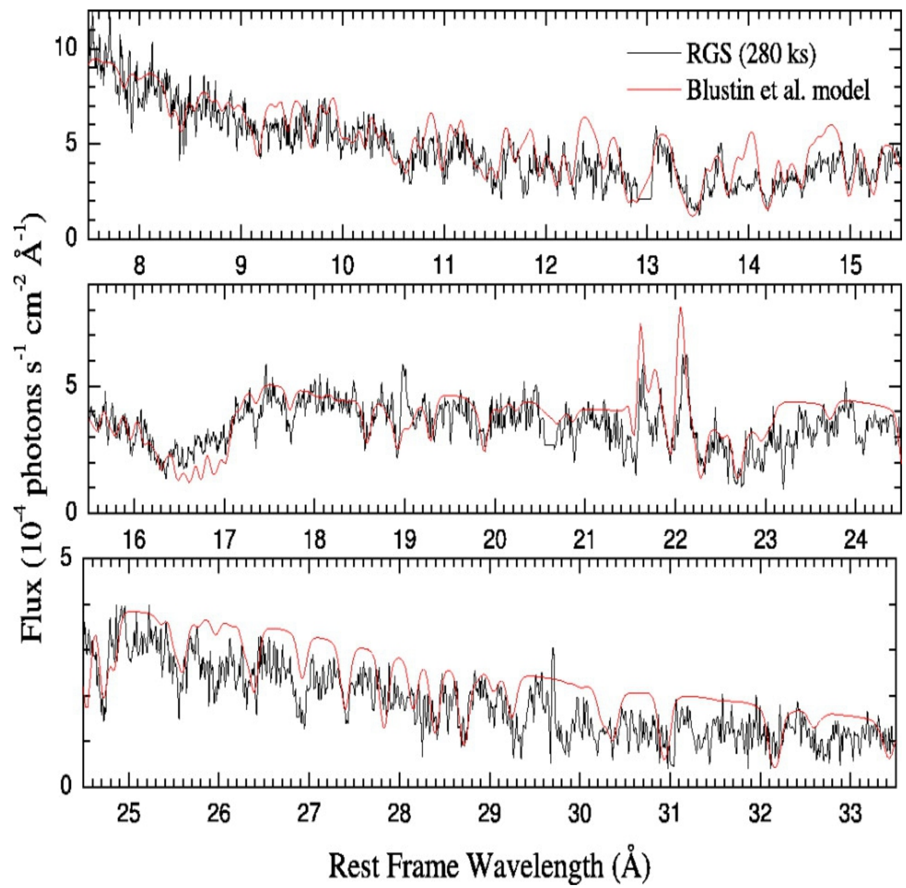

# Warm absorber in AGN:

**NGC 1068 Sy2** XMM-Newton Kinkhabwala + 2002.

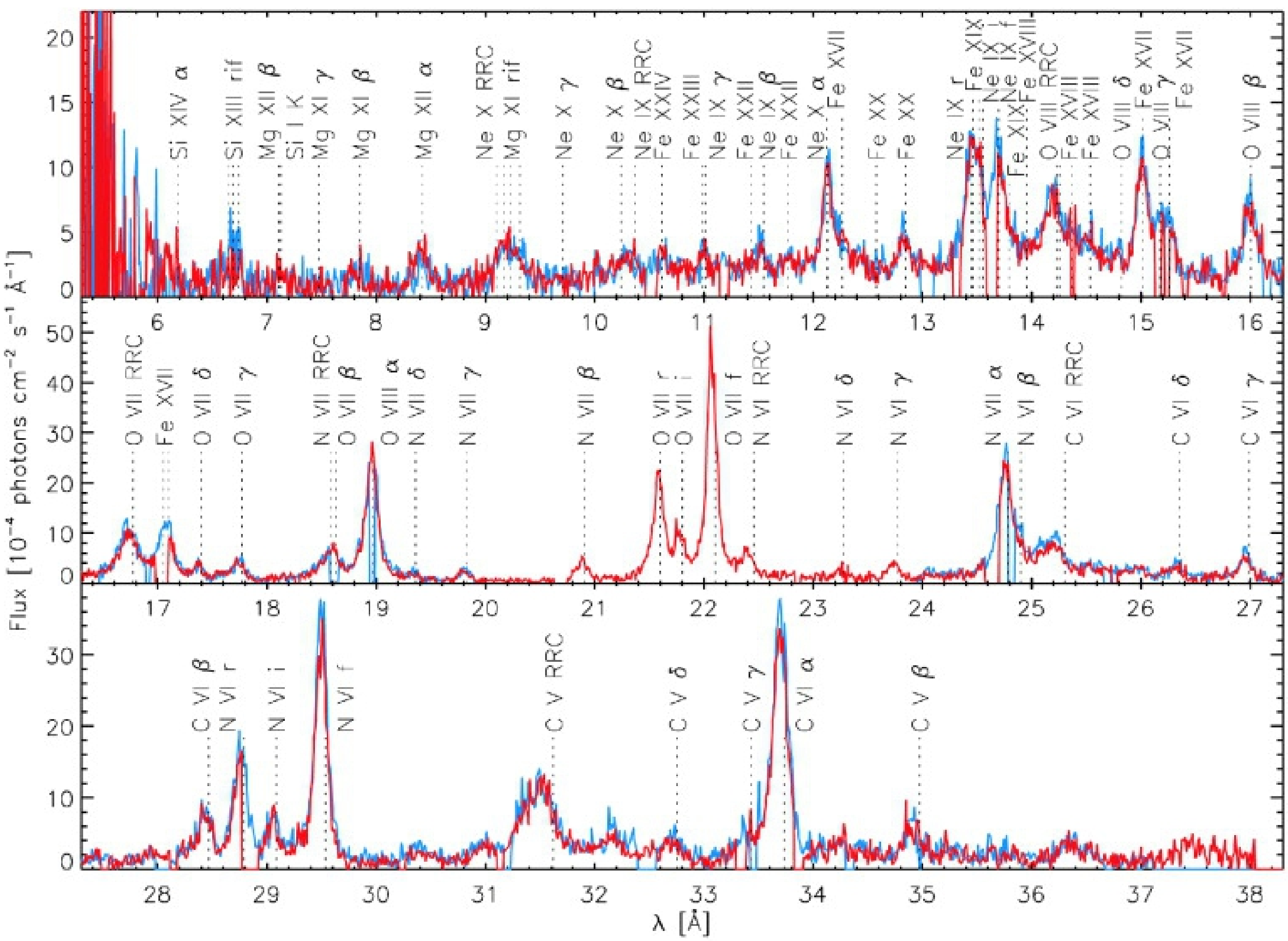

# Warm absorber in AGN – outflows in UV:

**HiBALs -   v  < 50,000 km/s**
**NALs    -   v < 60,000 km/s**
**WA       -    v < few x 100 km/s**

**HS1603+3820, z=2.54**
**Dobrzycki+ 2007,   MMT**
**22 absorbers in system A**

**SDSS J0838+2955, z=2.043,**
**Moe+  2009, APO**
**a,b,c  22,000    13,000    4900  km/s**

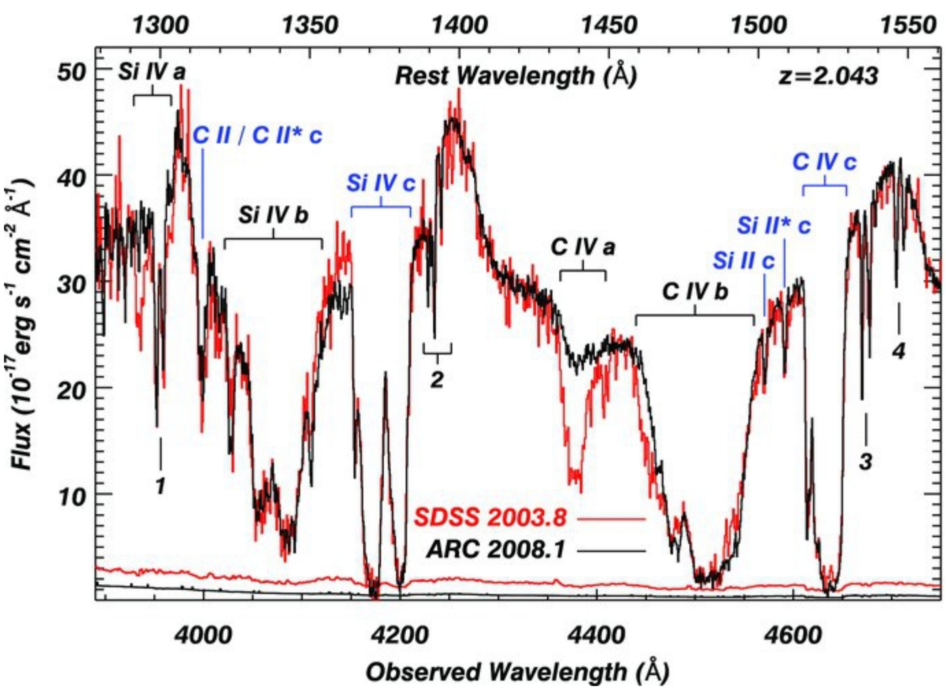


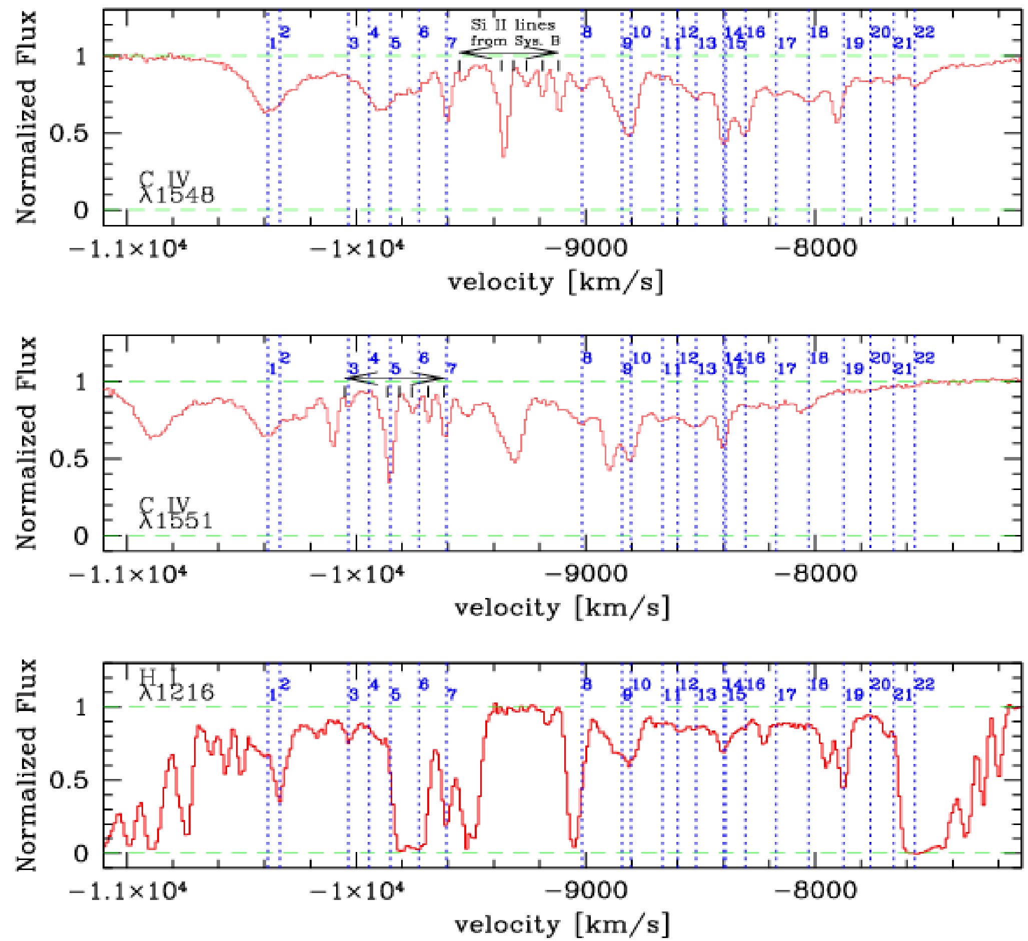

# Warm absorber in AGN – outflows in X-rays:

**Two cases of Sy1, when soft X-ray lines (WA) where fitted by the same velocity components as UV lines.**

**NGC 5548, Crenshaw+ 1999**

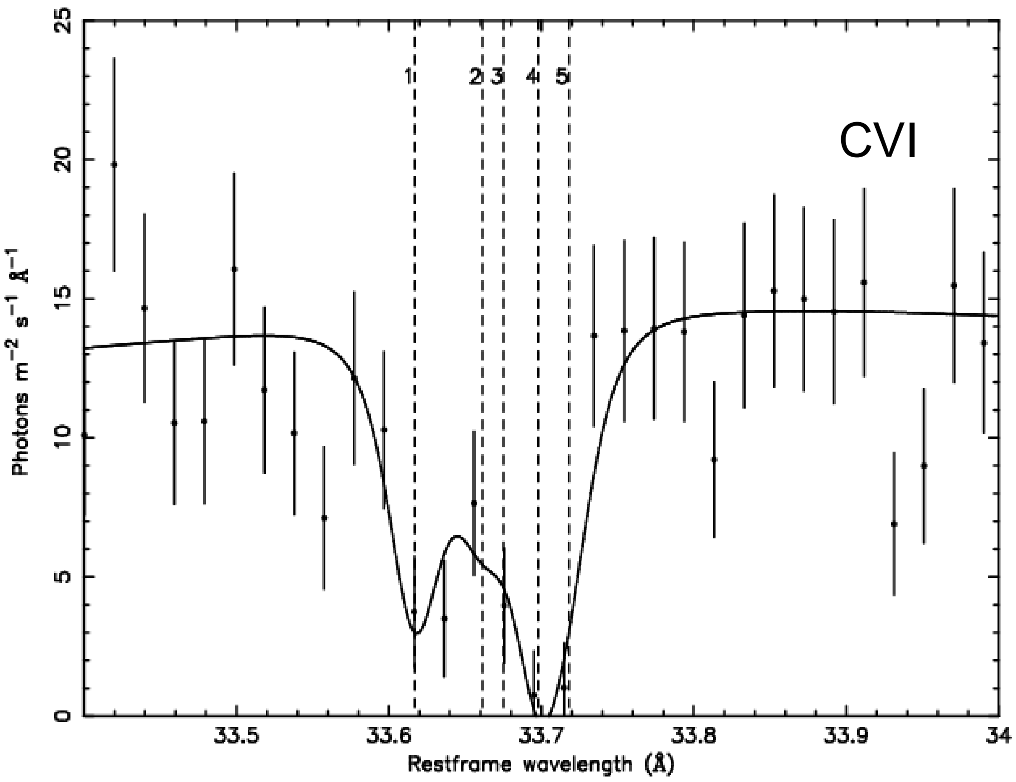


**NGC 3783, Gabel+ 2003**

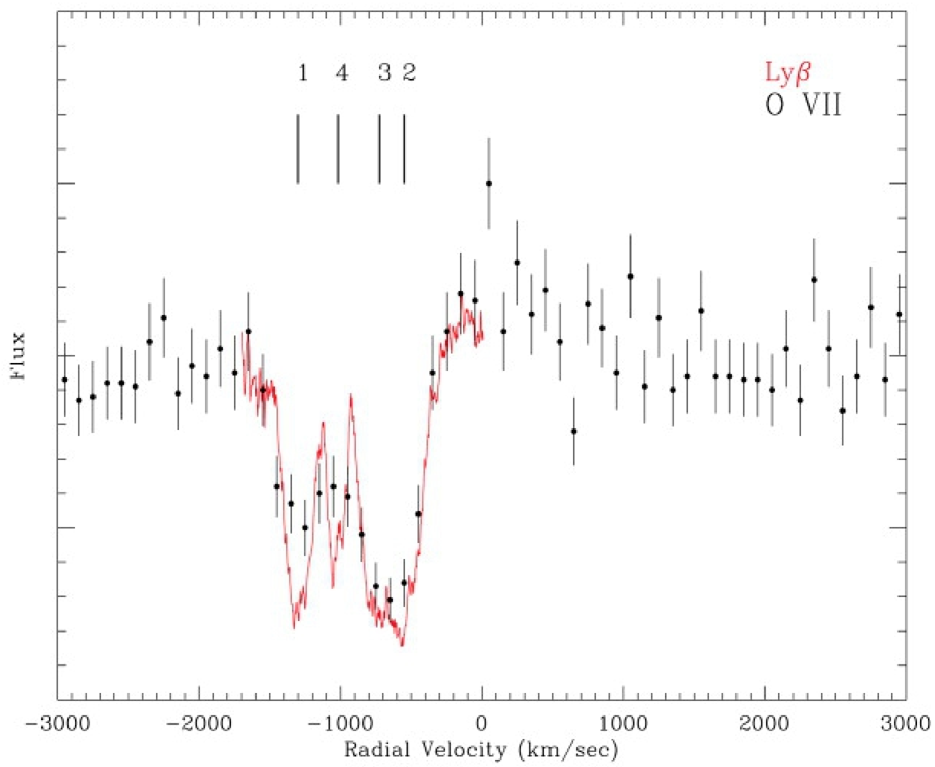


**1056, 669, 540, 340, 163 km/s,**
**Kaastra+ 2002**

# Warm absorber in AGN:

**Unified model of AGN with the Warm Absorber/Emiter**

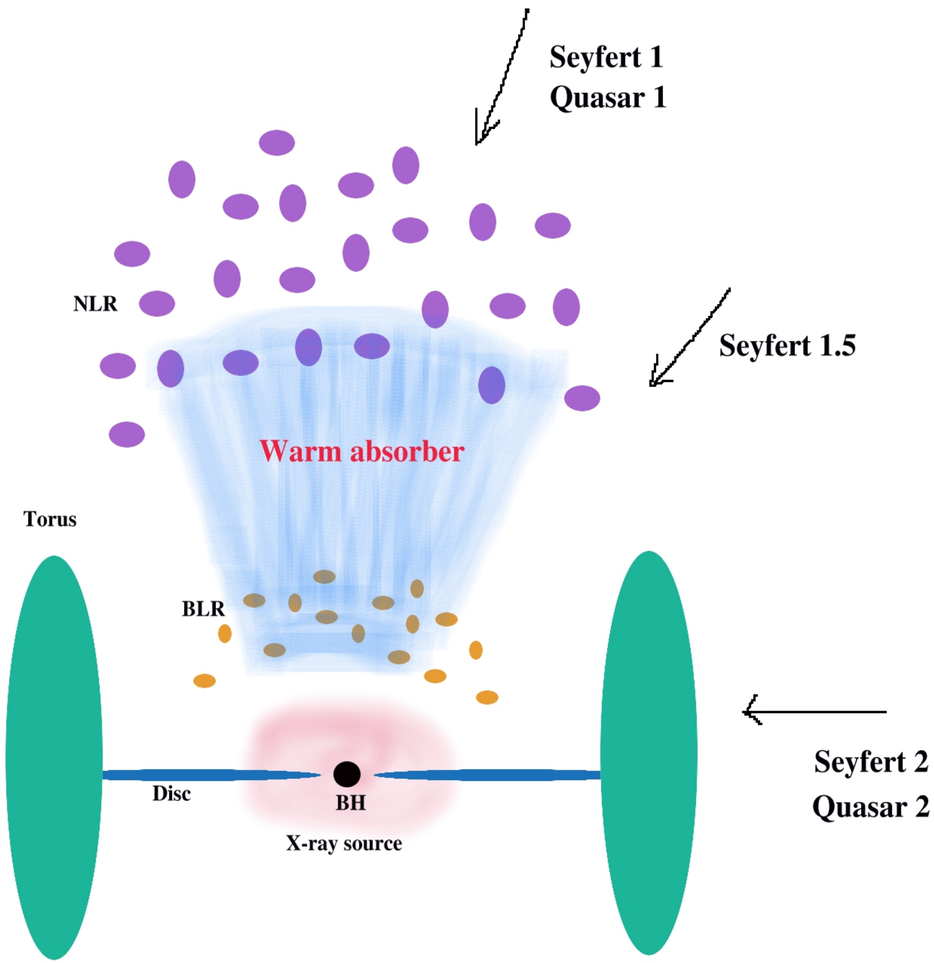


**Sy 1 – warm absorber on the line of sight to the observer**

**Sy2 – warm absorber off the line of sight to the observer.**

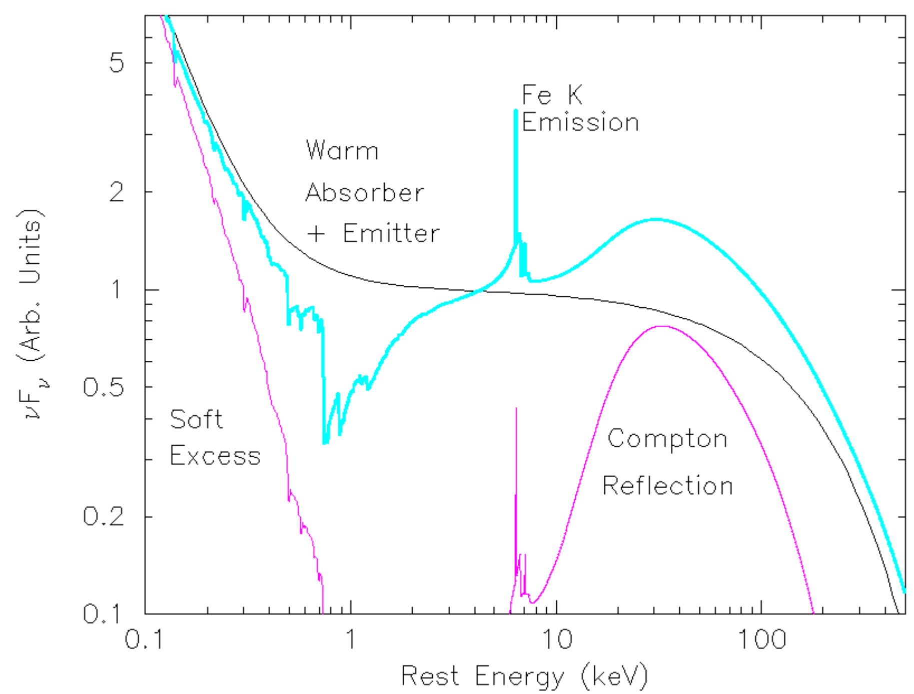

# Physical conditions of warm absorber:

- Highly ionized gas with column density about $10^{21-23}$ $cm^{-2}$.
- The gas contains heavy elements mostly in the form of helium and hydrogen like ions.
- The gas is located between BLR and NLR @ 0.01-0.1 pc from nucleus up to about 10 pc. (Krolik 2002, Behar+ 2003)
- The gas is illuminated by hard X-ray radiation originating next to nucleus.
- Warm absorber satisfies unified model of AGN.
- In some objects lines are detected while edges are not seen.
- In most objects more than one ionization component is detected.

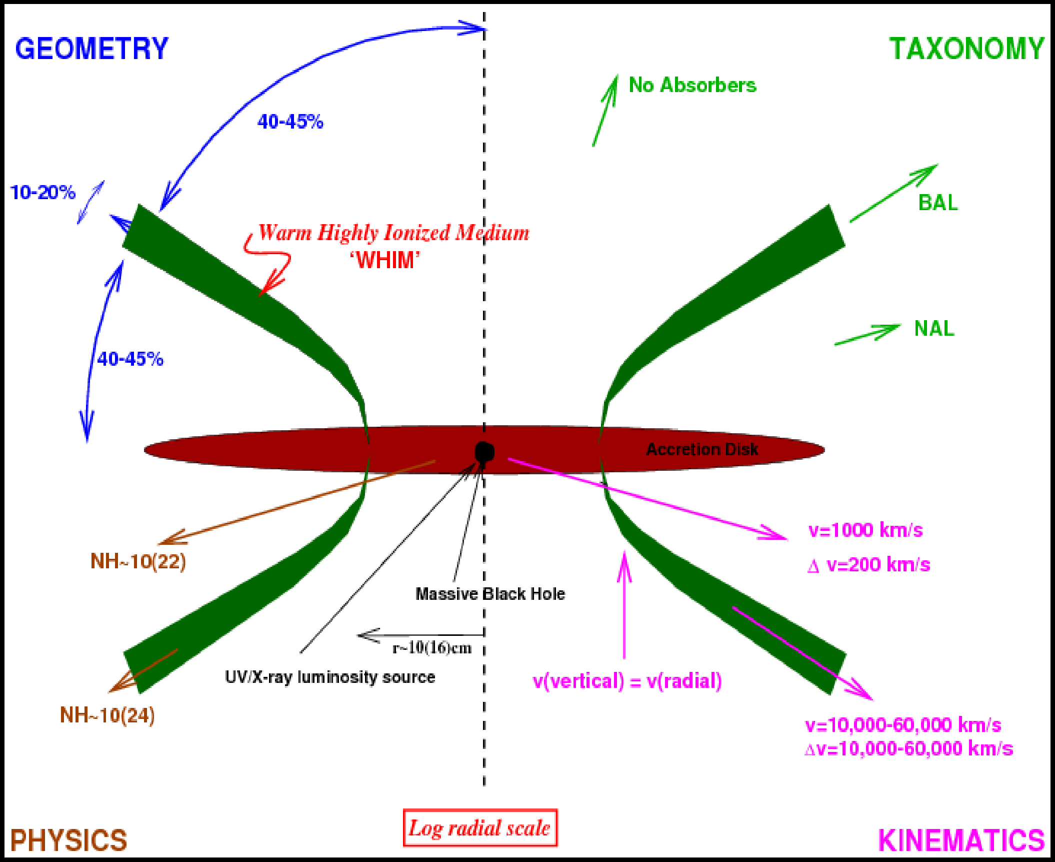


(Elvis, 2000, Fig. 1)

# Observational Surveys of the warm absorber:

- Winter + 2011, X-ray outflows in the *Swift* Sy1, OVII, OVIII edges
- Evans + 2011, SOARS – Survey of Outflows in AGN Resolved Spectroscopy.

## The Chandra SOARS Project

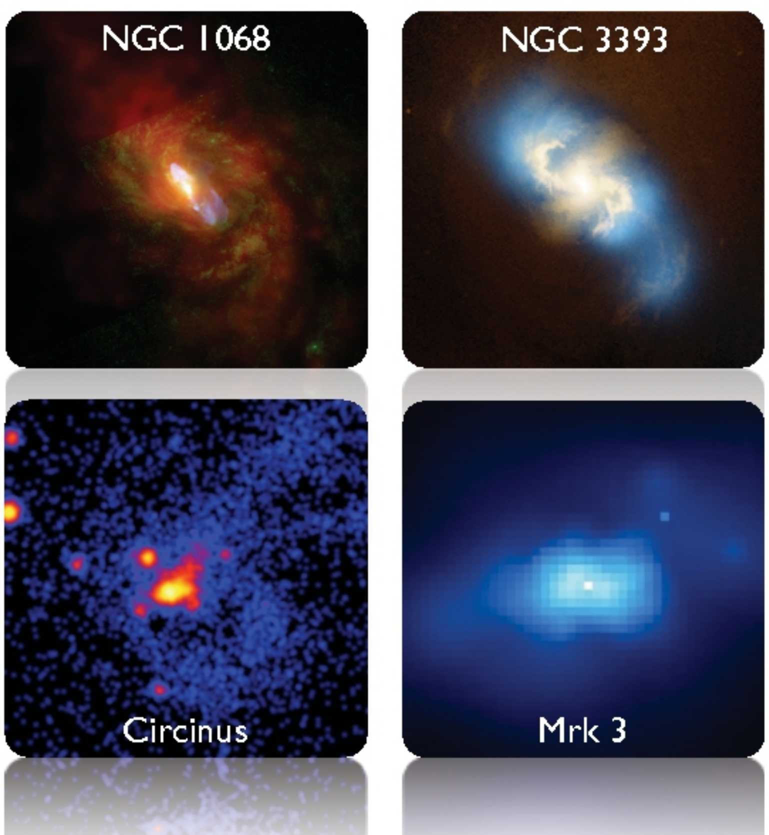


- **NGC 1068 (440 ks)**
  - $N_H > 10^{25}$ $cm^{-2}$ (Evans et al. 2010)
  - HST: Das, Crenshaw & Kraemer (2007)
- **NGC 3393 (350 ks)**
  - Binary BH (Fabbiano et al. 2011)
  - $N_H \sim 2x10^{24}$ $cm^{-2}$ (Fukazawa et al. 2011)
  - HST: Cooke et al. (2000)
- **Circinus (695 ks)**
  - $N_H \sim 2x10^{24}$ $cm^{-2}$ (Yang et al. 2008)
- **Mrk 3 (400 ks)**
  - $N_H \sim 1.1x10^{24}$ $cm^{-2}$ (Awaki et al. 2007)
  - HST: Crenshaw et al. (2010)

# Observational Surveys of the warm absorber:

# Circinus Galaxy (695 ks)

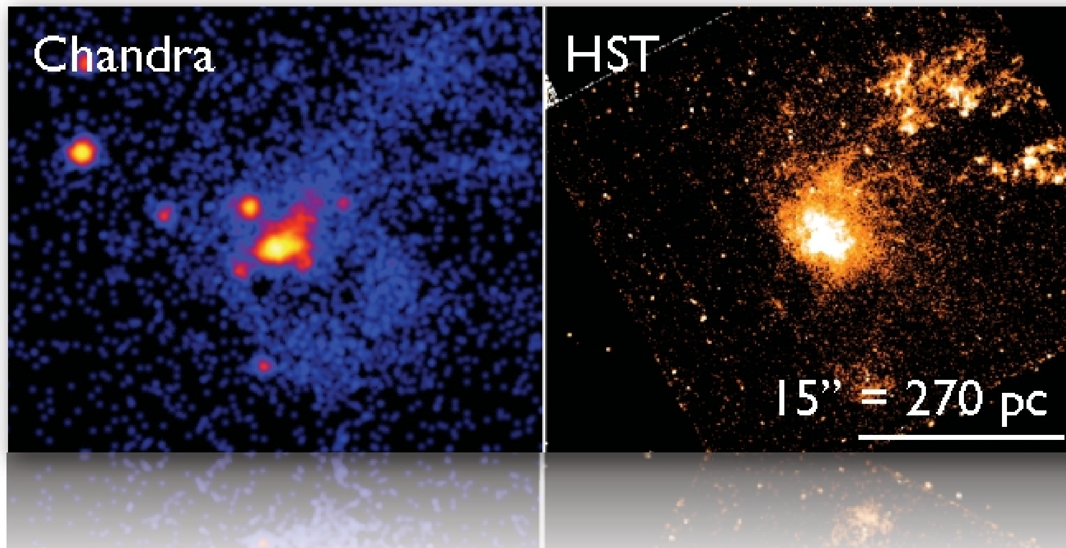


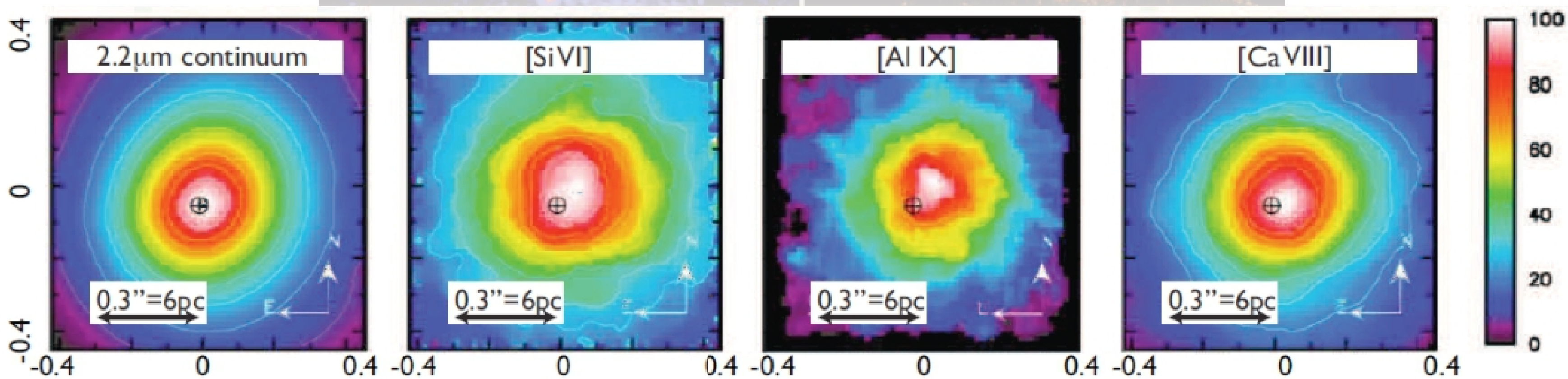


Mueller-Sanchez et al. (2006, 2011)

# Do we see absorption or emission?

XMM
Branduardi-Raymont + 2001

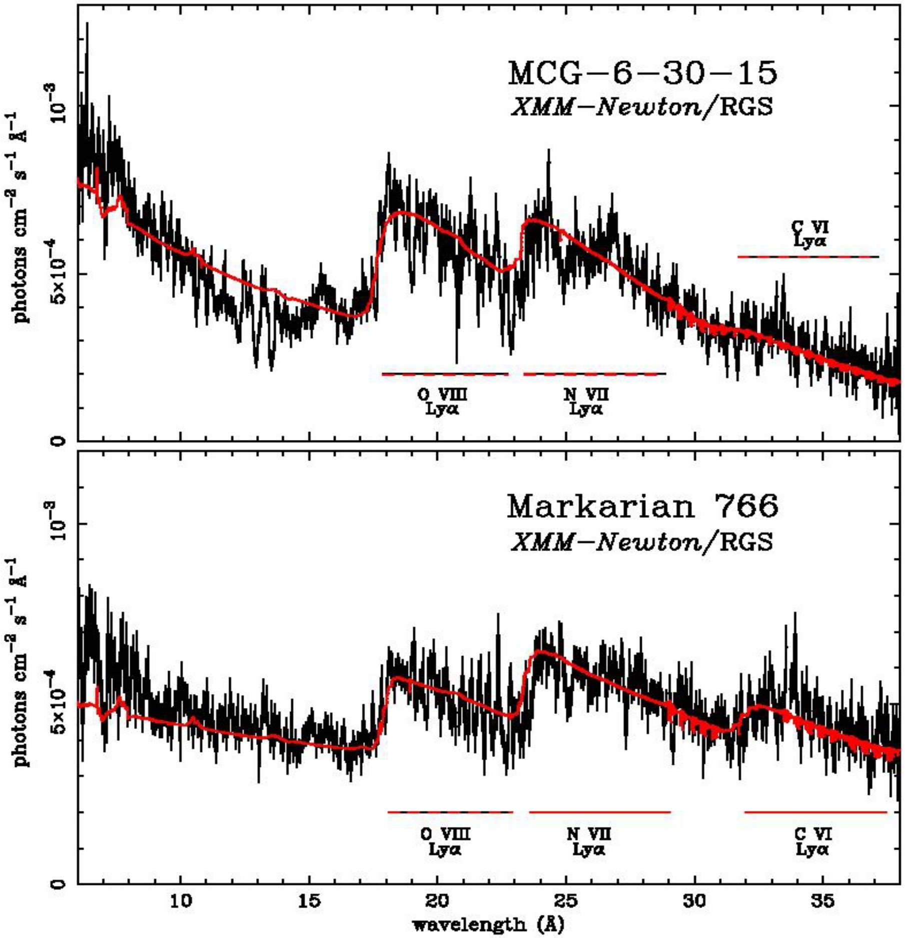


Chandra
Lee + 2001

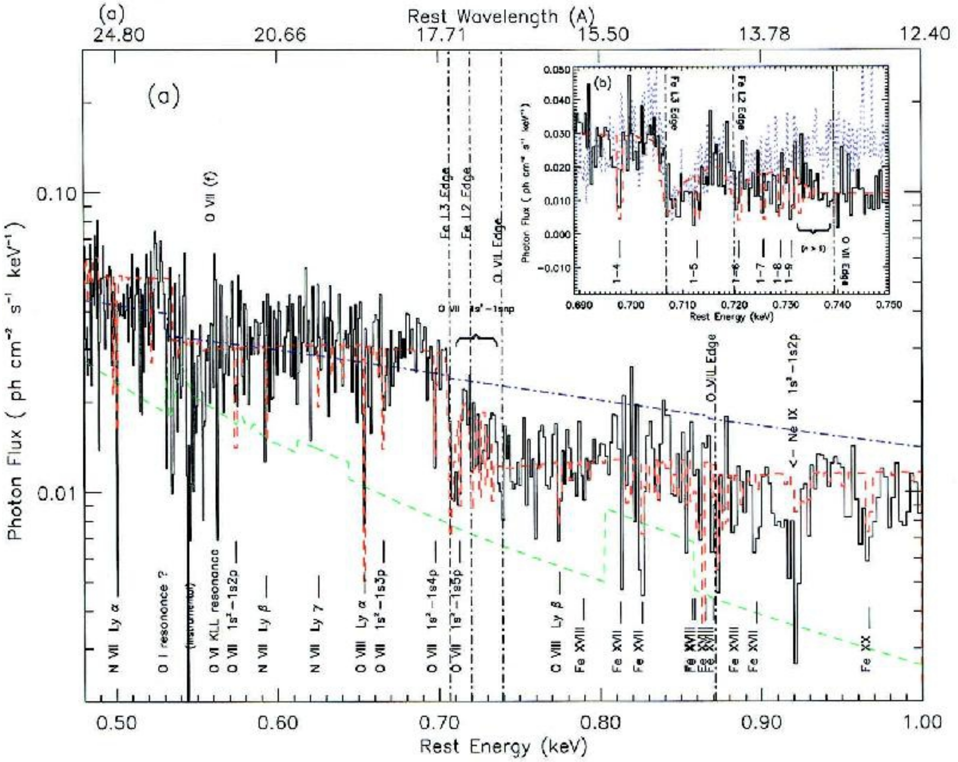


Next generation of satellites will answer this question.

# Typical X-ray Spectrum of Seyfert 1 Galaxies

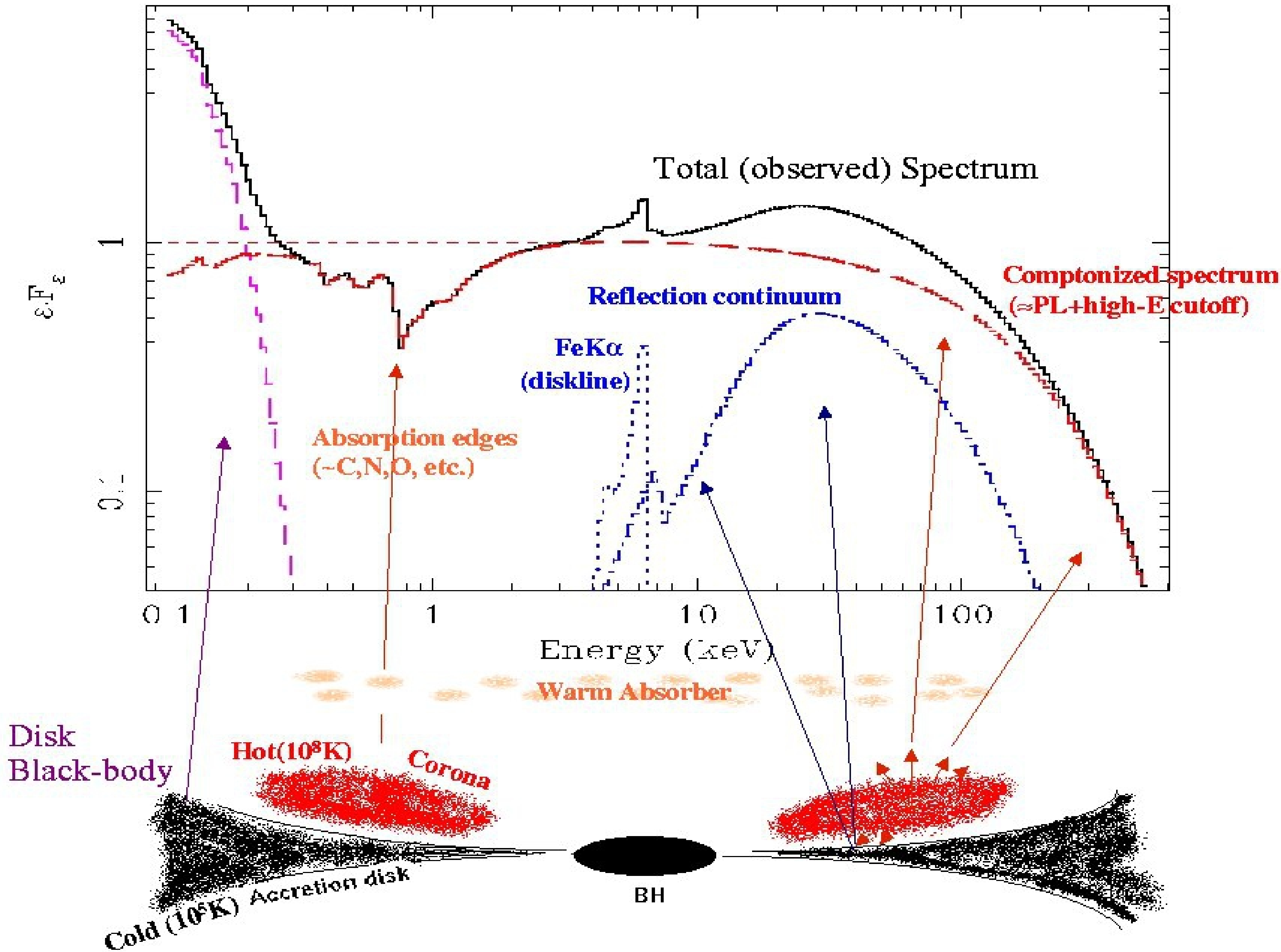

# Narrow Line Sy 1 galaxies (NLS1):

**Boller+ 1996, Rosat**

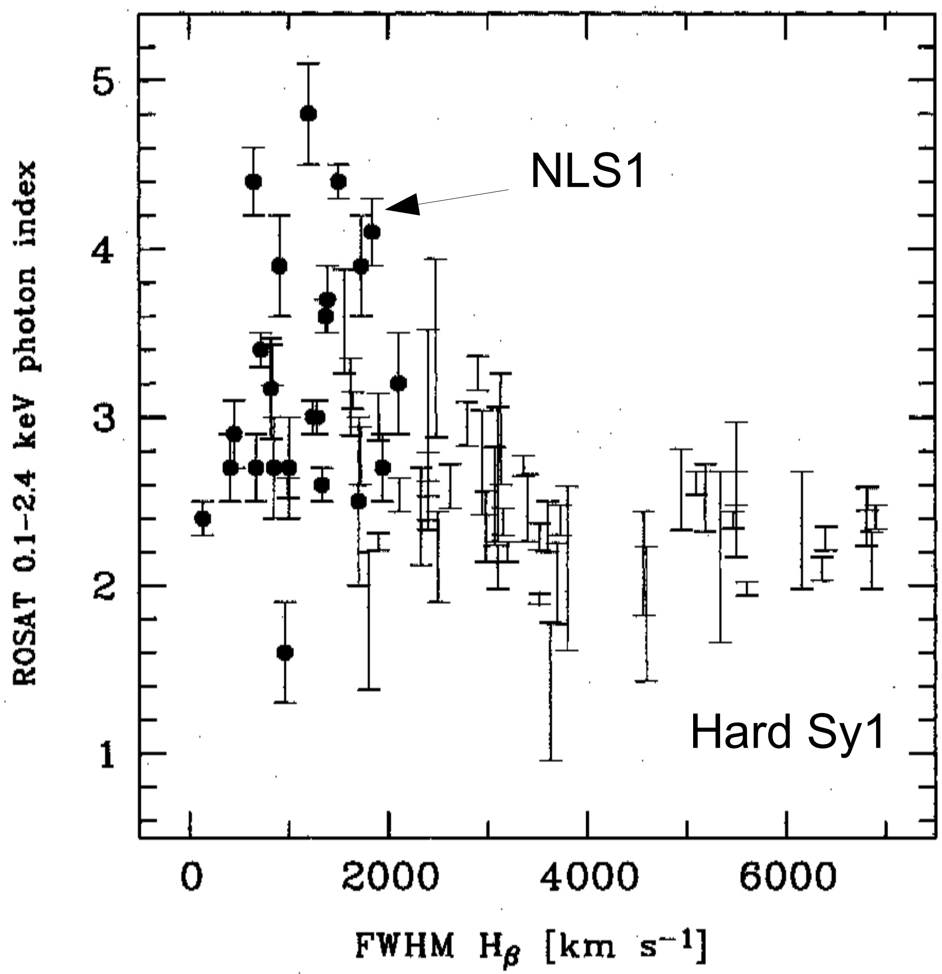


**Brandt + 1997, ASCA**

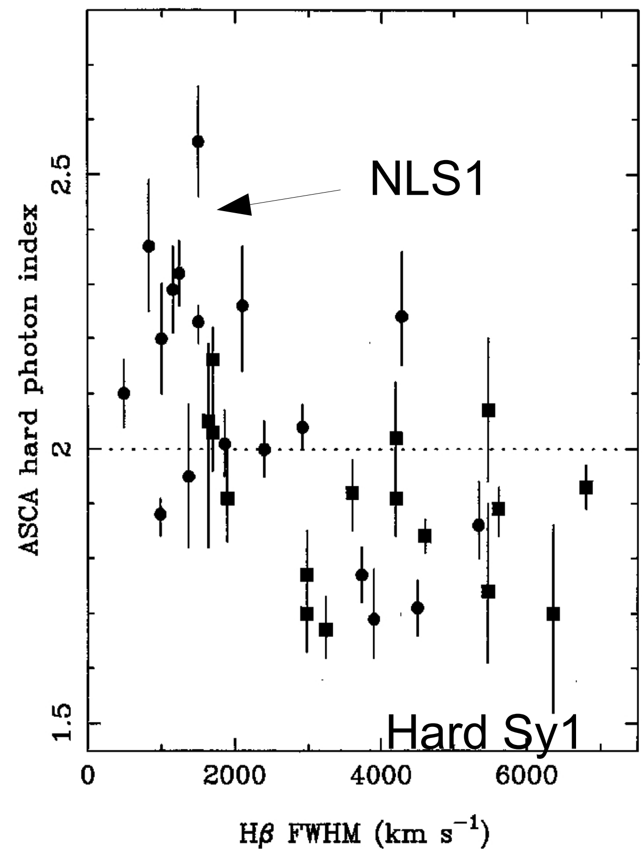


**Figure 1.** Plot of *ASCA* hard X-ray photon index versus FWHM of the Hβ line for Seyfert 1 type galaxies. Squares are Seyfert 1s from N97, and dots are other Seyfert 1s from the literature (see the text for details). The dotted line at $\Gamma=2$ is drawn for illustrative purposes.

Sy1 – flat continuum with a mean value of $\Gamma$=2.3
NLS1 – steep X-ray contiua with $\Gamma$>3

# Narrow Line Sy 1 galaxies (NLS1):

They are similar to X-ray binaries in soft state.

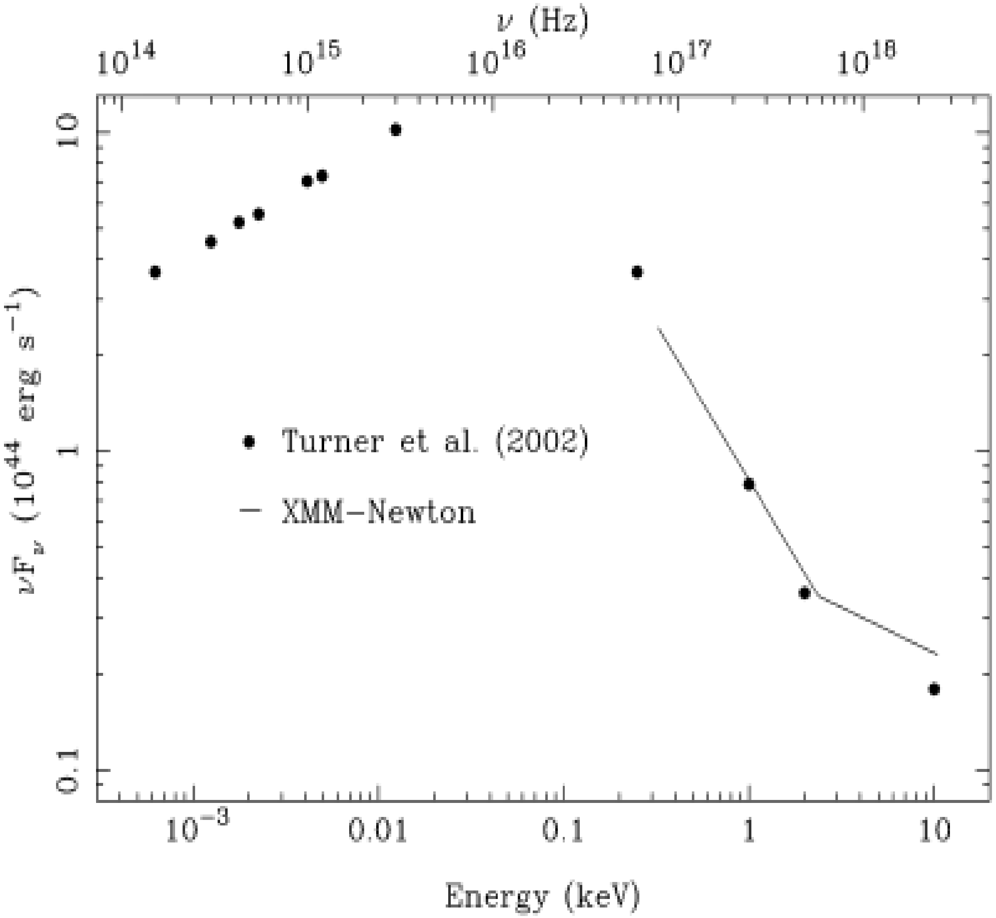


Ton S180

# Narrow Line Sy 1 galaxies (NLS1):

Soft X-ray excess of problematic origin:

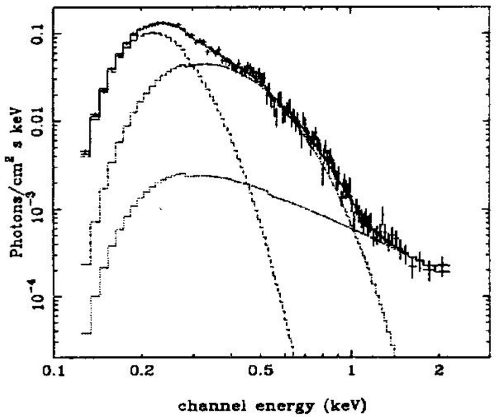


**Figure 1.** The deconvolved *ROSAT* PSPC data with a model consisting of an absorbed power law and two blackbody components, showing the dominance of the thermal emission component.

IRAS 13224

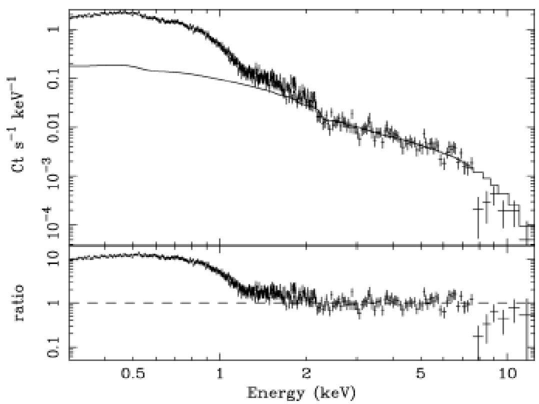


PG 1211+ 143

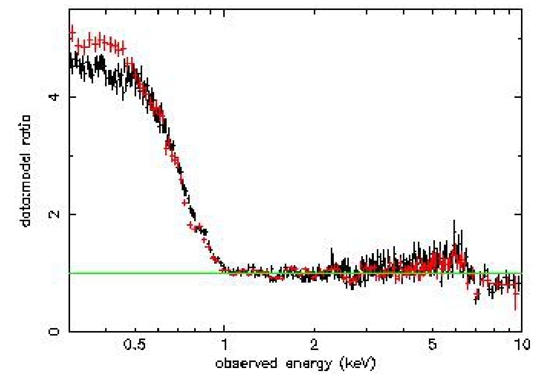


**Figure 3.** Extension to 0.3 keV of the 1-10 keV power law model fits for the pn (black) and MOS (red) spectral data, showing the strong soft excess in PG1211+143.

# Narrow Line Sy 1 galaxies (NLS1):

Soft X-ray excess of problematic origin:

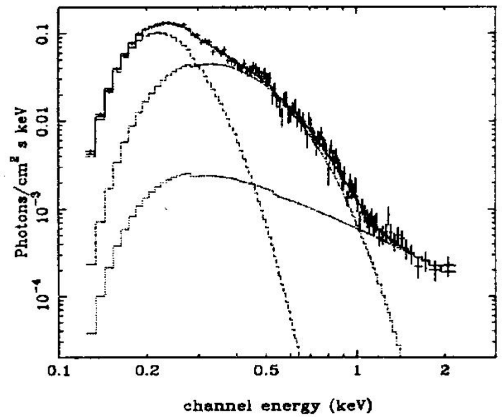


**Figure 1.** The deconvolved *ROSAT* PSPC data with a model consisting of an absorbed power law and two blackbody components, showing the dominance of the thermal emission component.

IRAS 13224

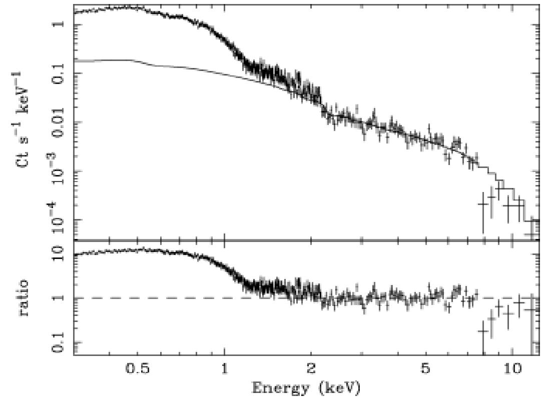


PG 1211+ 143

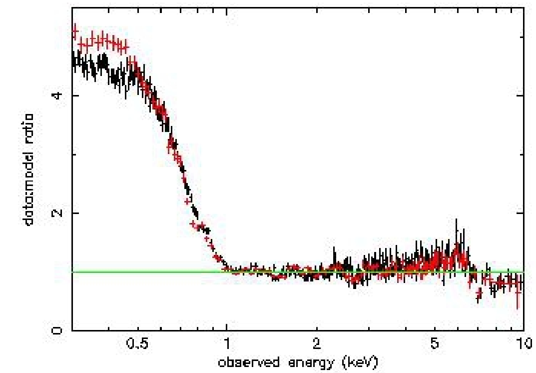


**Figure 3.** Extension to 0.3 keV of the 1-10 keV power law model fits for the pn (black) and MOS (red) spectral data, showing the strong soft excess in PG1211+143.

Relativistically blurred reflection
Fabian + 2007

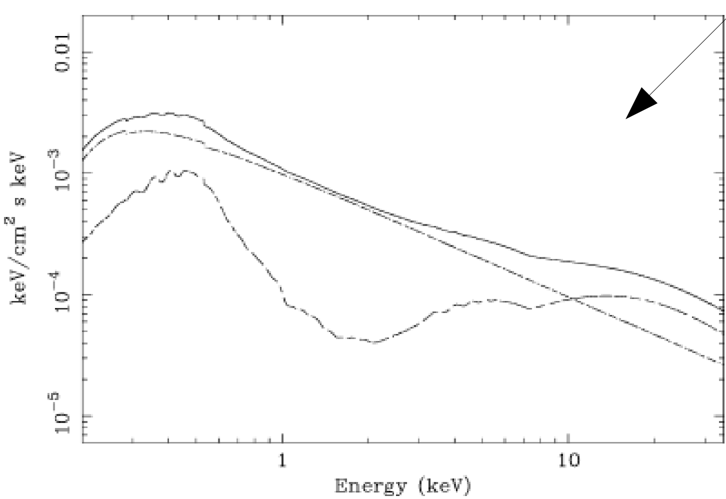


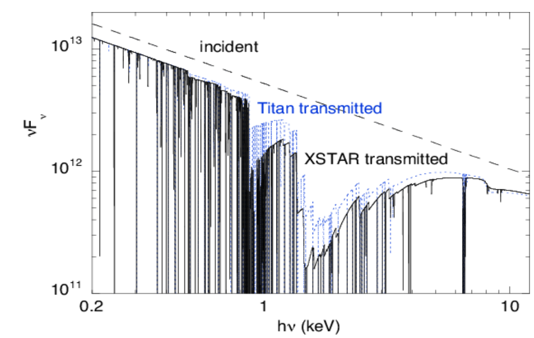


Relativistically blurred absorption
Schurch+ 2006

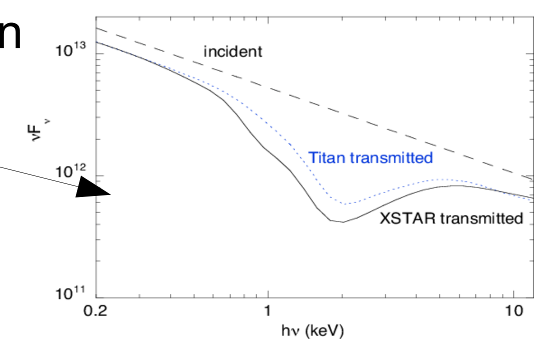

# Narrow Line Sy 1 galaxies (NLS1):

Mehdipour+ 2012, Mrk 509

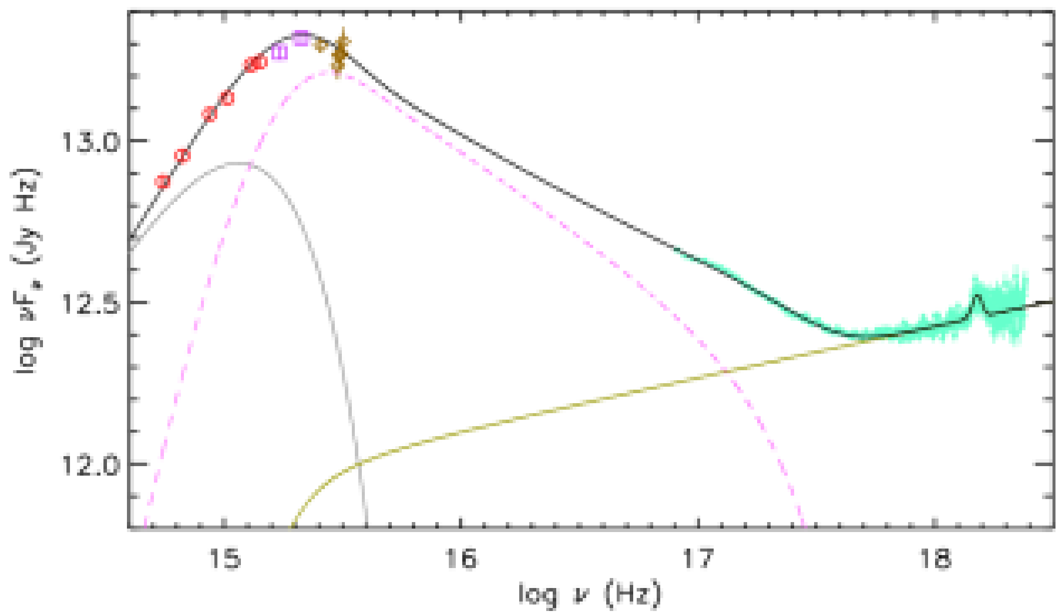


The best broad-band continuum with XMM-Newton data
- additional model is warm Comptonization as an explenation for Soft X-ray excess.

# Narrow Line Sy 1 galaxies (NLS1):

Petrucci + 2020, Mrk 509
Simulations by TITAN code

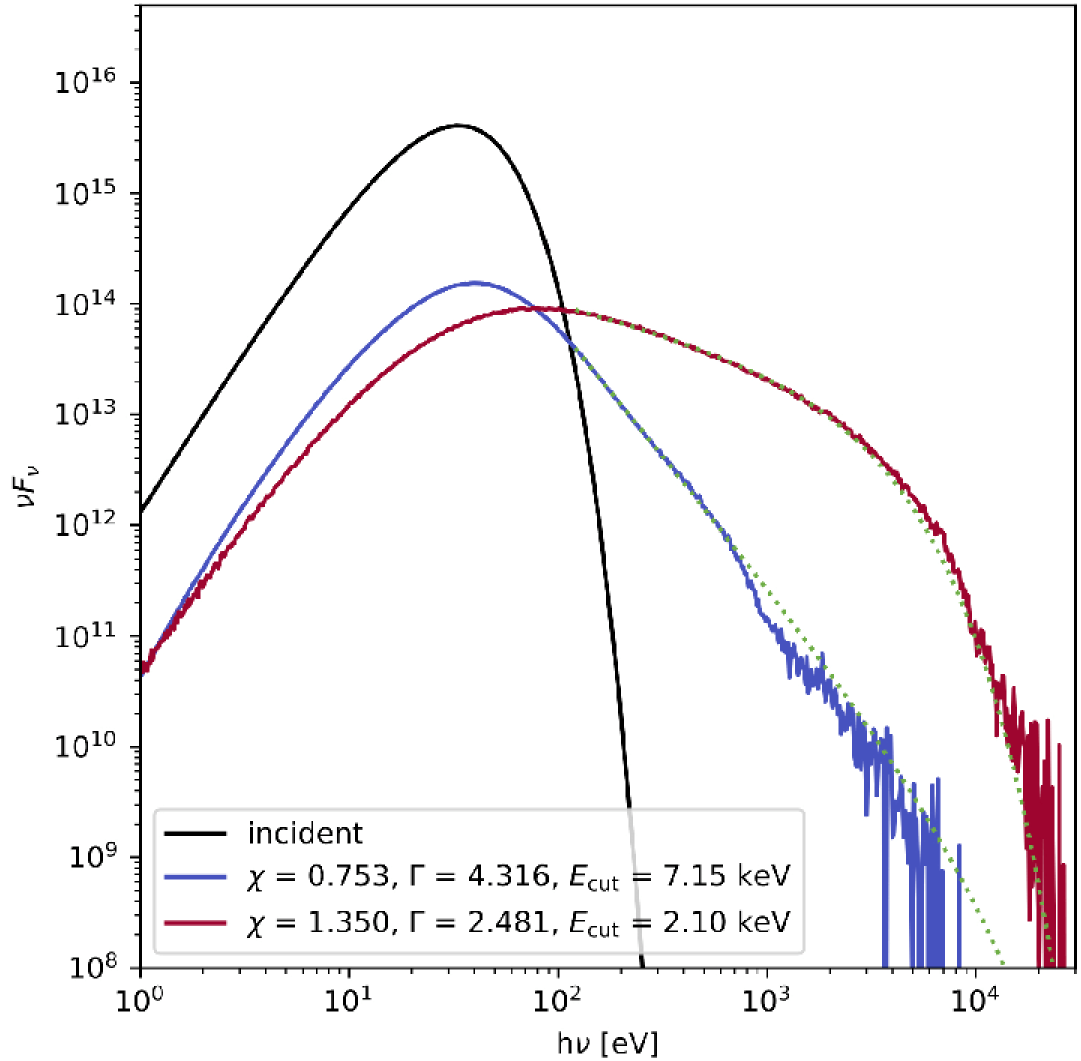


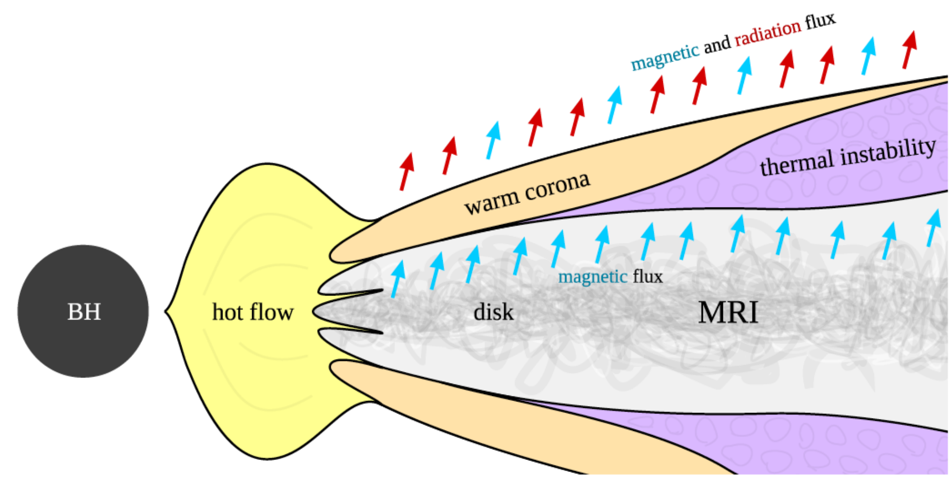


Figure 1.1: Schematic illustration of a slice through the disk plane (only one side was shown due to symmetry). Black hole is shown as the circle on the left. Grey area represents optically thick and geometrically thin disk when most of the accreting mass is located. Warm corona covering the disk in which the magnetic energy is released as radiation is marked in orange. Magnetic and radiative energy flux are represented by blue and red arrows, respectively. Part of the corona which possibly collapses due to thermal instability is shown in magenta. Inner optically thin and geometrically thick hot flow, although not considered in our model, is drawn in yellow for completion.

# Variability in X-rays:

## Blazars

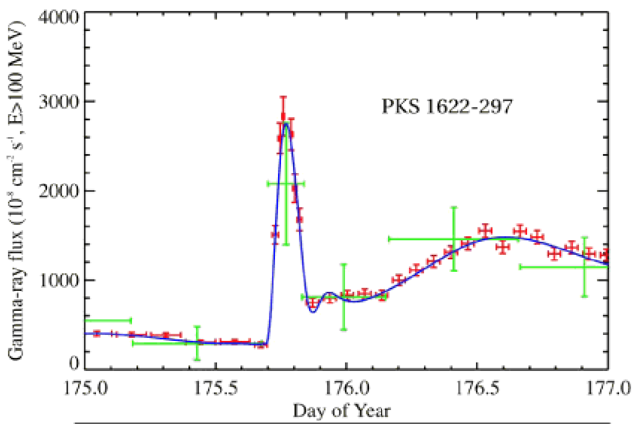


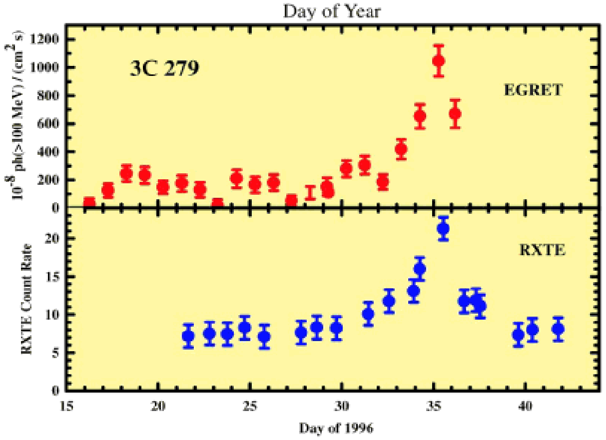


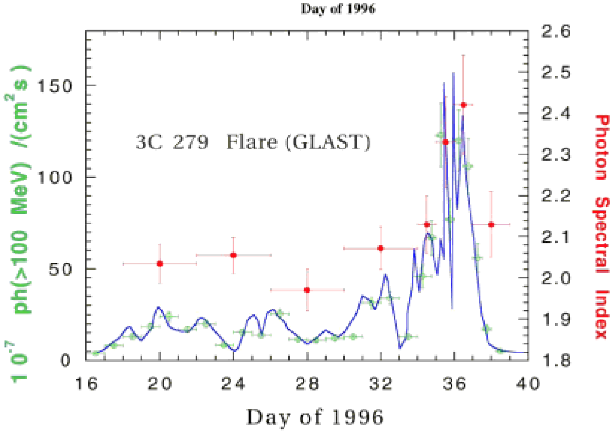


## NLS1

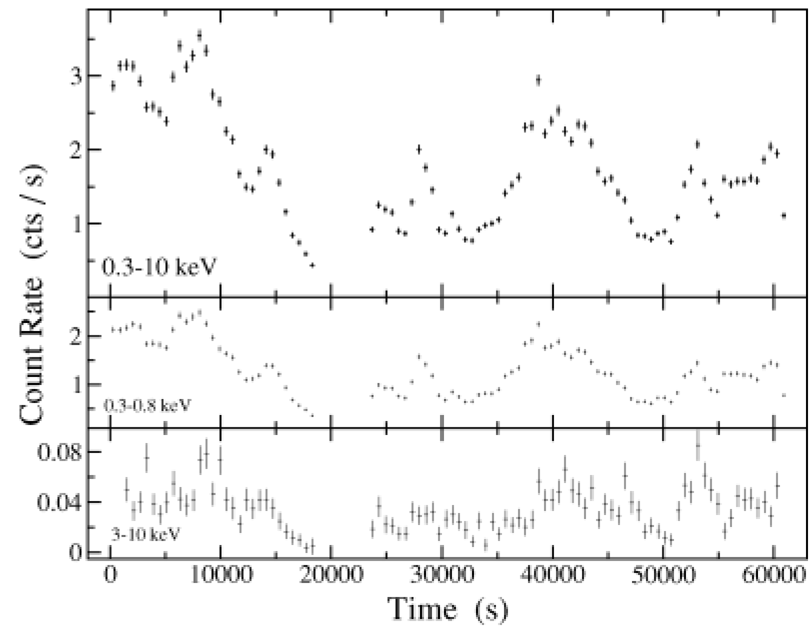


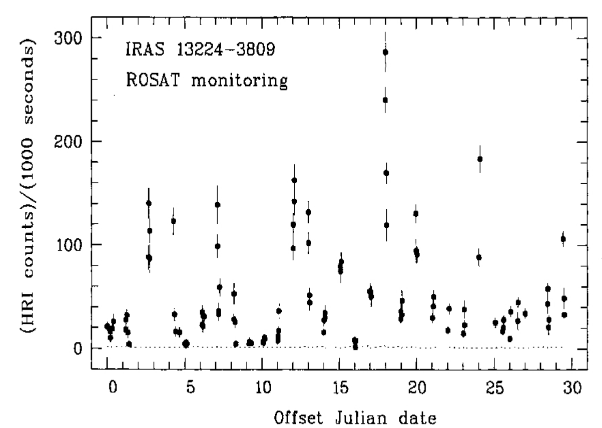


**Figure 1.** *ROSAT* HRI light curve for IRAS 13224–3809 obtained during a 30-d monitoring observation between 1996 January 11 and February 9. The abscissa label gives the Julian date minus 245 0093.523 d. Each data point is plotted at the middle of the exposure interval from which it was obtained, and the sizes of the exposure intervals lie within the data points themselves. The total exposure time is 111.313 ks, and the source is centred on-axis in the field of view. The dashed curve indicates the background counting rate within the source extraction circle as a function of time. At least five giant-amplitude variations are visible (see the text for details). We obtain similar results when ignoring HRI channels 1–3 and can exclude any ultraviolet leak from having serious effects.

# Variability in X-rays:

NGC 4051, McHardy + 2005

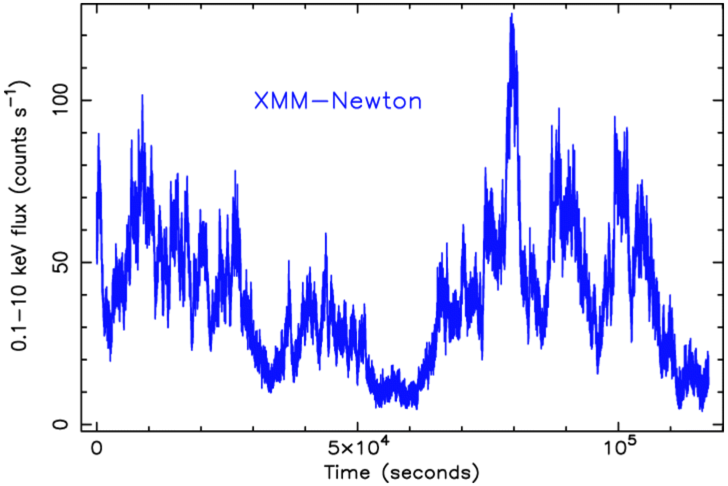


Power Density Spectra:

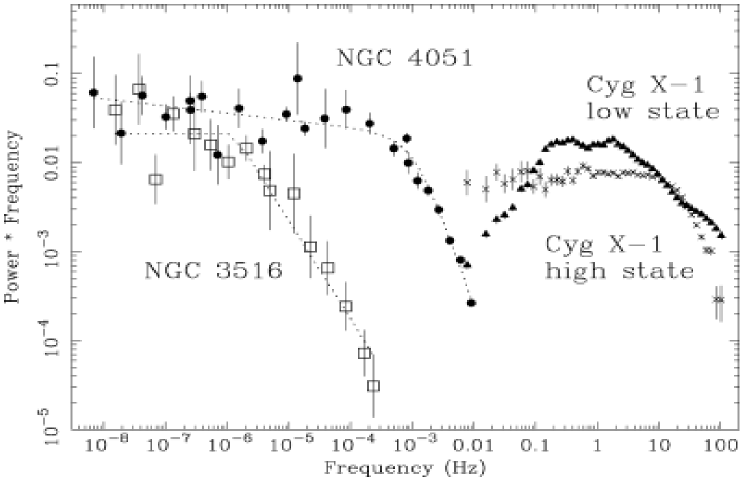

# Variability in X-rays:

NGC 4051, McHardy + 2005

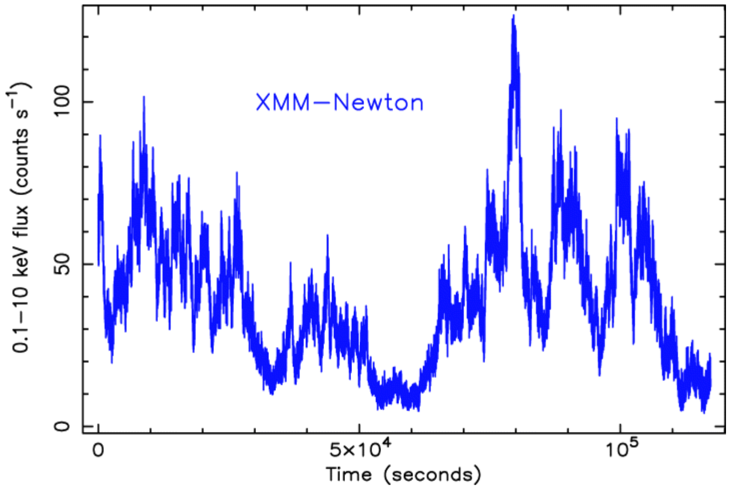


Power Density Spectra:

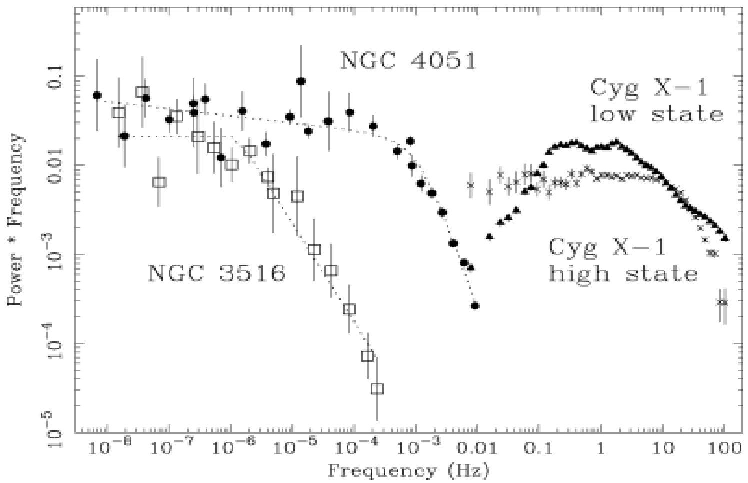


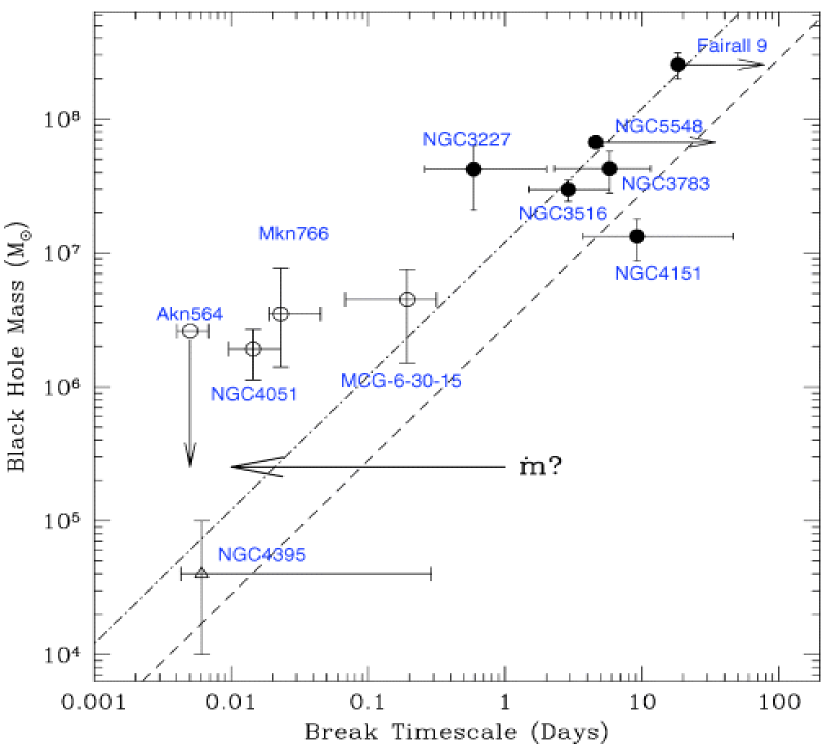

# Variability in X-rays:

Using X-ray normalized excess variance: Nikołajuk + 2009

$$M_{BH} = C \frac{T - 2\Delta T}{\sigma_{nxs}}$$

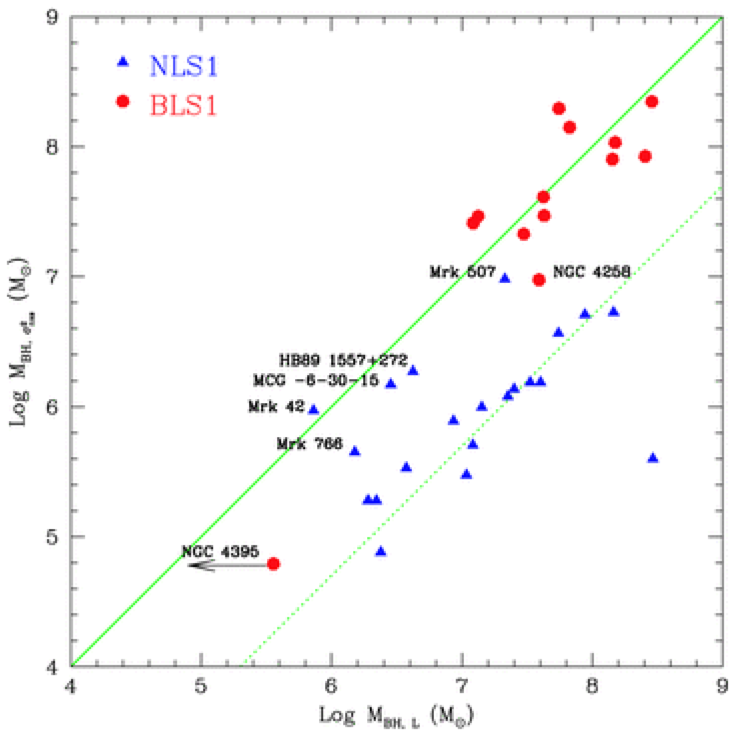


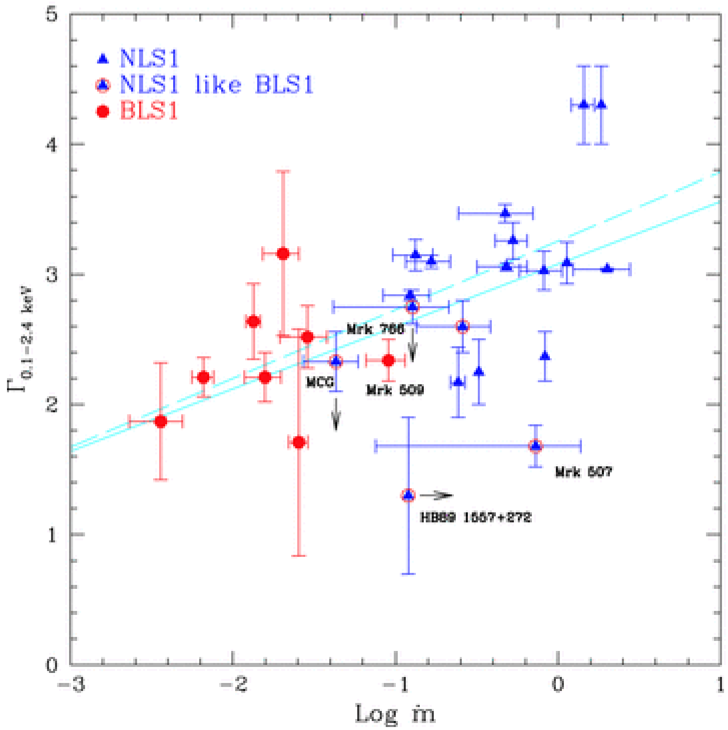

# Variability in X-rays - Iron Line:

MCG -6-30-15
Markowitz + 2001



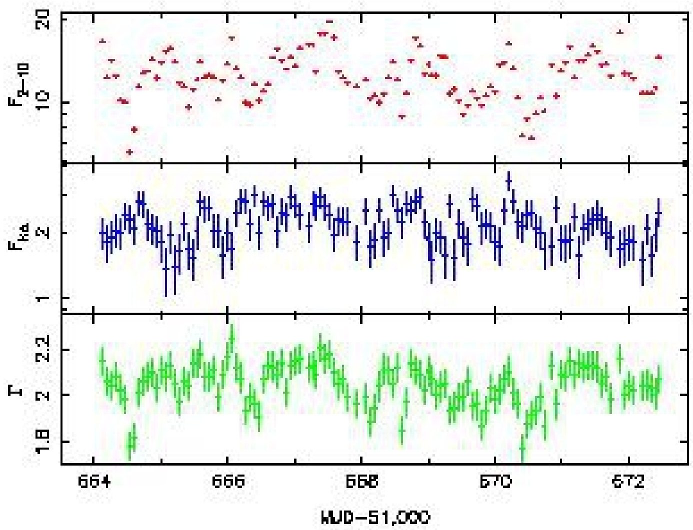


Figure 3. MCG–6-30-15 light curve for 2-10 keV flux (top; in ct sec$^{-1}$), Fe K$\alpha$ flux (middle; in $10^{-4}$ ph cm$^{-2}$ sec$^{-1}$), and 2-10 keV power-law slope Γ (bottom) derived from spectral fitting of each orbit during the *RXTE* 8-day observation. Note that the line flux shows significant rapid variability, but is NOT correlated with the continuum.

Flux in iron line changes within a day, but it is not correlated with continuum emission.

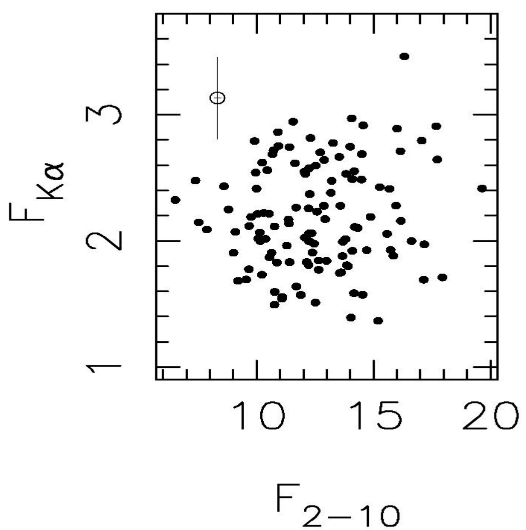

# Variability in X-rays - Iron Line:

DeMarco + 2009

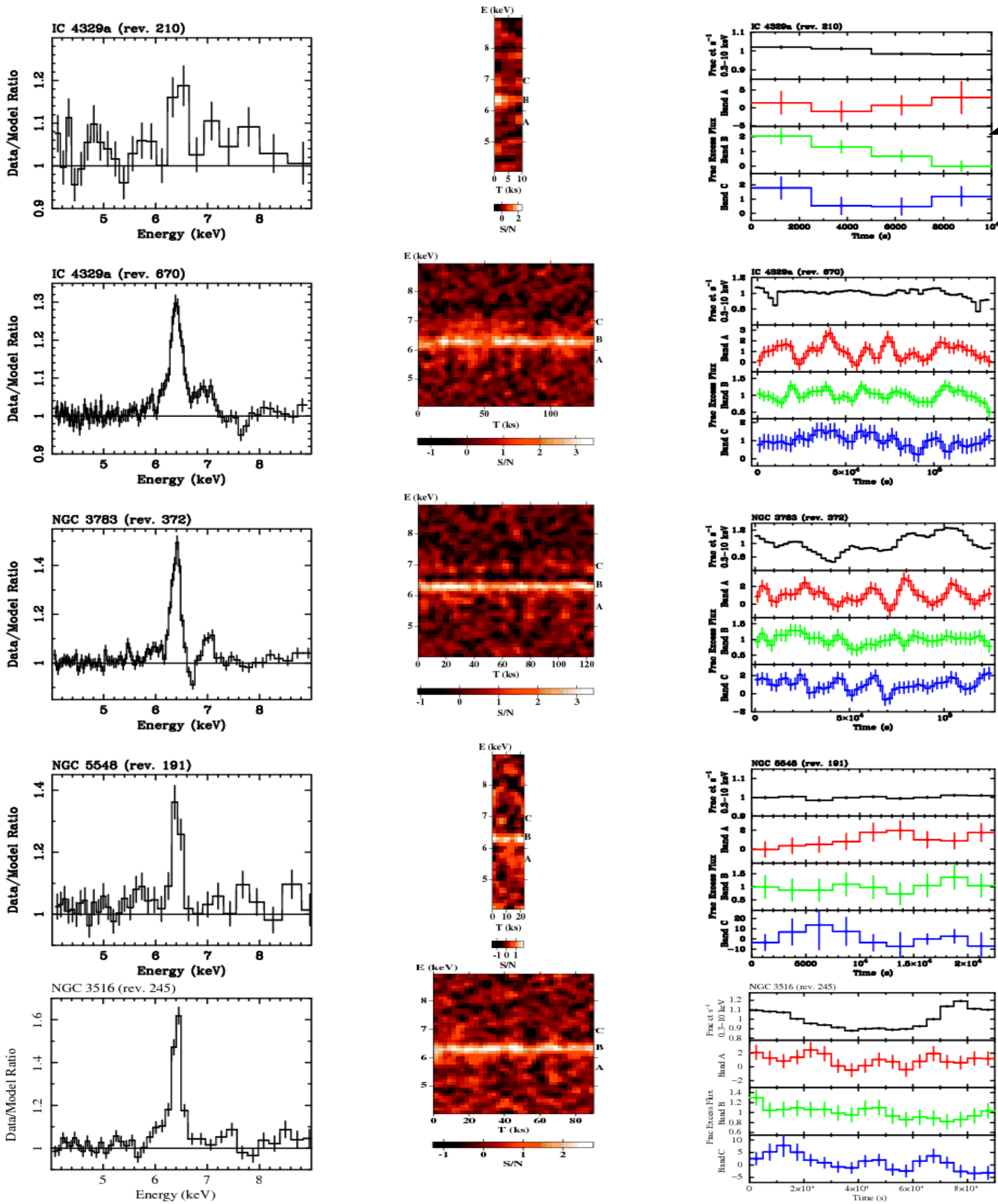


Miller+ 2006, Mkr 766

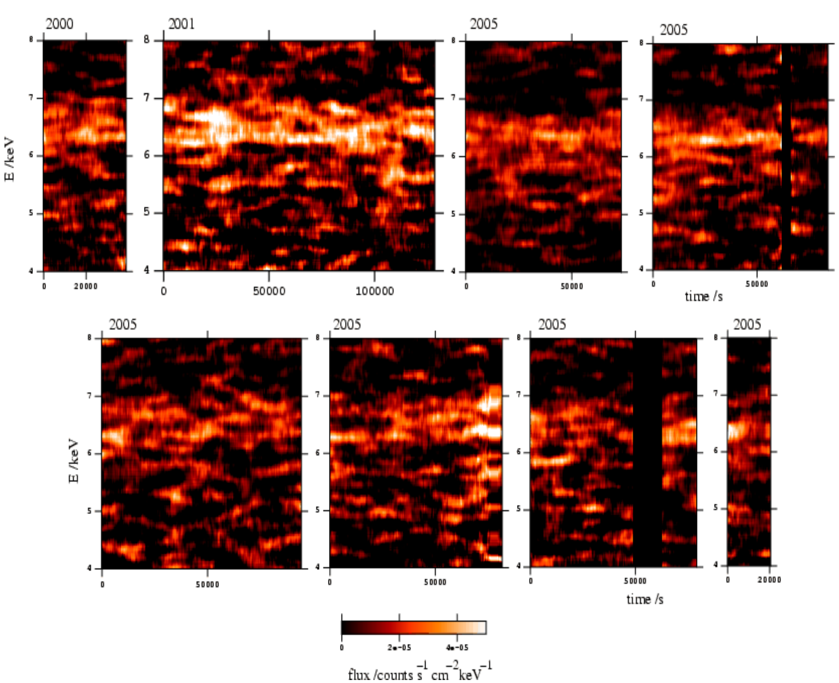

# Variability in X-ray, Soft X-ray Lags:

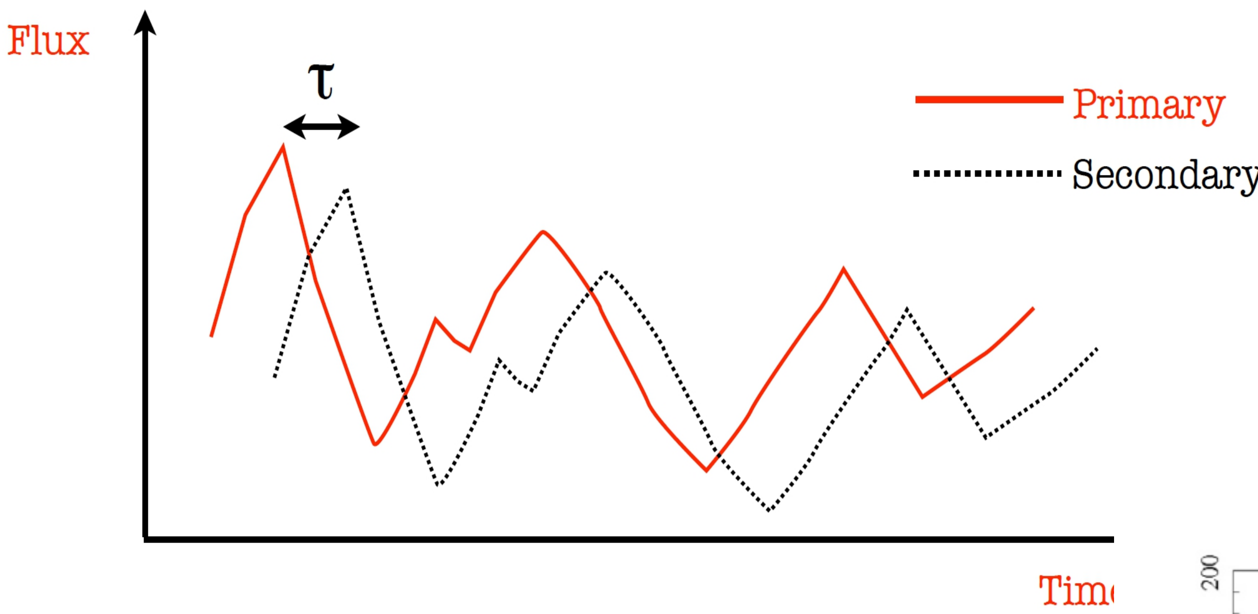


DeMarco + 2012

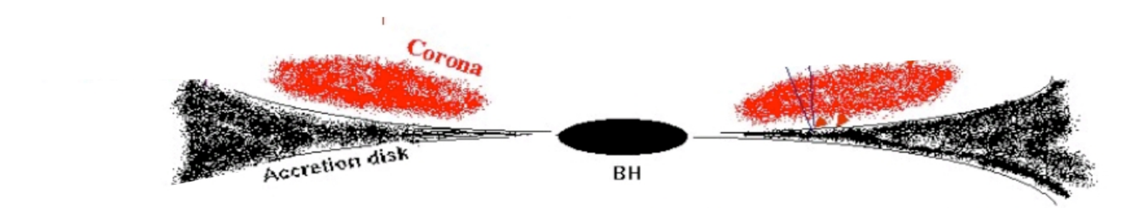


Haardt, Maraschi and Ghisellini (1994)

1H 0707-495

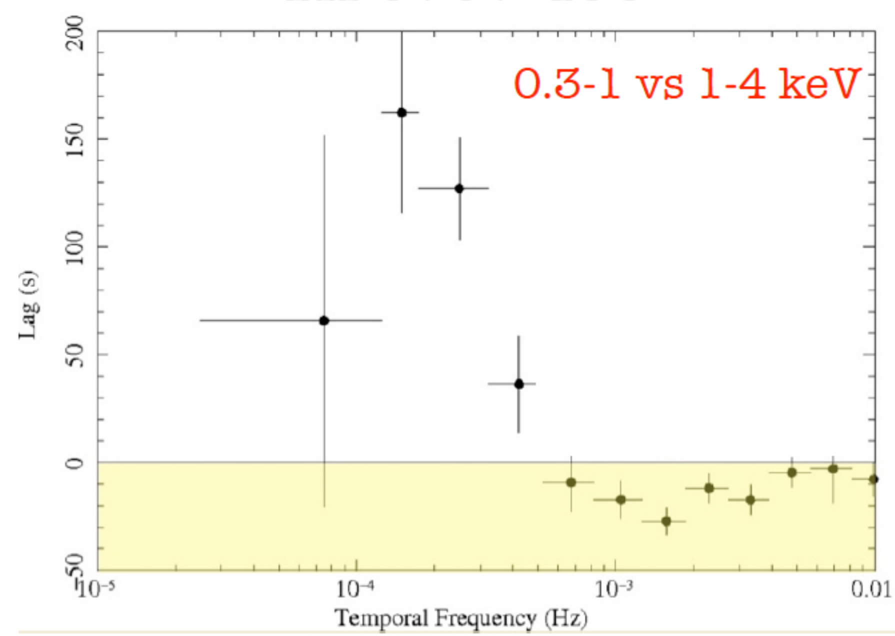


Fabian +09, Zoghbi +10, +11

# Variability in X-ray, Soft X-ray Lags:

DeMarco + 2012

## Inner disk reverberation

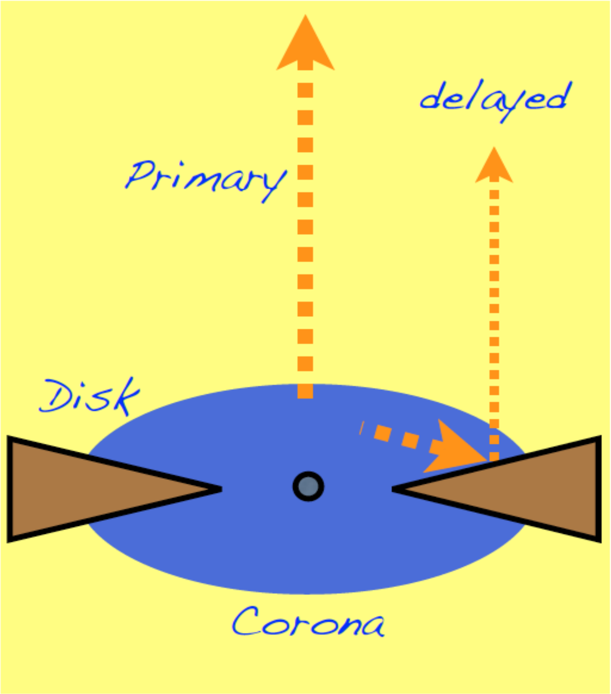


involved length scales

~rg

Zoghbi +11

## Distant reflector

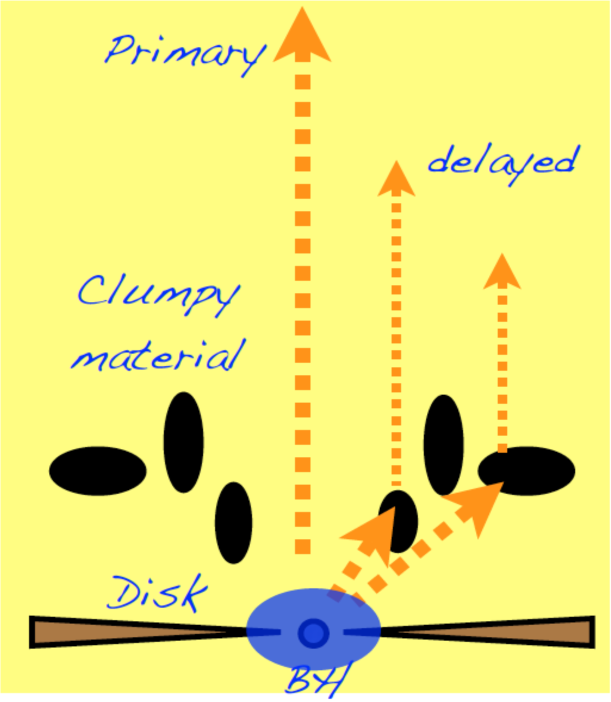


involved length scales

~1000 rg

Miller +11

# Variability in X-ray, Soft X-ray Lags:

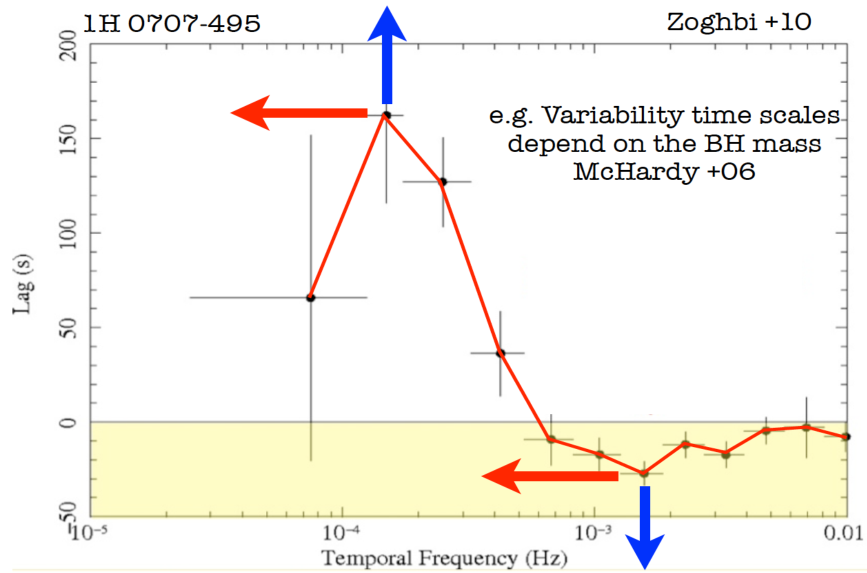


**DeMarco + 2012**

$M_{BH}$~2x10^6 Msol
Zhou & Wang 2005 (1H0707)

$M_{BH}$~ 2.4 (±0.7) x10^7 Msol
Kaspi et al. 2000 (PG1211)

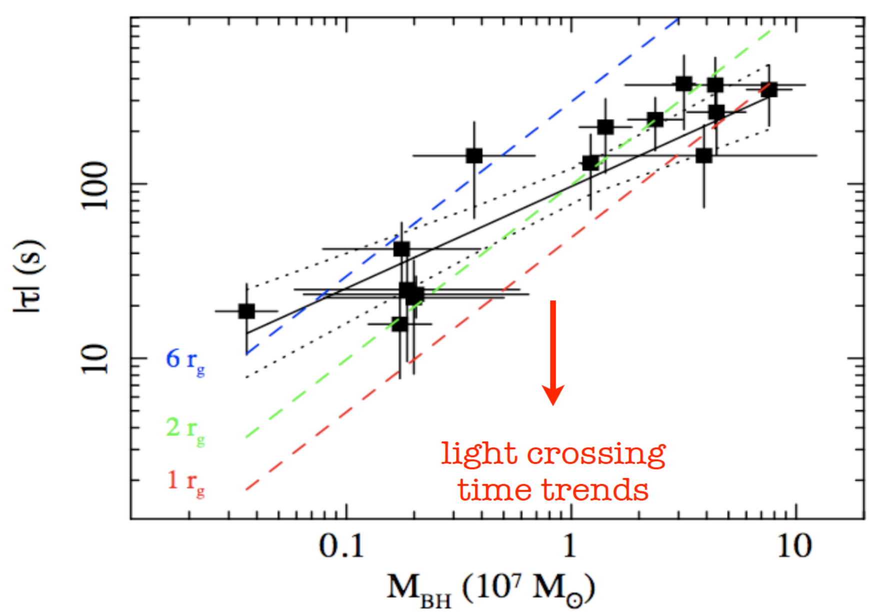


Involved distances are very small!!!!

# Tidal distruption event - TDE:

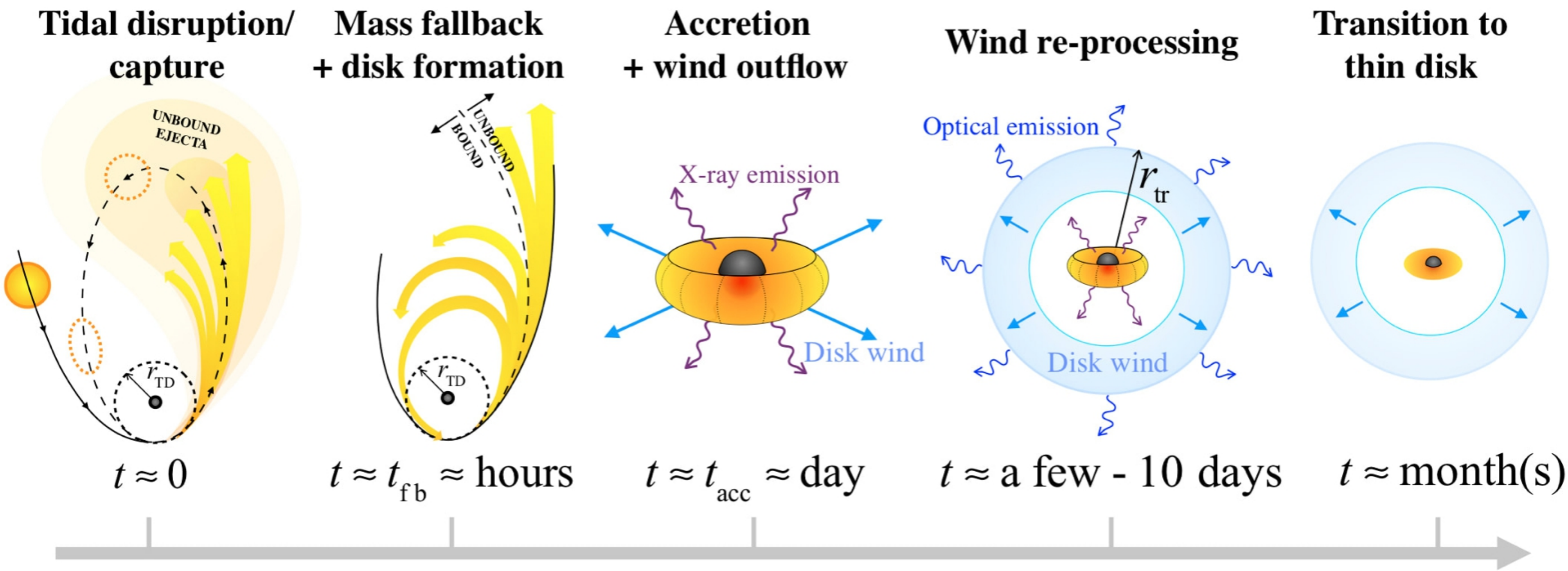


**Figure 1:** Adapted from Kremer et al. (2021a). Schematic of a stellar-mass black hole TDE including disk formation and evolution. From left to right: (1) Tidal disruption of the star, allowing for a possible initial partial disruption that unbinds a small fraction of material while the star is tidally captured, (2) Fallback of bound material to pericenter, (3) Rise time for X-ray emission (roughly 10^44 erg/s) through viscous accretion onto the black hole, (4) Reprocessing of the X-ray emission by disk wind at the trapping radius leads to bright optical emission (10^41-10^44 erg/s), (5) Transition to thin disk and prompt drop in mass transfer rate and luminosity.

# Tidal distruption event - TDE:

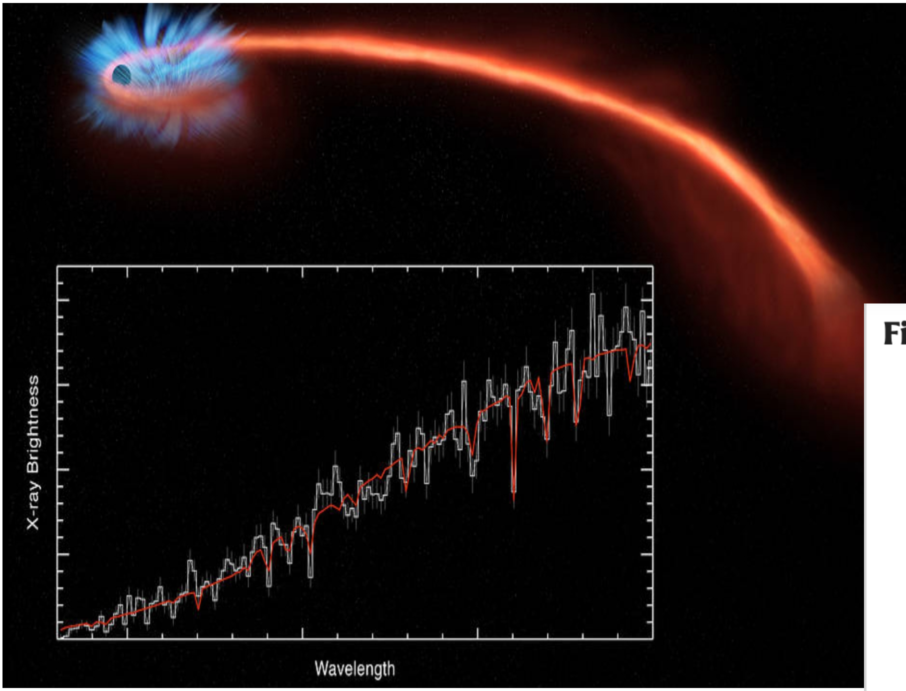


Fig. 1: UV-optical and X-ray light curve of OGLE16aaa.

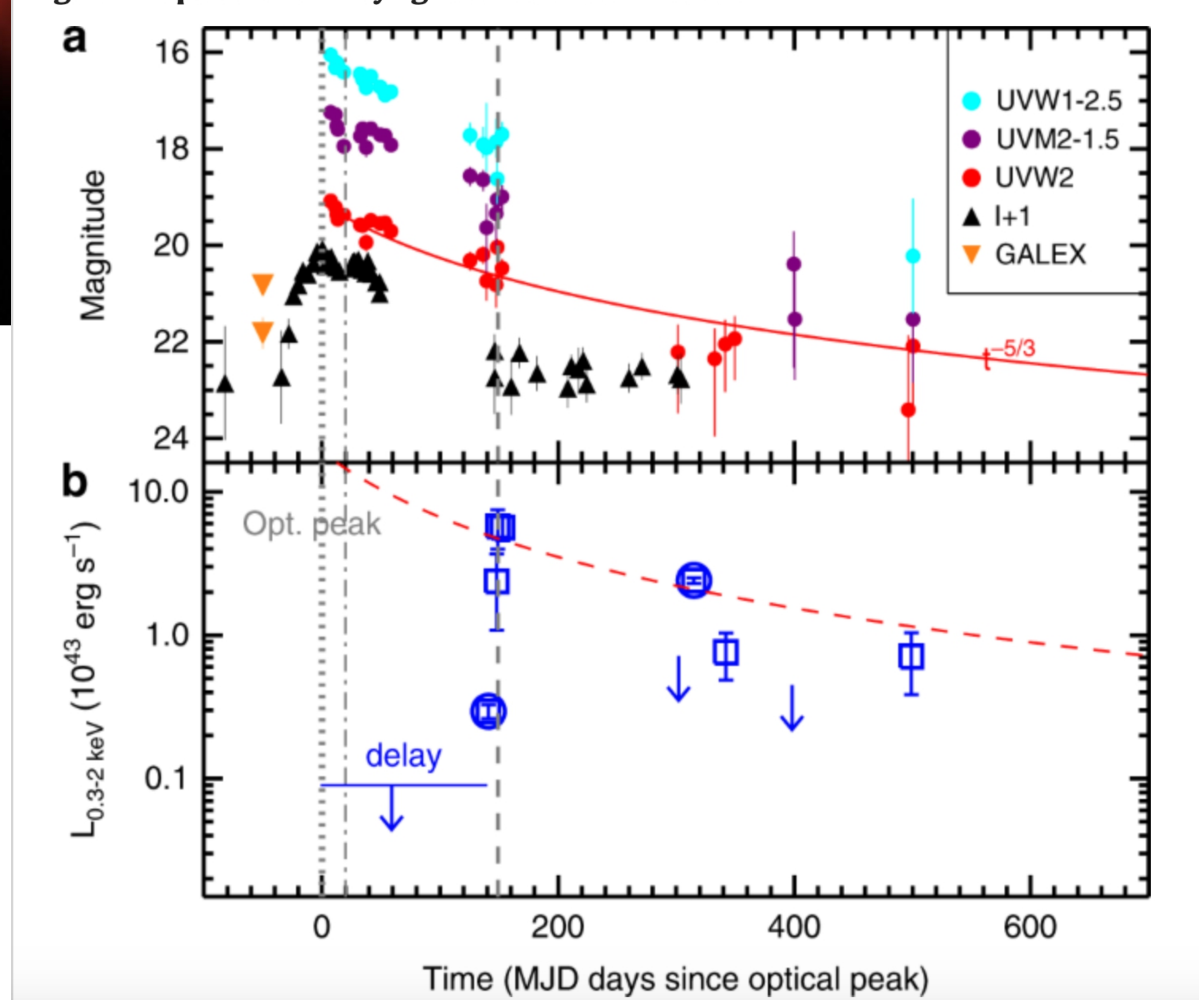

# XRB – mean spectrum of AGN:

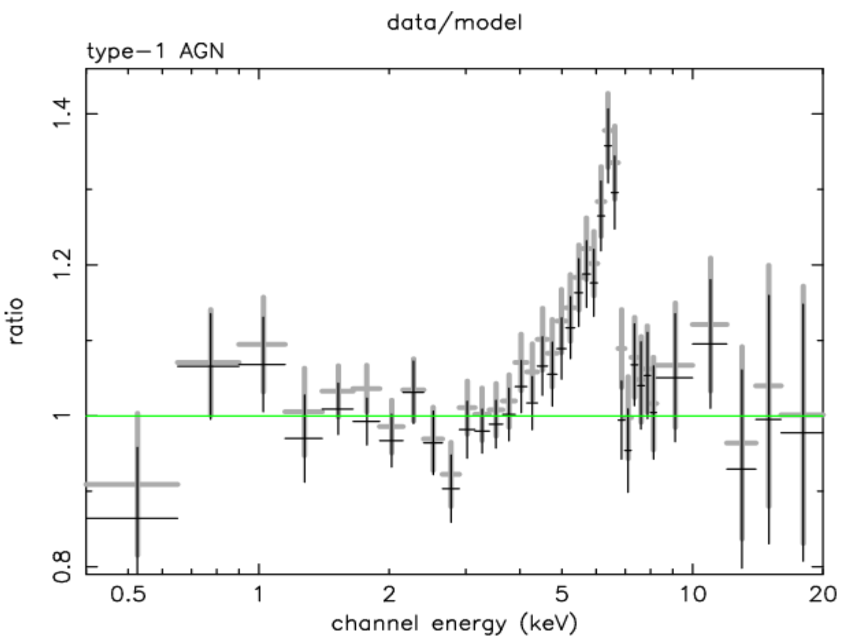


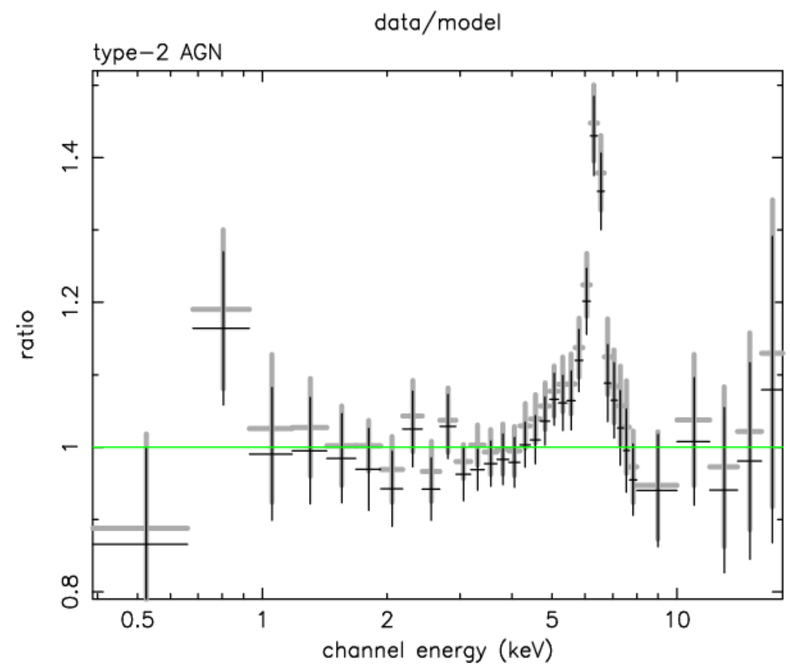


Over 100 AGN from XMM-Newton observations of Lockman Hole, Streblyanska + 2005.

# XRB – mean spectrum of AGN:

Zdziarski + 1995

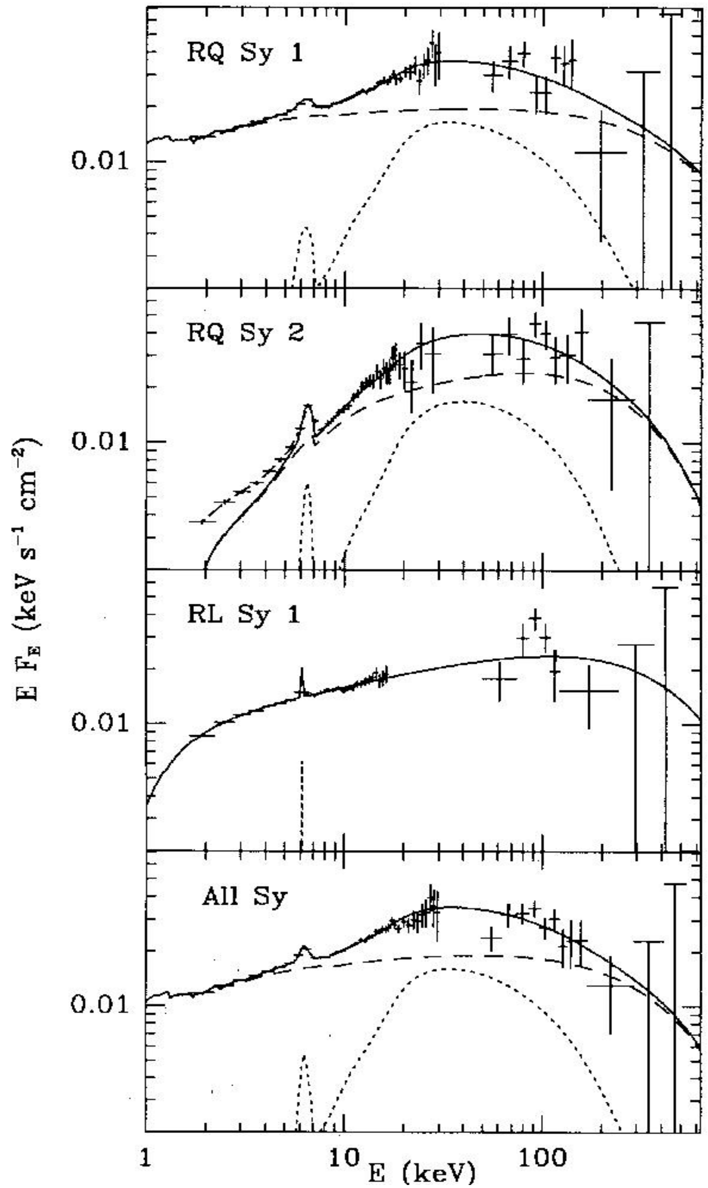


Gandhi+ 2003, XRB modeled by Compton thick ($N_H > 10^{24}$) and Compton thin ($N_H < 10^{24}$) AGN

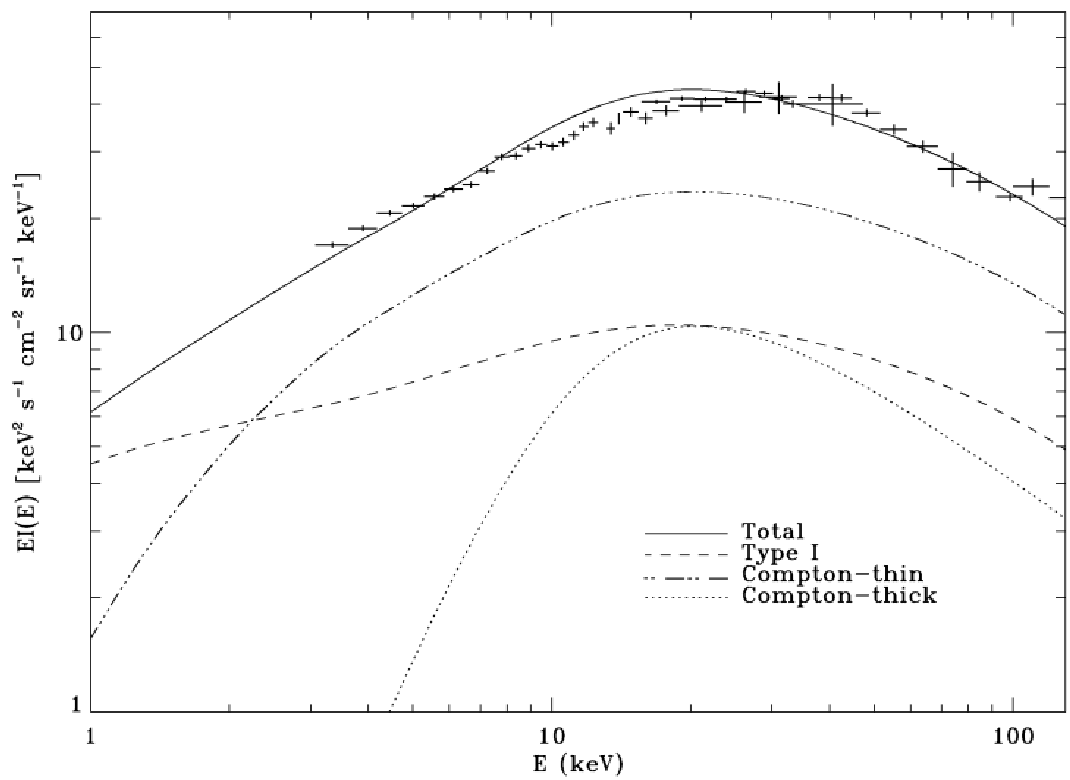

## XRB:

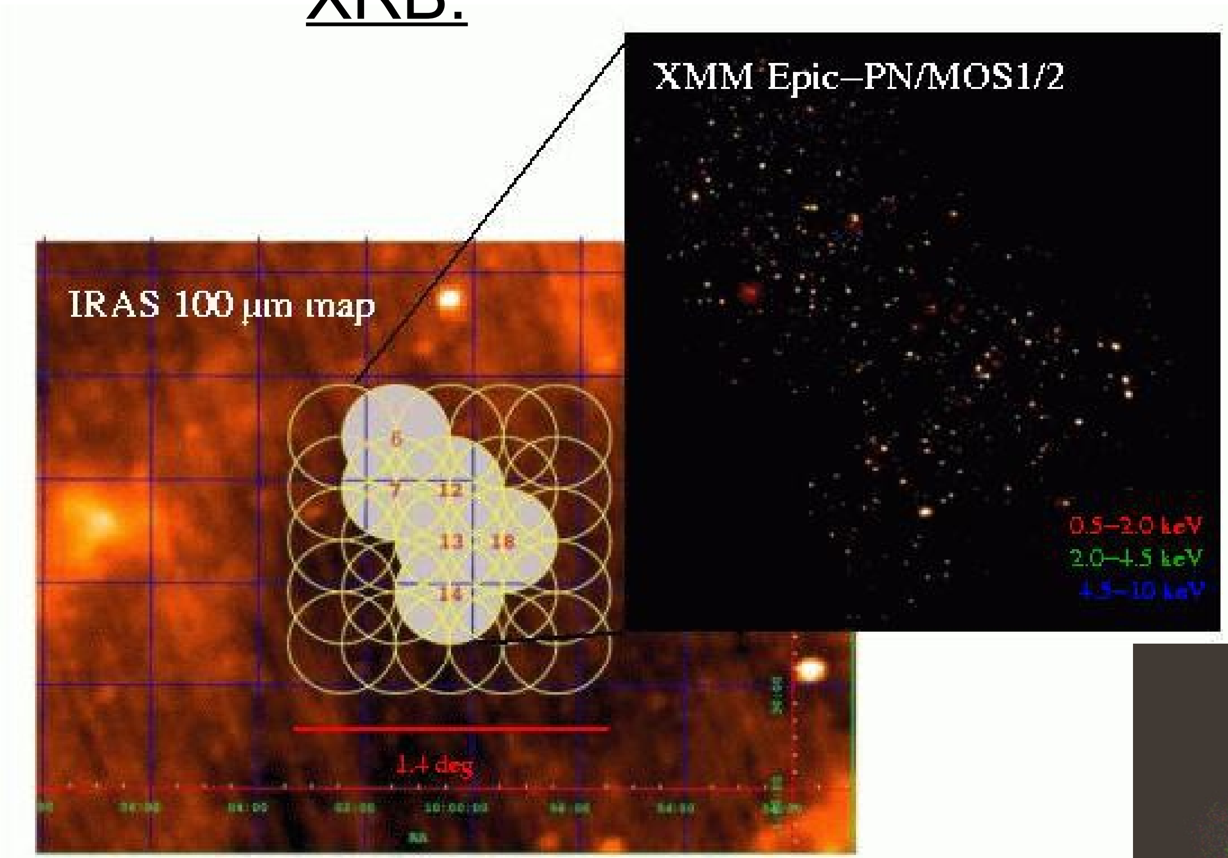


80% of point source are AGN

**Chandra Deep Field South**
**1 Ms, 20x20 arcmin**
**0.3-1 keV**
**1-3 keV**
**3-7 keV**

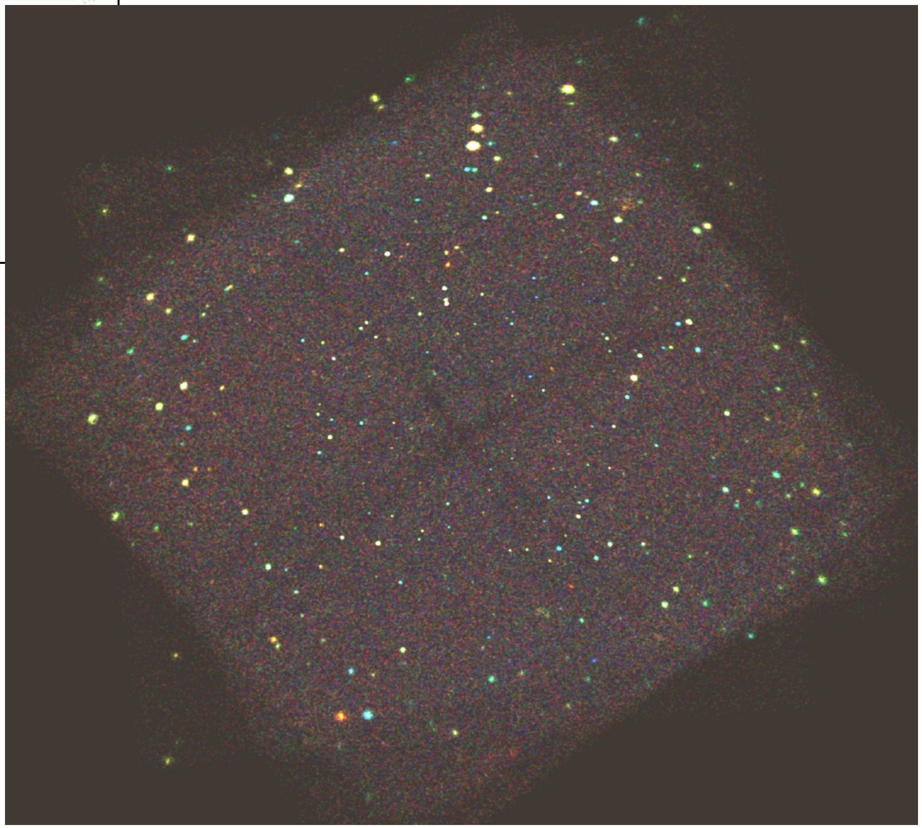

# XRB – log(N) – log(S) diagram:

Chandra, XMM, Beppo-Sax, ASCA, Gandhi+ 2003

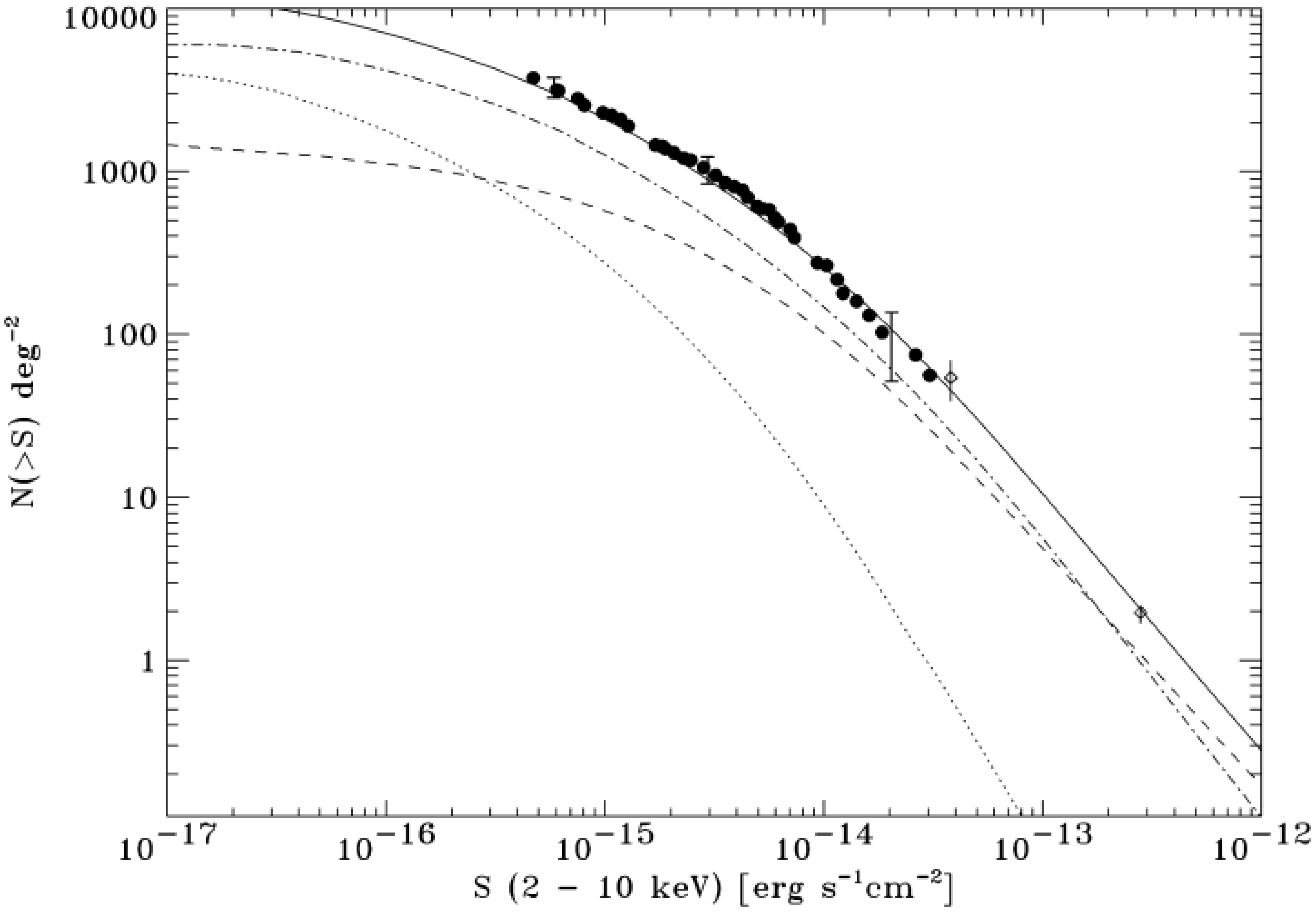

# XRB – absorbed AGN:

Model: Ricci+ 2011

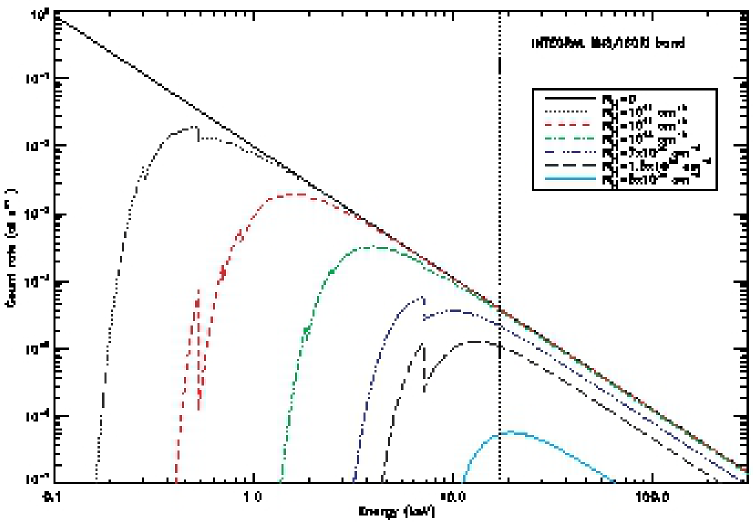


**Figure 2:** Effect of photoelectric absorption and Compton scattering on a power law model with a photon index of $\Gamma = 1.95$ in the X-rays.

# XRB – absorbed AGN:

Model: Ricci+ 2011

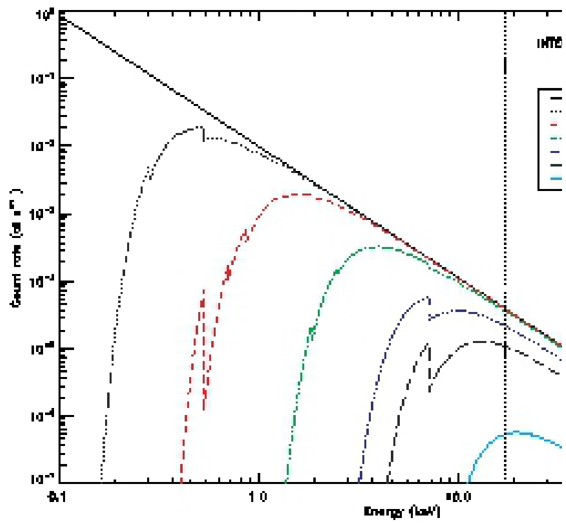


**Figure 2:** Effect of photoelectric absorption and Compton scattering
index of $\Gamma = 1.95$ in the X-rays.

Rosa+ 2008

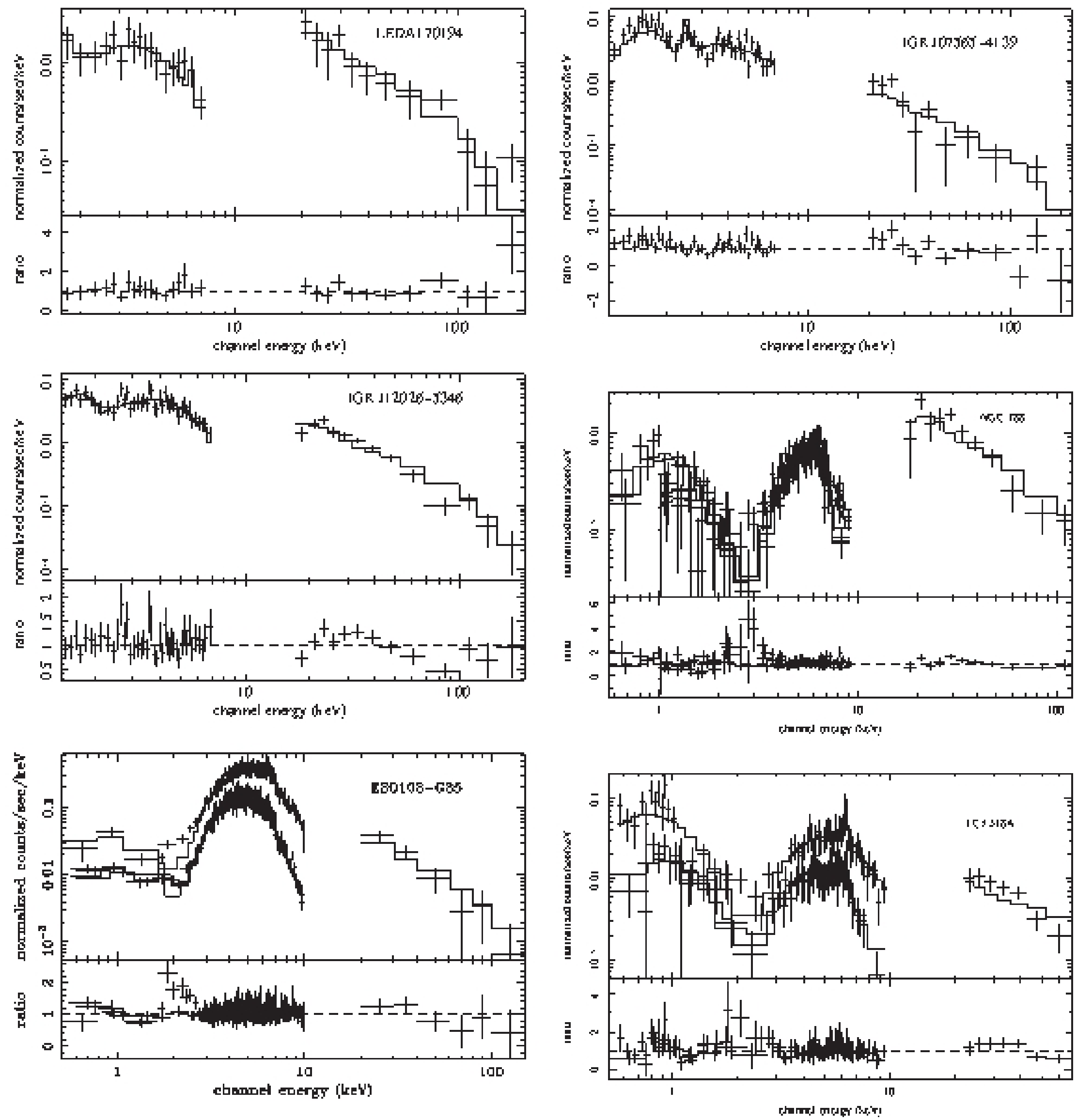


Integral + XMM-Newton

# XRB – absorbed AGN:

## Malizia+ 2009, INTEGRAL

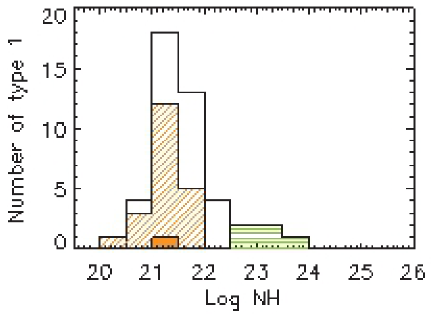


**Figure 5.** Column density distribution in the type 1 objects belonging to the complete sample. The horizontal dashed bins represent sources requiring complex absorption for which the higher value of $N_H$ has been used (see

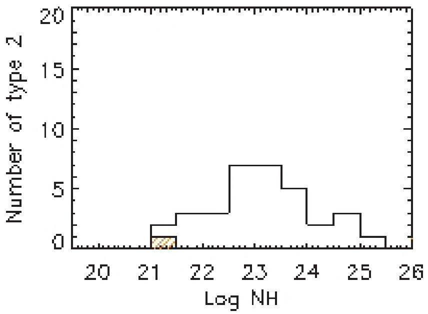


**Figure 6.** Column density distribution in the 33 type 2 AGN of the complete sample. Dashed bin represents IGR J16024−6107 where no absorption in excess of the Galactic one has been measured.

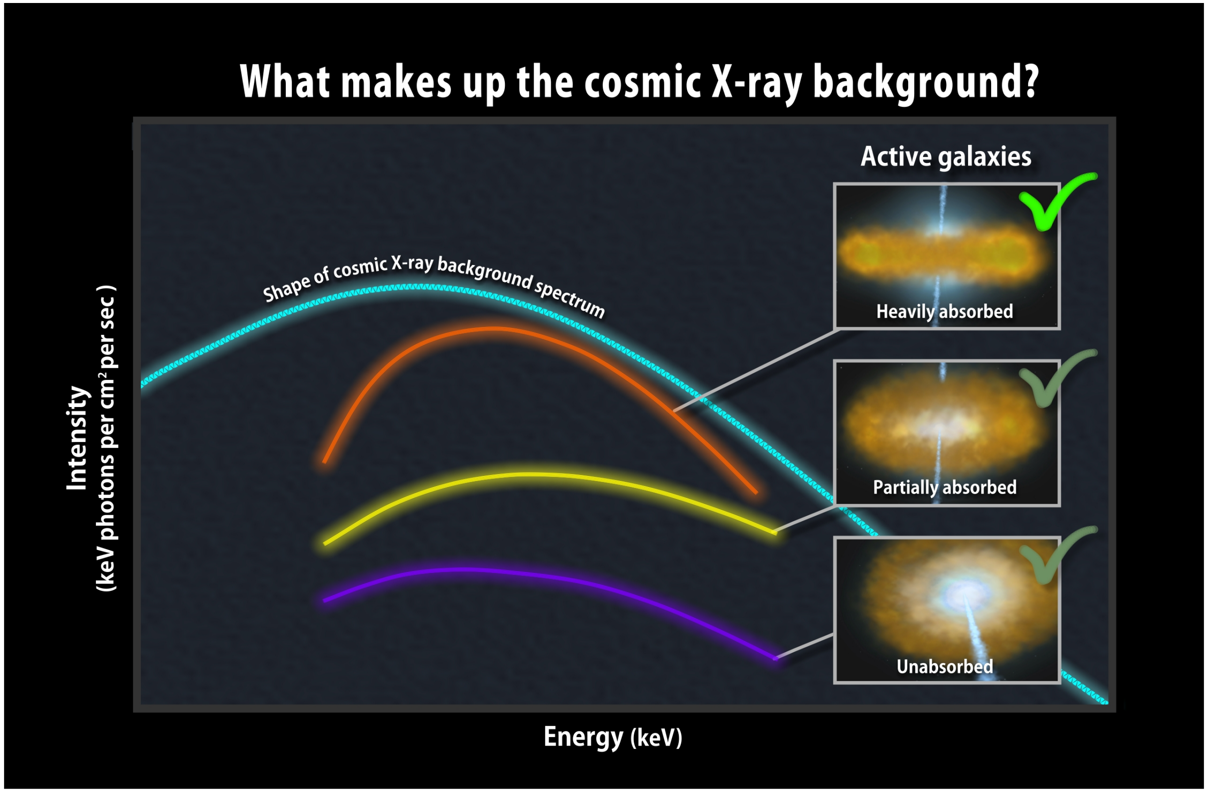

# XRB – luminosity density:

The redshift distribution of X-Ray Background (XRB)

Sołtan 2008, A&A, 490, 1039

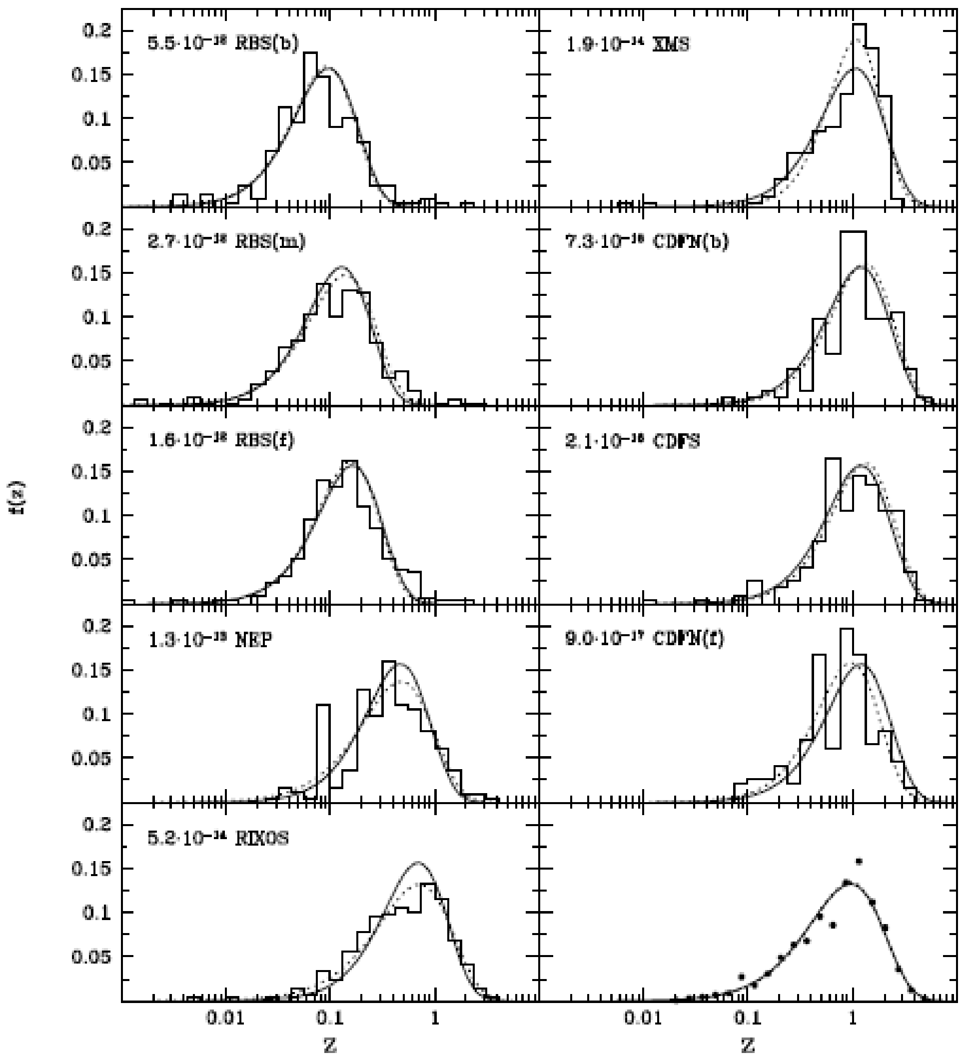


| Name | Flux limits (erg cm$^{-2}$ s$^{-1}$) | Number of sources all | extragalactic | AGN |
|---|---|---|---|---|
| RBS | $1.0\times10^{-12}-5.0\times10^{-11}$ | 1764 | 1054 | 681 |
| NEP | $5.0\times10^{-14}-1.0\times10^{-12}$ | 361 | 248 | 192 |
| RIXOS | $2.5\times10^{-14}-5.0\times10^{-13}$ | 393 | 318 | 235 |
| XMS | $1.0\times10^{-14}-2.0\times10^{-13}$ | 275 | 256 | 231 |
| CDFS | $5.0\times10^{-17}-1.0\times10^{-15}$ | 205 | 201 | 197 |
| CDFN | $1.5\times10^{-17}-5.0\times10^{-15}$ | 425 | 412 | 268 |

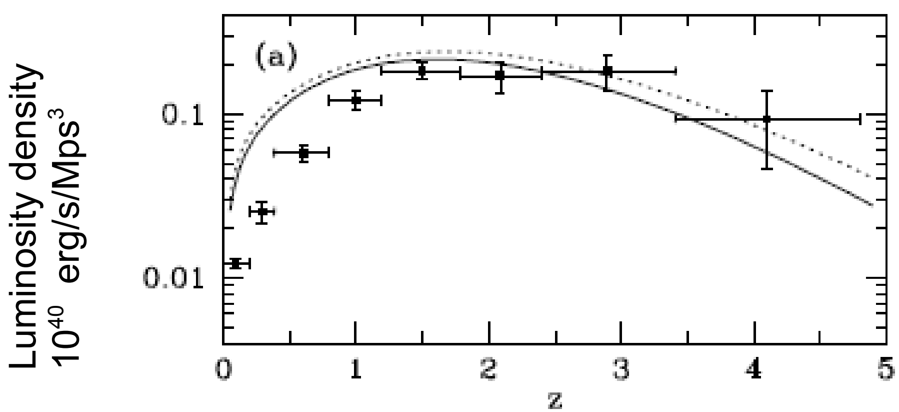

# THE END

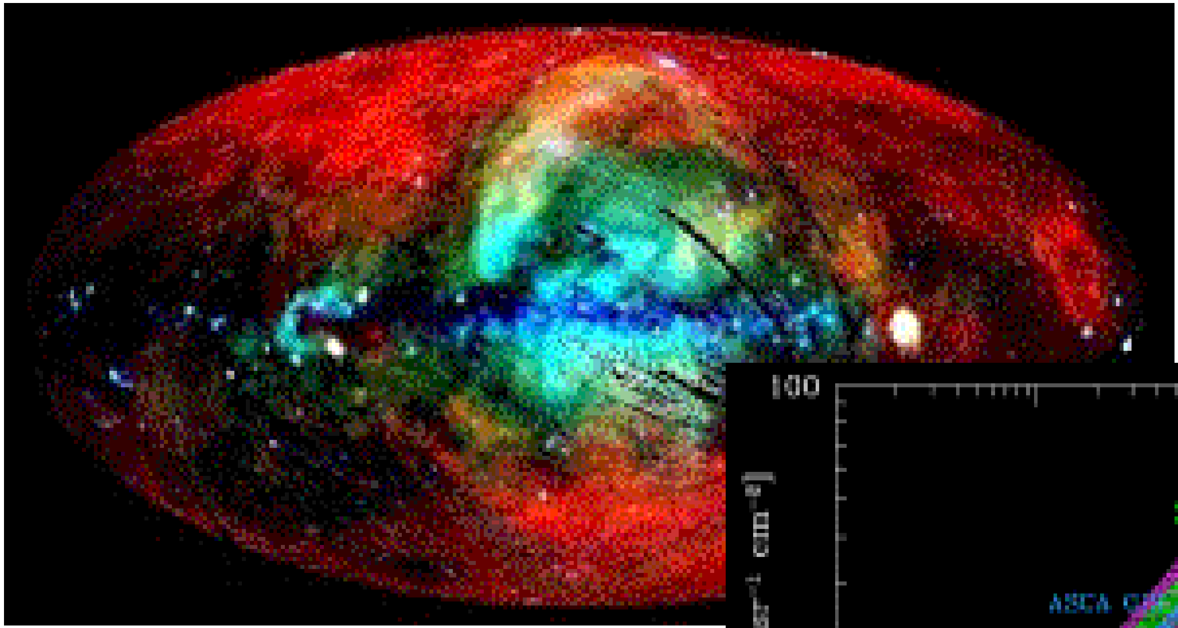

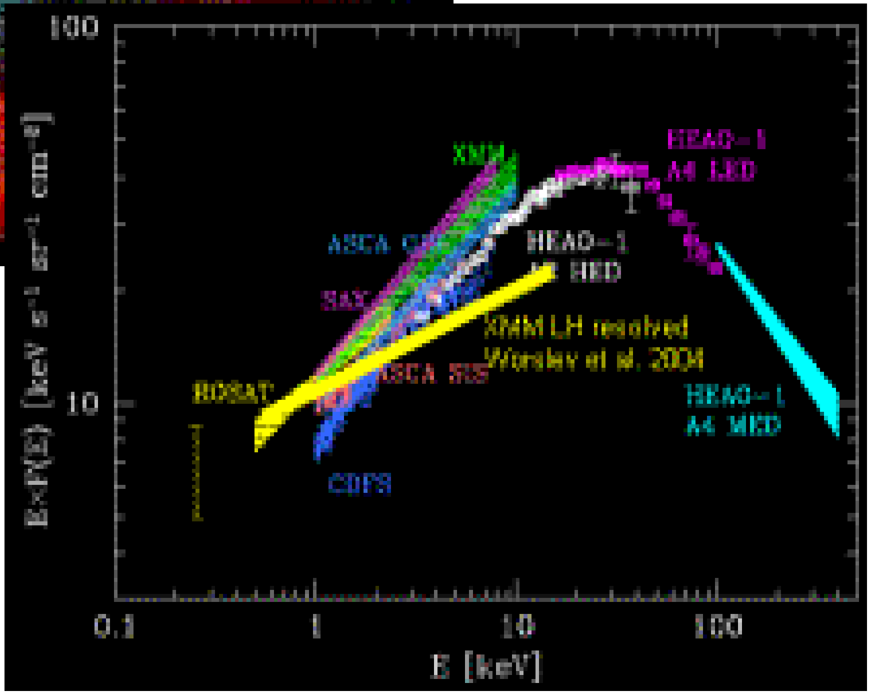

XMM
HEAO-1
A4 LED
ASCA GIS
HEAO-1
A2 HED
SAX
XMM LH resolved
Worsley et al. 2004
ROSAT
ASCA SIS
HEAO-1
A4 MED
CDFS
E×F(E) [keV s⁻¹ sr⁻¹ cm⁻²]
E [keV]
100
10
0.1
1
10
100